Ministry of Higher Education and Scientific Research
University of Carthage
Higher School of Communication of Tunis

A thesis submitted to obtain the degree of
Doctor of Philosophy in
Information and Communication Technologies

Cooperation and Coordination Strategies in Cognitive Radio Networks

By
Imen Sahnoun

Chair	Ridha Bouallegue	Professor at SUPCOM
Reviewers	Mohamed Slim Alouini	Professor at KAUST
	Noura Sellami	Professor at ENIS
Examiner	Leila Najjar Atallah	Associate Professor at SUPCOM
Supervisors	Mohamed Siala	Professor at SUPCOM
	Ines Kammoun Jemal	Associate Professor at ENIS

Acknowledgement

I would like to take this opportunity to express my sincere thanks to my supervisors Mr. Mohamed Siala, Professor at Supcom, and Mrs. Ines Kammoun Jemal, Associate Professor at ENIS, for sharing their outstanding expertise and knowledge, being a constant source of research ideas and inspiring words in times of needs. I learned a lot from their constructive comments and suggestions to improve the quality of this thesis. Thanks to them both, because without their encouragement and faith in me, this work could not be the same.

I am deeply grateful to all members of the jury for agreeing to read the manuscript and to participate in the defense of this thesis: Mr. Ridha Bouallegue, Professor at SupCom as a Chair, Mrs. Leila Najjar, Associate Professor at SupCom, as an external examiner, and Mr. Mohamed Slim Alouini, Professor at KAUST (Saudi Arabia), as well as, Mrs. Noura Sellami, Professor at ENIS, as reviewers.

I have also to thank Mr. Ridha Hamila, Professor at QU (Qatar), for his useful discussions and warm welcome during my experience as research assistant at Qatar University Lab.

Many thanks go to my beloved parents Brahim and Rebeh, to whom I dedicate this work. My every little success would not have been possible without their prayers.

Also, I would like to give my special thanks to my husband Zied for his patience, understanding and support through my PhD study.

Finally, I cannot forget my lovely children Mariem and Yahya who are the pride and joy of my life.

Abstract

Cognitive radio is an exciting emerging technology that has the potential of dealing with the stringent requirement and scarcity of the radio spectrum and offers the ability of radio sensing, self adaptation and dynamic spectrum sharing. In this thesis, we are interested in the case where secondary users are allowed to communicate concurrently with primary users provided that they do not create harmful interference to the licensed users. More precisely, the secondary transmission depends on a variable cost that reliably quantifies the interference power generated by the secondary user at the primary base stations. Here, we aim to improve the cognitive system performance in terms of throughput. For this aim, we first propose to use an adaptive modulation technique at the unlicensed user in order to maximize its data rate. We study the system behavior as a function of several parameters such as the maximum allowed cost, the number of base stations in the primary network, the secondary user location and its transmission power. Then, we propose to use cooperative techniques only if the resulting average interference power at the primary receiver is above a certain threshold. For relaying scenario, we adopt a space-time coding protocol based on Alamouti Space Time (ST) code as well as an Amplify and Forward (AF) protocol. Through simulations, we show that, these adaptive cooperative protocols have better performance compared with the classical cognitive system.

To further enhance the performance of the cognitive radio system, we propose, next, novel energy allocation schemes for the secondary users, considering the cooperative multi-hop transmission. Our optimization

problem is formulated as a maximization of the instantaneous received signal to noise ratio, under interference power constraints that are imposed to protect the primary network. In other words, we must maintain the interferences generated by the secondary transmissions to the primary network below an acceptable threshold level. We start by resolving geometrically our optimization problem for two and three hops. A variety of simulation results shows that our proposed energy allocation approach, combined with adaptive modulation, gives a better performance compared to the classical cooperative scheme with uniform energy distribution. Then, we propose an analytical optimal solution to the problem for the 2-hop case. We, also, show that the analytical resolution leads to the same results as the geometrical one.

Afterwards, we consider the case of multi-antenna secondary base station (BS-S) that does not have any prior information about the channel from the primary users. Hence, in order to maintain a limited interference during the downlink transmissions to the secondary users, the BS-S needs to get a perfect or partial knowledge of the primary users channels. For this aim, we investigate the identification problem of the primary active users and propose two solutions. We start by proposing an efficient and reliable method for a blind active primary users identification, without any energy or radio resource losses, based on randomly rotated constellations for each transmitted symbol at the primary users. Then, we consider the realistic non-line-of-sight (NLOS) environment, and propose a novel and efficient primary users identification, using compressive sensing (CS). Our focus is on the angular sparsity of the received signal at the BS-S, given an unknown number of primary user source signals impinging upon the antenna array from different directions of arrival (DOA). Given multiple snapshots, multiple measurement vectors (MMV) are available at the secondary base station and considered for primary channel detection over the angular domain using the regularized MMV-FOCal Underdetermined System Solver (M-FOCUSS) algorithm. Next, we develop novel methods for paths separation and primary channels estimation based on their autocorrelation matrix properties. Finally, we focus on the downlink transmissions and propose to design a beamforming vector at the BS-S, based on the estimated channels, that maximizes the desired signal power to each secondary receiver while minimizing the total interference towards all primary receivers.

Keywords: Cognitive Network, Adaptive Modulation, Interference, Amplify and Forward Relaying, Cooperative ST Alamouti, Energy Optimization, Relay Selection, Multi-Hop, Resource Allocation, Geometrical Optimization, Lagrange Multipliers, Multiple-Input-Single-Output, Users Identification, M-Sequences, Non-Line-Of-Sight, Compressive Sensing, Channel Estimation, Beamforming.

Contents

List of Figures

List of Tables

Chapter 1

Introduction

1.1 General Context and Motivation

Over the past several years, the radio spectrum is becoming a critical and limited resource for wireless communication networks due to the success of 3G and 4G systems and the explosion of high date rates hungry multimedia services [1]. A recent survey of spectrum utilization made by the Federal Communications Commission (FCC) has indicated that the actual licensed spectrum is largely underutilized in vast temporal and geographic dimensions [2]. In fact, conventional fixed spectrum allocation cannot successfully cope with the scarcity of radio frequency spectrum. Cognitive radio (CR) [3] [4] which is a promising technology to deal with this frequency scarcity resulting from the inflexible spectrum allocation policy, has been a topic of increasing research interest in recent years [5] [6]. Such paradigm has been originated by Mitola [7] [8] to promote the efficient use of the limited spectral resource [3] by seeking and opportunistically utilizing radio resources in time, frequency and space domains on a real time basis. In fact, CR allows the lower-priority secondary users (SUs) to share the licensed spectrum, originally allocated to the higher-priority primary users (PUs), provided that certain prescribed constraints are satisfied, thus having a potential to improve spectral utilization efficiency. One of the most important constraints consists

in maintaining the data transmissions of the licensed users protected [9] [10]. In other words, the interference generated by the cognitive transmissions to the primary network must be kept below an acceptable threshold level.

Different paradigms for the CR scenario have been discussed in [11] and are broadly classified into two main techniques according to the ways of accessing primary users 'spectrum: overlay and underlay CR systems [12]. In overlay networks, secondary users are allowed to access spectrum only when transmissions of primary users are considered absent. This approach requires that the secondary users sense the radio environment and identify the temporally vacant spectrum [10]. Quick and accurate detection of the presence of PUs is an important and difficult task [13] [14]. Furthermore, if the PUs occupy their spectrum too long that the SUs have no chance to access, the spectrum usage of such CR systems would not be efficient. However, for underlay networks, the secondary users can coexist with the primary users and exploit the same band being used by the PUs simultaneously based on interference limitation [11] [15]. This approach is especially appealing for practical deployment since it does not involve complex spectrum sensing mechanisms that require time consuming and power intensive processes [13] [14] [16]. Also, if the PUs and SUs can concurrently share the spectrum, the regional spectrum efficiency would be increased dramatically.

In this work, we focus on the underlay paradigm allowing the secondary users to operate in parallel with the primary users. During their transmissions, the SUs have to guarantee that the interference level they cause to the primary receivers is kept below a predefined threshold [17]. This constraint, associated with underlay systems, limits their transmission energies as well as their coverage areas. One possible solution is to use cooperative relaying techniques [18] [19] in order to make communication possible between two distant nodes. In this thesis, both non-regenerative and cooperative space-time coding protocols will be considered. In fact, it has been proved that cooperation based on space-time block codes (STBC) represents an effective way to introduce spatial diversity in various wireless systems [20]. Further, in most of the existing research activities on relaying, the cooperative diversity is used to reduce the bit error

rate. However, this reduction comes at the expense of the amount of required resources since additional channels are needed for relaying. Therefore, the throughput is reduced in cooperative networks. For this reason, we propose to use an adaptive modulation technique by the secondary users in order to compensate the throughput loss due to the relaying and maximize the data rate at the secondary destination [21] [22].

Furthermore, for each communication is allocated a total available power that must be well distributed among all involved nodes. In this context, and given that power is a critical resource, optimizing the usage of this resource is crucial. In the literature, several power allocation approaches for cooperative networks have been investigated considering different relaying schemes and optimization criteria. In [23] and [24], the authors proposed a power allocation scheme for multi-hop transmission systems that minimizes the outage probability under a total power constraint. In [23], the authors considered dual-hop transmission systems with and without diversity employing Decode and Forward (DF) and Amplify and Forward (AF) relaying protocols. In [24], both individual and total power constraints have been treated in the dual-hop case. The individual power constraint was however overlooked when resolving the multi-hop case. In [25] and [26], the total power consumption in a DF multi-hop network was minimized while keeping the Signal-to Noise Ratio (SNR) above a certain threshold [26], and the end-to-end Bit Error Probability (BEP) below a predefined target [25]. In [27], the authors aimed to maximize the instantaneous received SNR in an AF multi-hop network under short-term and long-term power constraints. A power allocation scheme was also proposed in [28] to maximize the achievable data rate in a multi-hop relay network, where both AF and DF relaying protocols were studied. In [29], a selection relay scheme combined with a power optimization was proposed, under both individual and total power constraints, to maximize the source-destination channel capacity. Therefore, the objective is to find new optimal energy allocation schemes for source and relays nodes that maximize the instantaneous SNR at the secondary destination in the underlay network.

Moreover, to avoid harmful interference to the primary system, quick and accurate detection of the presence of PUs is an important and challenging task. In the literature, a number of different methods have been proposed for identifying the presence of signal transmissions, such as matched filtering, energy detection,

and cyclostationary detection [30] [31] [32]. In these works, the authors assumed that perfect or partial instantaneous Channel State Information (CSI) of the PU channels are available at the CR transmitter. These CSIs are generally obtained at the CR network thanks to pilot symbols sent in parallel to data symbols by the different users of the primary network. However, in practice, the primary system does not need to intervene and be aware of the existence of the secondary users. In [33], the authors developed a novel iterative least square (ILS) based primary-system identification algorithm which can blindly detect the code channels utilized by primary users. Authors in [34] employed artificial neural network (ANN) to identify the primary users' presence by identifying the modulation type of the primary user.

More recently, Compressive Sensing (CS) [35] [36] has been considered as a promising technique that can be applied for primary users identification [37] [38] [39], by exploiting some inherent sparsity features of the received signal at the secondary base station. Most of the literature on CS deals with sparsity in the frequency domain to perform wideband spectrum sensing [40]. In [41], the authors investigated the angular sparsity for multiple antenna spectrum sensing and primary users detection considering a Line-Of-Sight (LOS) propagation. As we consider, in this work, the underlay scenario, characterized by its spectrum-sharing nature, the CR network inevitably operates in interference-intensive environments. Two conflicting challenges are how to maintain the interferences generated by the cognitive transmissions to the primary network below an acceptable threshold level, while maximizing the performance of the secondary network. In the literature, many interference mitigation techniques have been proposed [42] [15], including spectrum shaping, predistortion filtering and spread spectrum, to make the coexistence of primary and secondary networks possible. As for multiple-antenna CR networks, spatial processing, especially transmit beamforming, is an effective alternative [43] [44] [45] to balance between the interference minimization for primary users and the SINR maximization for secondary users, by adaptively form different beam patterns to enhance reception in the destination direction (intended user) and put nulls towards the directions of the interference (non-intended users). Various beamforming techniques have been developed that find optimal beams while maintaining the interference to the primary networks within an acceptable level. In

[46] and [47], authors combined beamforming and power allocation methods for CR systems in multiple access channels with tolerable SINR at PU systems. The authors in [47] proposed two different scenarios: with and without cooperation between the primary and secondary networks. In [48] [49] [50], zero forcing beamforming was used to null the self-interference among SUs chosen by the orthogonal user selection algorithms. In order to reduce the amount of required feedback and to increase the sum-rate of the CR systems, [51] and [52] propose a scheduling algorithm based on opportunistic beamforming. The orthogonal beams were calculated based on full [51] and partial primary users' CSI [52].

1.2 Thesis Contribution

In this work, we consider a spectrum-sharing cognitive radio (underlay CR network) where the coexistence of simultaneous primary and secondary communications in the same frequency channel may occur as long as the aggregated interference generated by the secondary users is below some acceptable threshold. The main purpose of this work is to secure the primary communications, while maximizing the data rate at the secondary destination. Thus, we define a maximum cost value above which the secondary user is not authorized to transmit.

Our first contribution is to use an adaptive modulation technique by the secondary user in order to maximize the data rate at the secondary destination. The performance of such adaptive cognitive system is studied with respect to several parameters such as the maximum allowed cost at the primary network, the secondary user location, its transmission energy and the number of primary base stations detected in the network.

Our second contribution consists in using cooperative techniques only if the SU cannot transmit through the direct link. By others words, if the aggregate interference of the direct link between the SU and the destination exceeds a critical threshold, a cooperative transmission is investigated. Otherwise, the SU is not allowed to transmit. For the cooperative transmission, both non-regenerative (AF) and cooperative Alamouti space-time (ST) coding protocols are studied and compared to each other. In fact, the Alamouti ST

coded cooperation approach is characterized by the properly exploitation of the whole energy transmitted by the source in both cooperation phases. We analyze the systems performance in terms of throughput under different influential factors and reveal some important tradeoffs.

Furthermore, to ensure data rate maximization at the secondary network, we propose a transmission energy optimization with respect to the tolerable interference power at the primary receiver. In fact, our third contribution consists in finding new optimal energy allocation schemes for both source and relay nodes that maximize the instantaneous received SNR without causing interference to the PU. To solve our optimization problem, we propose both geometrical and analytical approaches. Our study, is then generalized to the cognitive multi-hop case.In fact, the advantage of the geometrical method is to get more insight and makes the resolution tractable for more hops in the system. Note here that, up to our knowledge, our proposed geometrical optimization approach, as well as the analytical approach in the cognitive cooperative context, have not been considered in the literature.

In addition, our fourth contribution is to combine a selection scheme where only one "best" relay is chosen with an optimal energy allocation scheme for source and relay nodes to maximize the instantaneous received SNR under the system constraints. We compare the performances of adaptive AF based on Alamouti ST code system with optimized energy allocation over those with uniform energy allocation.

The fifth contribution of this work is to propose a practical embedded identification scheme of active primary users, where the secondary base station has no prior information about the channel from the PUs. The proposed approach is based on the use of random or pseudo-random sequences by the PUs to avoid extra signaling between primary and CR networks. Depending on the generated random sequence, the PU rotates or keeps unchanged its constellation for each transmitted symbol. Based on the signals received at the secondary BS antennas, we propose a simple and efficient processing to blindly identify all active primary users. We consider to use the m-sequences that have several important properties [53] [54] [55]and belong to the family of pseudo-random sequences. Some numerical results are provided to demonstrate the advantages of the proposed method.

Our sixth contribution consists in considering, unlike [41], a real case that is the Non-Line-of-Sight (NLOS) propagation, where several paths can originate from the same PU, and arrive to the secondary destination at different Directions Of Arrival (DOA). Using the compressive MMV sensing method. Then, we develop novel methods for paths separation and primary channels estimation based on their autocorrelation matrix properties.

Finally, we exploit the interference channels estimated in the latter part, and propose, as a seventh contribution, a beamforming design at the secondary base station that maximizes the throughput at the secondary network while minimizing the interference at the primary one. For this purpose, we adopt a Gram-Schmidt orthogonalization process [53] in order to create orthogonal beams to the PUs channels.

1.3 Publications

The work presented in this thesis has led to the following publications:

Conferences

1. I. Sahnoun, I. Kammoun, M. Siala. Throughput enhancement for secondary users in cognitive network. The IEEE 24th Annual International Symposium on Personal, Indoor, and Mobile Radio Communications, PIMRC, 2013.

2. I. Sahnoun, I. Kammoun, M. Siala. Joint adaptive modulation and cooperation for throughput enhancement in cognitive network. The International Conference on Communication and Networks, COMNET, 2014.

3. I. Sahnoun, I. Kammoun, M. Siala. Energy Allocation Optimization for Cooperative Cognitive Network. The IEEE 15th International Workshop on Signal Processing Advances in Wireless Communications, SPAWC, 2014.

4. I. Sahnoun, I. Kammoun, M. Siala. Optimal Energy Allocation Scheme for Throughput Enhancement in Cooperative Cognitive Network. The European Signal Processing Conference, EUSIPCO, 2014.

5. I. Sahnoun, I. Kammoun, M. Siala. Primary users identification in underlay cognitive radio. The International Multi-Conference on Systems, Signals and Devices, SSD, 2016.

6. I. Sahnoun, I. Kammoun, M. Siala. Embedded Primary Users Identification and Channel Estimation for Underlay Cognitive Radio Network based on Compressive Sensing. The IEEE 27th Annual International Symposium on Personal, Indoor, and Mobile Radio Communications, PIMRC, 2016.

Journals

1. I. Sahnoun, I. Kammoun, M. Siala, R. Hamila. Optimal resource allocation schemes for AF multi-hop in a cognitive radio system, submitted to Wireless Personal Communications (WPC) in august 2015 with no response until august 2016. Then, removed and submitted to International Journal of Communication Systems.

2. I. Sahnoun, I. Kammoun, M. Siala. Compressive sensing-based primary channel estimation followed by secondary downlink beamforming in cognitive radio network, submitted to IEEE Transactions on Wireless Communications.

1.4 Thesis Organization

In this section, we provide an outline of this thesis which organizes the previously detailed contributions on 4 chapters.

In chapter 2, we introduce the cognitive radio concept and main approaches. Then, we present the principle of our approach based on adaptive modulation and derive analytical formulation of the constraint imposed

on secondary users. We study the system performance in term of throughput considering the effect of several parameters on the system throughput, such as the maximum allowed cost at the primary network, the secondary user location, its transmission energy and the number of detected primary base stations. Then, we introduce the cooperation techniques in order to enhance the overall network capacity in terms of data rate and cell coverage. For the relaying scenario, both non-regenerative (AF) and cooperative space-time coding protocols based on Alamouti ST code are studied. We analyze the performance of our adaptive cooperative cognitive system under different influential factors and reveal some important tradeoffs.

In chapter 3, we consider an adaptive cognitive network based on cooperation and propose a novel energy allocation scheme for source and relay nodes. In fact, an optimization of the SU and the relay transmitted symbol energies is carried on to maximize the instantaneous received signal-to-noise ratio under power and interference constraints. The performance of such system in terms of throughput and outage probability is evaluated and compared to that of the conventional fixed allocation scheme where the energy is uniformly distributed to each node. Moreover, we end the chapter by combining selective-relay cooperative communication, where only one "best" relay is chosen, with optimal energy allocation scheme. For the cooperation, we consider the Alamouti AF protocol.

In chapter 4, we propose new energy optimization schemes for the AF multi-hop cognitive system that maximize the instantaneous SNR at the secondary destination. We start by resolving geometrically our optimization problem. In particular both the two and the three hop cases are studied. Then, we propose an analytical optimal solution to the problem of the 2-hop case. Simulation results are also given for both methods.

Chapter 5 is dedicated to blindly identify all active primary users and estimate their channels. First, we propose and study a practical embedded identification scheme of active primary users based on the use of pseudo-random sequences, where both Binary Phase-Shift Keying (BPSK) and Quadrature Phase-Shift Keying (QPSK) modulations are considered. Second, we consider a Non-Line-of-Sight (NLOS) propagation, where several paths can originate from the same PU, and arrive to the secondary destination at different

directions of arrival. We begin by sensing the uplink primary channels based on the CS method. Then, we develop novel methods for paths separation and primary channels estimation. Through simulations, we study the recovery performance of the proposed approach in terms of false alarm and average minimum square error (MES) between the true and the estimated primary channel, over the conventional maximum to minimum eigenvalue (MME) detector. Finally, we end the chapter by generating a beamforming design at the secondary base station (BS-S), based on the estimated channels, that maximizes the desired signal power to its corresponding secondary receiver while minimizing the total interference towards all primary receivers.

Finally, the dissertation is concluded in chapter 6, by giving a summary of our contributions, perspectives to the carried work and suggestions for open research topics.

Chapter 2

Throughput Enhancement for Secondary Users in a Cognitive Network

2.1 Introduction

In this chapter, we are interested in the case where secondary users are allowed to communicate concurrently with primary users provided that they do not create harmful interference to the licensed users. More precisely, the secondary transmission will depend on a variable cost that reliably quantifies the interference power generated by the secondary user at the primary base stations. Here, we aim to improve the unlicensed system performance in terms of throughput. For this aim, we propose to use an adaptive modulation at the secondary user in order to compensate the throughput loss due to the relaying. Then, we propose to introduce cooperative techniques, such that cognitive and cooperation may work jointly to form a promising paradigm to significantly enhance the overall network capacity in terms of data rate and cell coverage. Here, the cooperation is used only if the resulting average interference power at the primary receiver is above a certain threshold. For relaying scenario, we propose to use an amplify and forward

relaying protocol as well as a cooperative protocol based on Alamouti ST code. Through this chapter, we investigate the system performance under different sets of conditions. We compare also the performances of these proposed adaptive cooperative protocols with the classical cognitive system and the ST coding protocol with the AF scheme.

The first part of this chapter starts with an overview of the cognitive radio networks. Then, we present our adopted cognitive approach and the principle of the adaptive modulation technique. Next, we derive analytical formulation for our constraint imposed on secondary users. We end the first part by analyzing the proposed system performance in terms of throughput. In the second part, we introduce an adaptive cognitive cooperative network based on both AF protocol and Alamouti ST code respectively. Then, we give the corresponding constraints imposed on secondary users for both cooperative schemes. Finally, we provide some simulation results to evaluate the proposed system and compare it to the non cooperative case.

2.2 Cognitive Radio System Overview

2.2.1 Cognitive Radio Principle

Cognitive radio (CR) is a paradigm for wireless communication in which either a network or a wireless node changes its transmission or reception parameters to communicate efficiently avoiding interference with licensed or unlicensed users. This alteration of parameters is based on the active monitoring of several factors in the external and internal radio environment, such as radio frequency spectrum, user behavior and network state. Therefore, CR is a promising solution to the problem of overcrowded spectrum. In fact, it brings a concept shift as a well regarded agile technology that allows opening up the frequency bands to concurrent operating users in a non-interfering mode. Accordingly to make possible spectrum sharing without causing harmful interference to existing traffics, cognitive users should possess a minimum of information about their surrounding non cognitive users. Depending on the access technology to coexist

with the primary network, cognitive radio approaches fall into two main classes: Overlay and Underlay [12].

2.2.2 Cognitive Radio Approaches

2.2.2.1 Overlay approach

The overlay approach have been proposed in the objective of enabling secondary users to occupy the spectrum holes that has been left vacant by primary users. Theoretically, it does not cause any interference to the primary system, that is, only white spaces of the primary system are exploited by the secondary network [42].

In order to facilitate the coexistence of both primary and secondary traffics within the same network in an opportunistic transmission mode, the surrounding environment should be observed to be able to predict the state of each portion of the frequency spectrum. In other words, the secondary users must conduct sensing operations permanently and reliably in order to detect the absence of primary user signals in space, time, or frequency [13] [14].

2.2.2.2 Underlay approach

The underlay paradigm allows simultaneous primary and secondary transmissions, as long as the interference level at the primary user is maintained below a specific level without causing any outage on primary operations [42][56]. In fact, exceeding the predefined tolerable interference threshold, may degrade dramatically the primary signal. To implement this underlay strategy, the primary receiver has to provide CR systems the information of how much interference it can tolerate across the spectrum. This approach is also called interference-tolerant CR. Many advanced signal processing techniques have been proven to be very efficient for interference avoidance and mitigation, among which we find the beamforming technique [43] [44].

In this thesis, the underlay strategy is considered, and our main objective is to secure the primary communications, while maximizing the data rate at the secondary destination.

2.3 Throughput Enhancement using Adaptive Modulation

2.3.1 Cognitive System Model

As shown in Figure 2.1, we consider a cognitive radio network consisting of one secondary terminal denoted by SU, one secondary base station denoted by BS-S and N primary base stations denoted by BS-P$_n$ where $n \in \{1,..,N\}$.

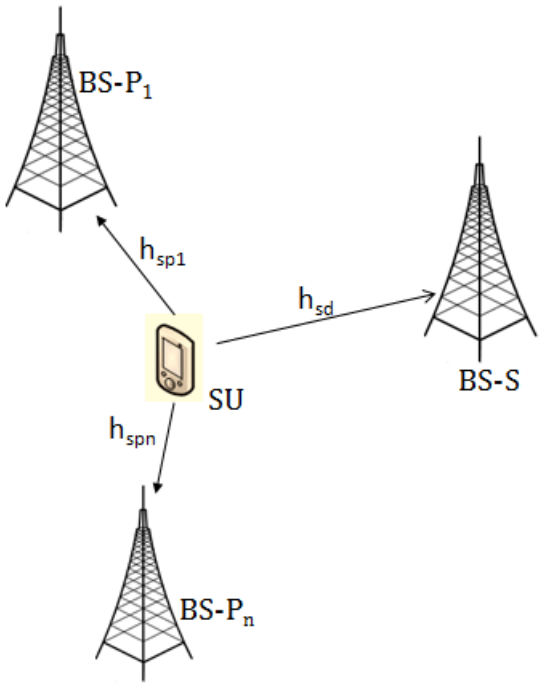

Figure 2.1: Channel model.

All links between terminals are assumed to be independent. Each link consists of Rayleigh, slow fading

channel, so that we can consider its coefficients as constant during the transmission of at least one frame. We denote respectively the propagation channel attenuations between SU-(BS-S) and SU-(BS-P$_n$) by h_{sd} and h_{sp_n}. Let b_{sd} and b_{sp_n} are the additive white Gaussian noise terms corrupting respectively the two links SU-(BS-S) and SU-(BS-P$_n$) with a common variance N_0. Furthermore, to investigate the effect of the path loss into the channel model, the coefficients L_{sd} and L_{sp_n} corrupting respectively SU-(BS-S) and SU-(BS-P$_n$) channels, follow a propagation model of $1/d^{\alpha}$, where α denotes the path loss factor. We assume that the distance between the primary and the secondary base station is fixed to some distance d_0. The shadowing effect is also considered here and the presence of correlation between channels is taken into account where S_i follows a log-normal distribution with parameter σ. We note that the shadowing, disturbing each propagation link, is due to the contribution of both nodes involved in the transmission on that channel link. For example, the shadowing, seen by the SU-(BS-S) link, is the contribution of both shadowing effects near the secondary user SU and the secondary base station BS-S. The SU, BS-S and BS-P$_n$ shadowing contributions are independent random distributed Gaussian variables. Hence, the shadowing effect S_{ij} , (i = s (SU), d (BS-S); j = s (SU), p$_n$ (BS-P$_n$)) disturbing the channel link ij is expressed by

$$S_{ij} = S_i + S_j. \tag{2.1}$$

Additionally, we assume that the shadowing effects near the secondary and primary base stations are similar. Therefore, for our shadowing model, we consider that

$$var(S_d) = var(S_{p_n}) = (1-\beta)\sigma^2 \tag{2.2}$$

and

$$var(S_s) = \beta\sigma^2. \tag{2.3}$$

Here, σ is a term in dB and β is a factor that assesses the SU shadowing contribution when compared to the secondary or primary base stations contributions. Typically, this factor can be chosen to be equal to 0.5.

In order to optimize our system performance and especially to maximize the throughput at the secondary destination, always under the interference constraints, an adaptive modulation is used by the secondary user.

2.3.2 Adaptive Modulation: Principle and Decision Table

In the adaptive transmission scheme, the transmitter changes its constellation size based on the instantaneous received Signal to Noise Ratio E_a/N_0 to decide for the constellation size of the next transmitted frame. We assume that all terminals have perfect knowledge of the channels coefficients. Hence, the source terminal can easily estimate the total received *SNR* at the destination.

In general, the look-up tables for the modulation choice are established by fixing a target Bit Error Rate (*BER*). Since our goal is to maximize the system throughput, we proposed in a previous work [22] a novel criterion for the determination of the decision table based on the maximization of system data rate. For this aim, we represented the throughput of a direct transmission from a source to a destination on a Gaussian channel as a function of instantaneous *SNR* for different modulations. Table 2.1 shows the obtained decision table. We note that E_a is the transmitted energy per symbol and N_0 is the variance of the Gaussian channel.

2.3.3 Constraint Imposed on Secondary Users

We propose a cognitive radio scenario where concurrent primary and secondary communications are allowed. Nevertheless, in cognitive systems, the unlicensed users have to be designed to efficiently share the spectrum at the same time without causing harmful interference to the licensed users. To address this problem, we define a maximum cost power at the primary base station, denoted by C_{max}, so that secondary

Table 2.1: Decision table based on throughput criterion

Modulation	$(E_a/N_0)\,dB$
BPSK	$E_a/N_0 \leq 6.69$
4QAM	$6.69 \leq E_a/N_0 \leq 11.66$
8QAM	$11.66 \leq E_a/N_0 \leq 13.98$
16QAM	$13.98 \leq E_a/N_0 \leq 17.46$
32QAM	$17.46 \leq E_a/N_0 \leq 20.87$
64QAM	$20.87 \leq E_a/N_0 \leq 23.57$
128QAM	$23.57 \leq E_a/N_0 \leq 26.83$
256QAM	$E_a/N_0 \geq 26.83$

transmissions are possible only if their aggregate interference does not exceed this critical threshold. Otherwise, the SU is not allowed to transmit. More details on interference cost generated by the SU at the primary base station will be given in the next section.

2.3.3.1 Generated Cost due to SU Transmission

Let I_n denote the cost at the n^{th} primary base station BS-P$_n$ generated due to the SU transmission. This cost can be expressed as follows

$$I_n = \frac{P_e \left|h_{sp_n}\right|^2}{L_{sp_n} S_{sp_n}}, \tag{2.4}$$

where P_e is the SU transmitted power. In the presence of several primary base stations, the overall cost function C will be the maximum of cost values at the different primary base stations as follows

$$C = max_n(I_n) = max_n \left(\frac{P_e \left|h_{sp_n}\right|^2}{L_{sp_n} S_{sp_n}} \right). \tag{2.5}$$

The cost function can also be written as

$$C = max_n \left(\frac{E_a R |h_{sp_n}|^2}{L_{sp_n} S_{sp_n}} \right), \tag{2.6}$$

where $R = 1/T_s$ denotes the symbol rate and E_a is the SU transmitted symbol energy.

2.3.3.2 Threshold Cost Expression: C_{max}

In theory, the authorized noise rise is defined as the ratio of maximum received wideband power to the noise power authorized at a BS-P

$$NR_{auth} = 10 \log_{10} \left(\frac{C_{max} + P_b}{P_b} \right), \tag{2.7}$$

where P_b is the noise equivalent power and C_{max} is the maximum cost tolerable at the primary base station. We consider that the NR_{auth} value is fixed at each BS-P and is known by the secondary user. Thus, we have

$$C_{max} = \left(10^{\left(\frac{NR_{auth}}{10} \right)} - 1 \right) N_0 R. \tag{2.8}$$

We assume for the rest of this work that the maximum cost tolerable at the primary receiver C_{max} is known at the secondary source.

2.3.4 Throughput Evaluation

2.3.4.1 Performance Metric

As a performance metric, we consider the normalized throughput which is defined as the total number of information bits per second per hertz received without error. For M transmitted packets, the normalized throughput is the ergodic average, expressed in ((bits/s)/Hz), as follows

$$Th = \sum_{m=1}^{M} \frac{L(1-P_{e,m})}{RT_m}, \tag{2.9}$$

where L is the packet length in bits and $P_{e,m}$ is the average probability of error for BPSK or QAM modulated symbols within the m^{th} packet. This symbol error probability can be obtained by simulations or derived as in [31] to accelerate the throughput calculation. Here, T_m is the cumulated transmission time needed to send the M packets. We notice that, during a packet transmission, even if the SU is not authorized to transmit, the T_m is incremented. Also, we consider here, a non-sporadic data flow system where M is chosen great enough to approach the analytical throughput value.

2.3.4.2 Simulation Results

As we adopt adaptive modulation, the calculated SNR is used by the secondary user to decide for the constellation size of the next transmitted frame. For our simulations, we use a path loss exponent of $\alpha = 4$ and a shadowing correlation coefficient between channels $\beta = 0.5$. A preliminary analysis of the system normalized throughput evolution at the secondary destination under certain conditions is given in Figure 2.2 and Figure 2.3, when one primary base station is considered in the network. Moreover, we assume that the SU is located at the line connecting the BS-S and the BS-P.

More precisely, Figure 2.2 illustrates the system throughput as a function of $(E_a/N_0)(d_0/d)^\alpha$ for several SU locations with respect to the two base stations BS-S and BS-P. We multiply (E_a/N_0) with $(d_0/d)^\alpha$ in order to normalize the SNR value. In this Figure, the authorized noise rise is fixed at 0.5dB. We notice that d is the distance between the source and the secondary destination and d_0 is a reference distance. We can clearly depict from these curves that the maximum throughput value is reached for certain optimal source energy E_a^{opt}. Moreover, the achievable throughput at the secondary destination decreases sharply at higher transmission energy values, since more and more the interference cost at the primary user increases and the SU will not be authorized to transmit beyond the threshold value. On the other hand, as it is expected

in Figure 2.2, the system throughput is better when the SU is near to the secondary destination and that the performance degrades as long as the SU gets closer increasingly to the primary base station.

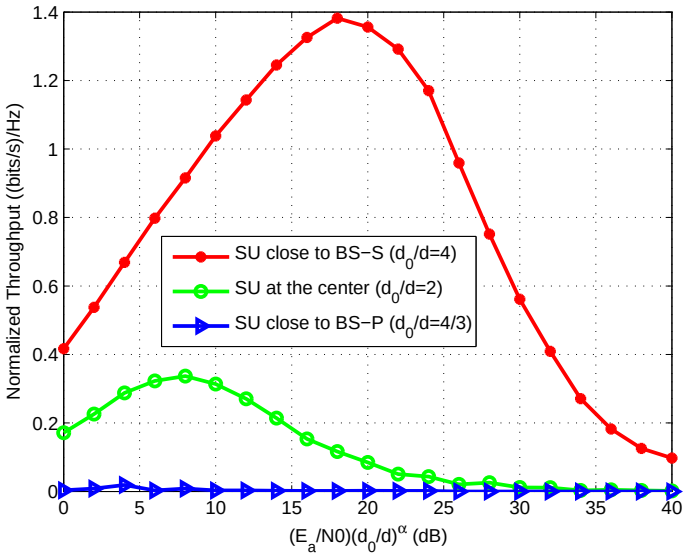

Figure 2.2: Throughput behavior as a function of $(E_a/N_0)(d_0/d)^{\alpha}$ for different SU positions.

Figure 2.3 shows the system throughput as a function of $(E_a/N_0)(d_0/d)^{\alpha}$, for different values of the authorized noise rise, namely, $NR_{auth} = 0.1$, 0.5 and 0.9dB so that a threshold cost of $C_{max} = 6.68$, 13.87 and 16.63dB respectively. We assume that the SU is located at the center of the line connecting the secondary and primary base stations. In addition, we notice from Figure 2.3 that the throughput at BS-S is strictly limited by the prescribed tolerable interference power at the primary receiver. In fact, a higher authorized NR_{auth} provides significant gain in terms of throughput, when compared to the cases of more stringent interference constraints. These results will be shown more in details in the remaining figures. Figure 2.4 depicts the impact of the SU position on the throughput of our adaptive cognitive network. In fact the top subplot shows the throughput behavior for several energy values when NR_{auth} is fixed to 0.5dB. We notice remarkable degradations in system performances when SU is close to the primary destination due to the rise of generated interference that avoid secondary user transmissions. In the low subplot, the throughput

evolution at the secondary user is illustrated for several values of allowed NR_{auth}, we choose $E_a/N_0 = 0$dB.

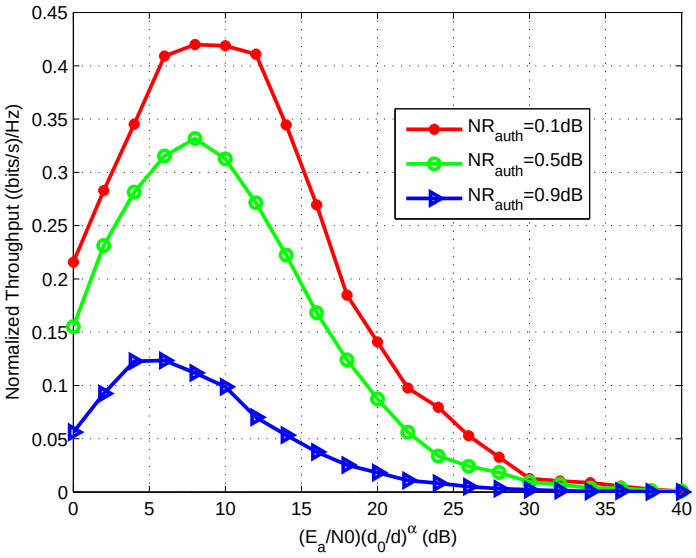

Figure 2.3: Throughput behavior as a function of $(E_a/N_0)(d_0/d)^{\alpha}$ for different NR_{auth} values.

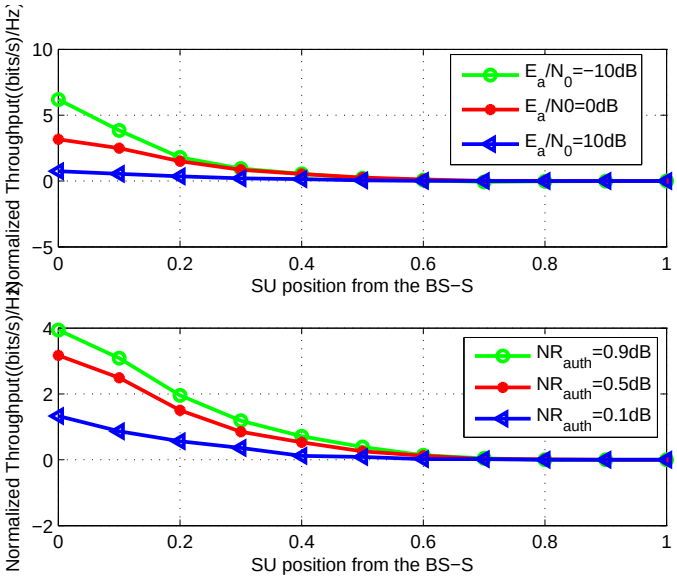

Figure 2.4: Throughput behavior as a function of SU position.

To carry out our simulations with more general view, we consider for the next simulations a rectangular pattern with a secondary destination located at the cell center. The SU position is varied along the cell area while keeping the BS-S and the BS-P locations unchanged. As we can see, Figure 2.5 and Figure 2.6 illustrate once again the previous performance analysis when the throughput becomes better at SU location close to the secondary destination and have progressively remarkable degradations when it moves away. It is clear from Figure 2.4 and Figure 2.5 that a better throughput is obtained using the transmission energy ($E_a/N_0 = -10$dB). However, a higher energy ($E_a/N_0 = 10$dB) deteriorates the achievable data rate (less than $0.8(bits/s)/Hz$) as an increase of generated cost avoid the SU transmissions. Figure 2.5 demonstrates one again that the resulting throughput of the cognitive network is strictly limited by the prescribed tolerable cost power imposed at the primary receiver, so that worse performances are denoted with the more stringent interference constraint ($NR_{auth} = 0.1$dB).

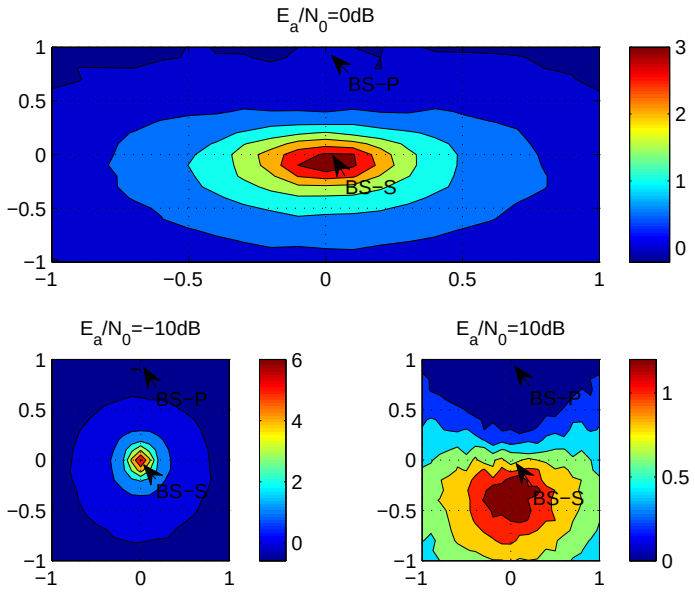

Figure 2.5: Cell area repartition of throughput system for several E_a/N_0 values ($NR_{auth} = 0.5dB$).

Next, since the transmit energy of SUs should be limited by the cost generated at the primary receiver, we

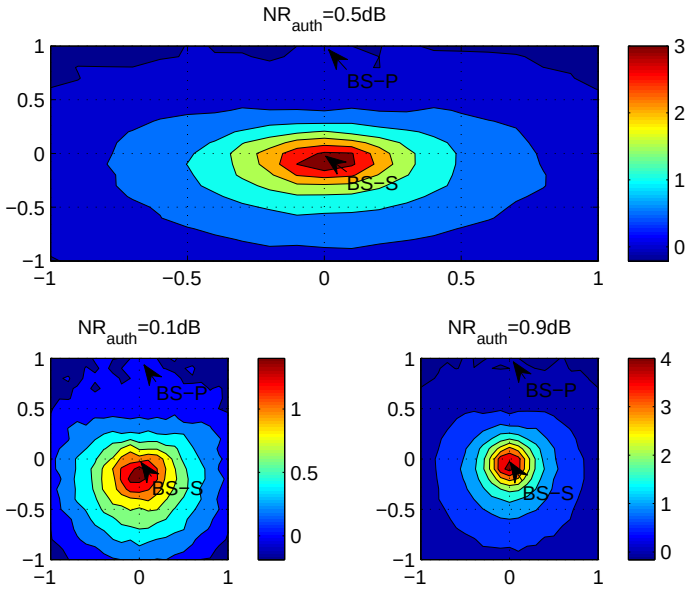

Figure 2.6: Cell area repartition of throughput system for several cost threshold values ($E_a/N_0 = 0dB$).

aim, according to the curves of Figure 2.2 and Figure 2.3, to find out for each SU position, the optimal transmission energy that provides maximum achievable throughput always with respecting that their interference onto PUs remains below the prescribed tolerable level. This is perfectly shown in Figure 2.7 which illustrates the optimal energy repartition over the cell area when the NR_{auth} is fixed to 0.5dB. We notice that when the SU is far away the BS-P and BS-S, higher transmitted energies are permitted and offer maximum throughput values, while low energies are recommended in the vicinity of the secondary and primary base stations. The resulting throughput is shown in Figure 2.8.

Finally, we would like to study the effect of detecting more than one primary base station in the network. Thus, the cost function becomes as defined in (2.6). Figure 2.9 shows the effect of the number of primary base stations, N, on our cognitive network performances, where the normalized throughput is plotted for N varying from 1 to 4. In particular, when $N = 2$, the second BS-P is located such that the BS-S is in the middle of these two BS-Ps. When $N = 4$, the 4 BS-Ps are located in the middle of the four edges. We depict

from Figure 2.9 that, with increasing the number of BS-Ps, the achievable data rate decreases significantly.

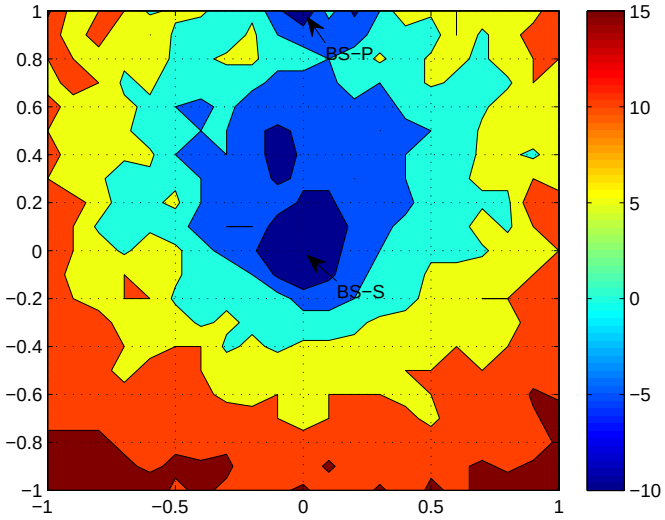

Figure 2.7: Cell area repartition of the optimum SU transmission energy ($NR_{auth} = 0.5dB$).

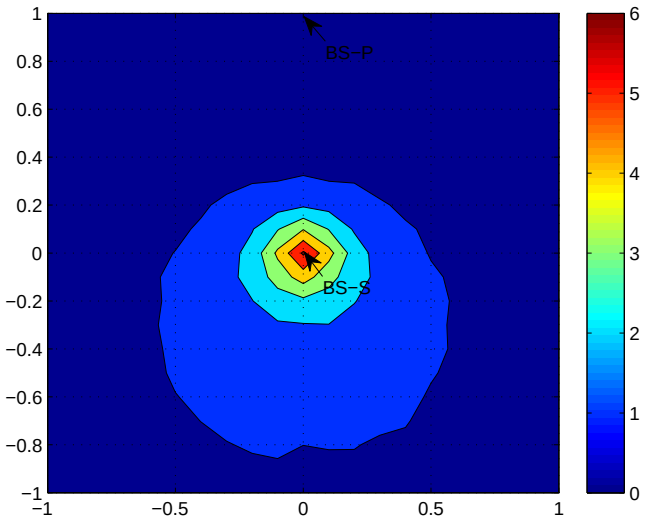

Figure 2.8: Cell area repartition of the optimized throughput ($NR_{auth} = 0.5dB$).

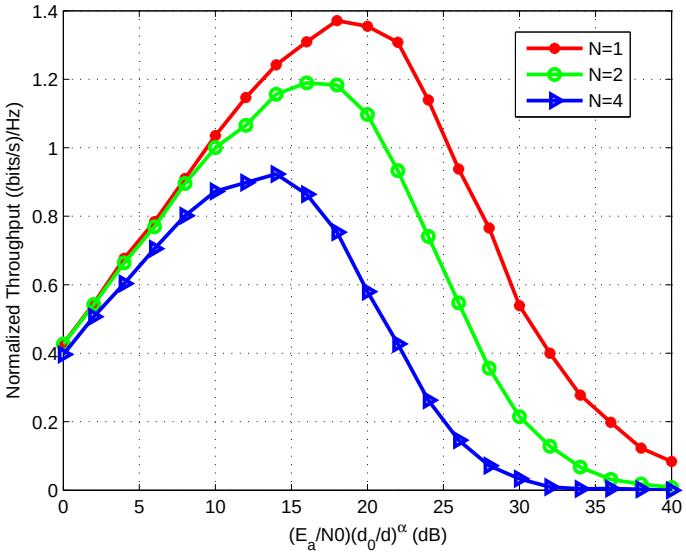

Figure 2.9: Throughput behavior as a function of $(E_a/N_0)(d_0/d)^{\alpha}$ for different number of BS-Ps.

2.4 Throughput Enhancement using Adaptive Modulation and Cooperative Techniques

The interference power constraints associated with underlay systems allow only short-range communication. Therefore, we propose to introduce cooperative techniques in order to enhance the secondary network performances.

2.4.1 Adaptive and Cooperative System Model

As shown in Figure 2.10, we consider N primary base stations denoted by BS-P$_n$ where $n = 1,..,N$ and a secondary radio network consisting of one terminal, one base station and one relay denoted respectively by SU, BS-S, and R. All links between terminals are assumed to be independent. Each link consists of Rayleigh, slow fading channel, so that we can consider its coefficients as constant during the transmission

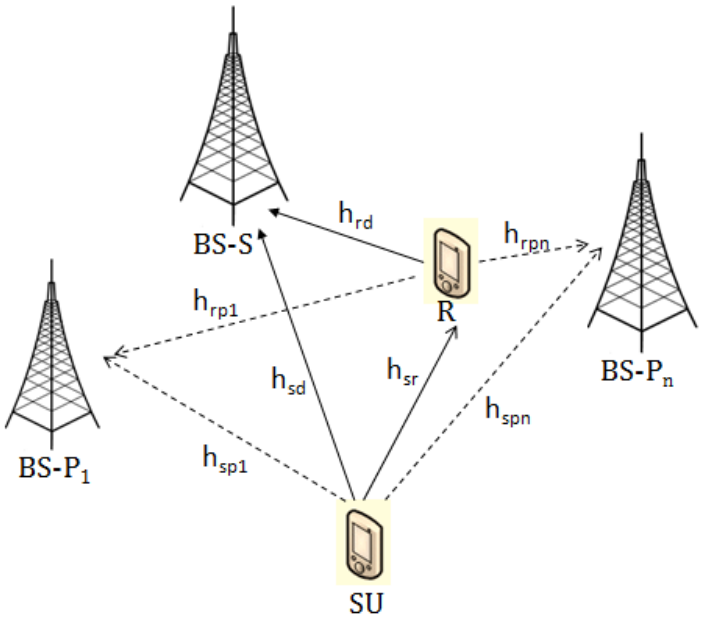

Figure 2.10: Cooperative Channel model.

of at least one frame. Furthermore, to investigate the effect of the path loss into the channel model, the coefficients L_{ij} corrupting respectively the channel link between node i and j, follow a propagation model of $1/d^{\alpha}$, where α denotes the path loss factor. The shadowing effect is also considered here. The presence of correlation between channels is taken into account where S_i follows a log-normal distribution with parameter σ. For our shadowing model, we assume that the shadowing effects near the different nodes are as follow

$$var(S_s) = var(S_{p_n}) = var(S_r) = (1-\beta)\sigma^2 \tag{2.10}$$

and

$$var(S_s) = \beta\sigma^2, \tag{2.11}$$

where β is the correlation factor. Typically, it can be chosen to be equal to 0.5.

In our contribution, if the interference cost generated by the SU still below the prescribed threshold at the primary network, the SU can transmit directly to the secondary destination. Otherwise, the SU tries to have recourse to cooperative techniques in order to transmit with lower energy as well as to maximize its own coverage and performance. Both non-regenerative (AF) and cooperative space-time coding protocols based on Alamouti ST code will be studied.

2.4.1.1 Cooperation Based on AF Protocol

In the first phase of cooperation, the SU sends a signal to the relay and the BS-S. For a given symbol a transmitted from the source, the signals received at the relay and at the destination are respectively

$$y_{sr} = \frac{\sqrt{E}h_{sr}}{\sqrt{L_{sr}S_{sr}}}a + b_{sr} \tag{2.12}$$

and

$$y_{sd} = \frac{\sqrt{E}h_{sd}}{\sqrt{L_{sd}S_{sd}}}a + b_{sd}, \tag{2.13}$$

where h_{sr} and h_{sd} are the propagation channel attenuations between SU-R and SU-(BS-S) and b_{sd} and b_{sr} are additive white Gaussian noise (AWGN) corrupting respectively the link between SU-R and SU-(BS-S) with a variance N_0 . To provide a fair comparison platform, we will consider the same total energy consumed in both cooperative and non-cooperative networks. Then, $E = E_a/2$ is the transmitted symbol energy for each of the source and the relay, where E_a is the symbol energy of the source in the direct transmission. In the second phase of the cooperation, the relay amplifies the received signal from the source with a factor γ before forwarding it to the destination. This factor is given by

$$\gamma = \frac{1}{\sqrt{\frac{|h_{sr}|^2}{L_{sr}S_{sr}} + \frac{N_0}{E}}}. \tag{2.14}$$

The received signal in the indirect branch is given by

$$y_{rd} = \gamma \frac{h_{rd}}{\sqrt{L_{rd}S_{rd}}} y_{sr} + b_{rd}, \tag{2.15}$$

where h_{rd} is the propagation channel attenuation between R-(BS-S) and b_{rd} is the additive white Gaussian noise of the R-(BS-S). As we adopt an adaptive modulation, the calculated SNR is used by the secondary user to decide for the constellation size of the next transmitted frame. Next, the secondary destination combines the two received signals using a Maximum Ratio Combining (MRC) [22]. We show that the total SNR expression can be written as

$$SNR_T = \frac{E}{N_0} \left(\frac{|h_{sd}|^2}{L_{sd}S_{sd}} + \frac{\gamma^2 \frac{|h_{sr}|^2}{L_{sr}S_{sr}} \frac{|h_{rd}|^2}{L_{rd}S_{rd}}}{1 + \gamma^2 \frac{|h_{rd}|^2}{L_{rd}S_{rd}}} \right). \tag{2.16}$$

2.4.1.2 Cooperation Based on Alamouti ST Code

In this section, we use an adaptive AF protocol based on the Alamouti space-time code [22] [57]. This protocol requires 4 channels used to send 2 symbols. As schematized in Table 2.2, in the first cooperative phase, the secondary source sends successively the first line of the code matrix: a_1 and $-a_2^*$. In the second phase, the relay sends an amplified version of the received signal, and the SU sends the second line of the code matrix: a_2 and a_1^*. During these two phases, we assume an energy transmitted by each of SU and R common to all symbols and equal to $E' = E_a/3$.

Table 2.2: Alamouti AF protocol.

Instant	t_1	t_2	t_3	t_4
SU	a_1	$-a_2^*$	a_2	a_1^*
R	y_{r1}	y_{r2}	γy_{r1}	γy_{r2}
BS-S	y_1	y_2	y_3	y_4

For two successive symbols a_1 and a_2 transmitted by SU, the signals received by the BS-S during the second phase are expressed as follows

$$\mathbf{z} = \mathbf{H}\mathbf{a} + \mathbf{n}, \tag{2.17}$$

where

$$\mathbf{z} = \begin{bmatrix} y_1 \\ y_2 \end{bmatrix}, \mathbf{a} = \begin{bmatrix} a_1 \\ a_2 \end{bmatrix}, \tag{2.18}$$

$$\mathbf{H} = \begin{bmatrix} \gamma\sqrt{E'}\frac{h_{sr}}{\sqrt{L_{sr}S_{sr}}}\frac{h_{rd}}{\sqrt{L_{rd}S_{rd}}} & \sqrt{E'}\frac{h_{sd}}{\sqrt{L_{sd}S_{sd}}} \\ \sqrt{E'}\frac{h_{sd}^*}{\sqrt{L_{sd}S_{sd}}} & -\gamma\sqrt{E'}\frac{h_{sr}^*}{\sqrt{L_{sr}S_{sr}}}\frac{h_{sd}^*}{\sqrt{L_{sd}S_{sd}}} \end{bmatrix} \tag{2.19}$$

and $\mathbf{n}$ is a noise vector. At the output of the MRC combiner, the final total SNR expression for Alamouti cooperative protocol can be written as follows

$$SNR_T = \frac{E'\left(2\frac{|h_{sd}|^2}{\sqrt{L_{sd}S_{sd}}} + \gamma^2\frac{|h_{rd}|^2}{\sqrt{L_{rd}S_{rd}}}\left(\frac{|h_{sr}|^2}{\sqrt{L_{sr}S_{sr}}} + \frac{|h_{sd}|^2}{\sqrt{L_{sd}S_{sd}}}\right)\right)}{\left(1+\gamma^2\frac{|h_{rd}|^2}{\sqrt{L_{rd}S_{rd}}}\right)N_0}. \tag{2.20}$$

2.4.2 Generated Cost due to Secondary Network Transmission

Without loss of generality, we assume here the presence of one primary base station.

2.4.2.1 Cost Expression in Non-Cooperative Case

The expression of the overall cost function C in non-cooperative case as well as the considered threshold C_{max} are given in the subsection (2.3.3). In fact, in the presence of one primary base station, we have

$$C = \frac{E_a R |h_{sp}|^2}{L_{sp} S_{sp}}. \tag{2.21}$$

2.4.2.2 Cost Expression when using AF Protocol

Since cooperation is conducted in two phases, the cost at the primary base station BS-P generated after SU and R transmissions can be written respectively as follows

$$C_1 = \frac{ER |h_{sp}|^2}{L_{sp} S_{sp}} \tag{2.22}$$

and

$$C_2 = \frac{ER |h_{rp}|^2}{L_{rp} S_{rp}}. \tag{2.23}$$

Hence, the overall cost function generated after the cooperative transmission will be the maximum cost of the two phases such as

$$C_{AF} = max(C_1, C_2). \tag{2.24}$$

2.4.2.3 Cost Expression when using Alamouti AF Protocol

For the cooperation based on Alamouti ST code, at the first and second time slots, only the secondary user is transmitting, so we have

$$C_1' = \frac{E'R|h_{sp}|^2}{L_{sp}S_{sp}}. \tag{2.25}$$

As for the third and fourth time slots, both SU and R are transmitting to the secondary destination. Thus, the cost function at the primary destination will be the sum of these two transmissions' costs

$$C_2' = \frac{E'R|h_{sp}|^2}{L_{sp}S_{sp}} + \frac{E'R|h_{rp}|^2}{L_{rp}S_{rp}}. \tag{2.26}$$

Finally, the overall cost function will be as follows

$$C_{Alamouti} = max\left(C_1', C_2'\right) = \frac{E'R|h_{sp}|^2}{L_{sp}S_{sp}} + \frac{E'R|h_{rp}|^2}{L_{rp}S_{rp}}. \tag{2.27}$$

2.4.3 Throughput Evaluation of the Proposed System

For our simulations, we use a path loss exponent of $\alpha = 4$ and a shadowing correlation coefficient between channels $\beta = 0.5$. We assume that the maximum cost tolerable at the primary receiver C_{max} is known at the secondary source and fixed at $0.5dB$. We note that the system throughput behavior as a function of C_{max} in non-cooperative case is studied in a previous work [58].

A preliminary analysis of the system normalized throughput evolution at the secondary destination under certain conditions is given in Figure 2.11 and Figure 2.12, when one primary base station is considered in the network. Moreover, we assume that the SU is located at the line connecting the BS-S and the BS-P. More precisely, Figure 2.11 illustrates the system throughput as a function of $(E_a/N_0)(d_0/d)^{\alpha}$ for several relay locations with respect to the two base stations BS-S and BS-P. Figure 2.12 shows the system throughput as a function of $(E_a/N_0)(d_0/d)^{\alpha}$, for both proposed schemes. We assume that the relay is located at the center of the line connecting the SU and the BS-S.

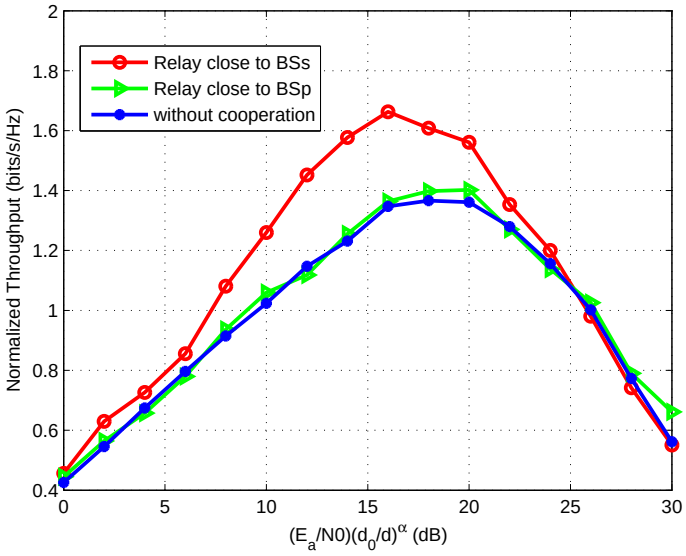

Figure 2.11: Throughput behavior as a function of $(E_a/N_0)(d_0/d)^{\alpha}$ for different Relay positions.

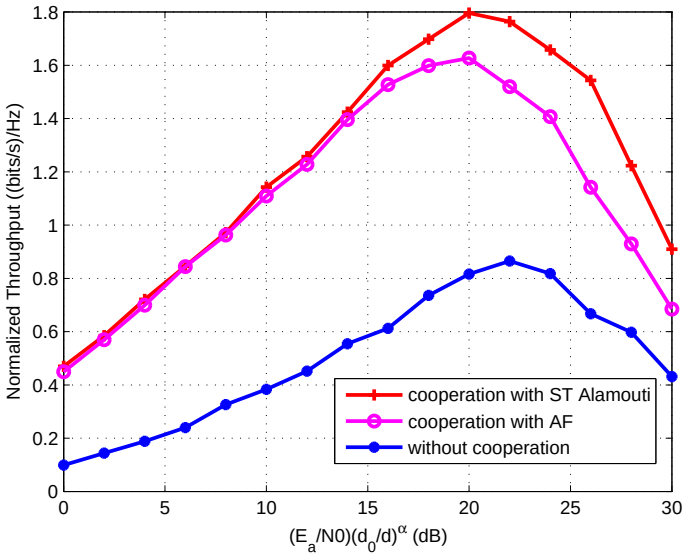

Figure 2.12: Throughput behavior as a function of $(E_a/N_0)(d_0/d)^{\alpha}$ for different schemes.

We can clearly depict from these curves that the maximum throughput value is reached for certain optimal

source energy. Moreover, the achievable throughput at the secondary destination decreases sharply at higher transmission energy values, since more and more the interference cost at the primary user increases and the SU will not be authorized to transmit beyond the threshold value. It is clear from Figure 2.11 that using cooperation when the SU is not authorized to transmit with that energy through the direct link is more advantageous especially when the chosen relay isn't far from the BS-S. In addition, we notice from Figure 2.12 that using AF relaying based on ST Alamouti scheme can improve the achievable data rate mainly at higher SU 'transmission energies.

To carry out our simulations with more general view, we consider in Figure 2.13 and Figure 2.14 a rectangular pattern with a secondary destination located at the cell center. Let the SU be at the center of the line connecting the secondary and primary base stations. The Relay position is varied along the cell area while keeping the BS-S, the SU and the BS-P locations unchanged. Figure 2.13 and Figure 2.14 illustrate once again the previous performance analysis when the throughput becomes better at relay location close to the secondary destination and have progressively remarkable degradations when it moves away and that worst throughput is obtained when the chosen relay is more and more close to the primary base station.

Finally, we would like to study the effect of detecting more than one primary base station in the network. So, we consider the general cost function as in (2.6). Figure 2.15 shows the effect of the number of primary base stations on our system performance, where the normalized throughput versus $(E_a/N_0)(d_0/d)^{\alpha}$ is plotted with several values of N. In particular, when $N = 2$, the second BS-P is located such that the BS-S is in the middle of these two BS-Ps. When $N = 3$, the three BS-Ps are located in the middle of the area edges. In such cases, it is observed from Figure 2.15 that, with increasing the number of BS-Ps, the achievable data rate decreases significantly and demonstrate once again the effectiveness of our proposed schemes to improve the throughput at the secondary destination.

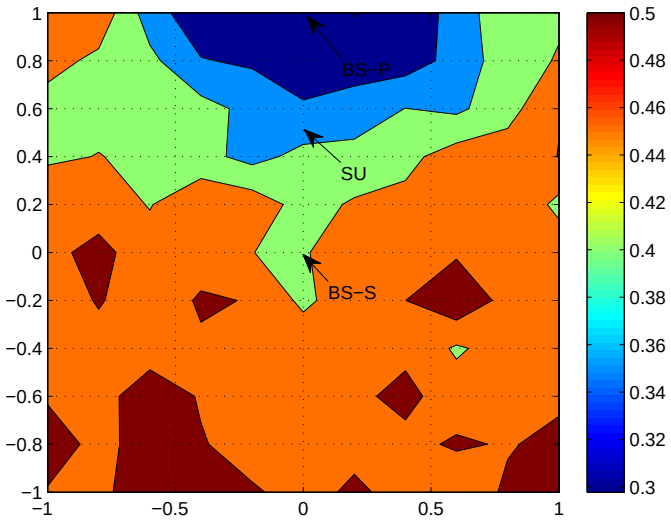

Figure 2.13: Throughput behavior as a function of relay location when $E_a/N_0 = -8dB$.

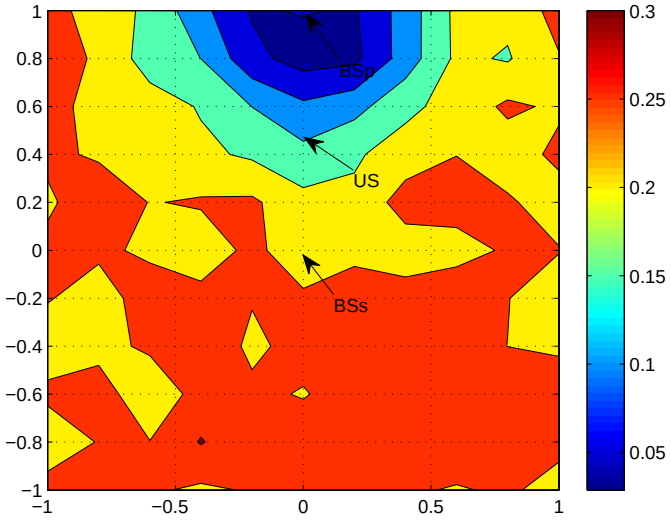

Figure 2.14: Throughput behavior as a function of relay location when $E_a/N_0 = -15dB$.

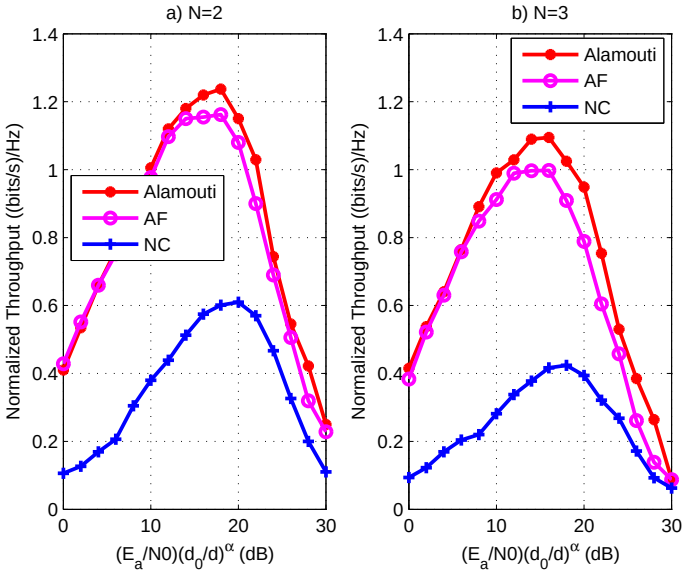

Figure 2.15: Throughput behavior as a function of a function of $(E_a/N_0)(d_0/d)^{\alpha}$ for different numbers of BS-P.

2.5 Conclusion

This chapter studied an adaptive cognitive strategy where the secondary user can share the spectrum concurrently with the primary user on condition that its generated cost remains below a certain threshold. Furthermore, an adaptive cognitive strategy based on cooperation technique is proposed, when the secondary user is not allowed to transmit through the direct link. Two cooperative techniques are considered that are conventional and Alamouti Amplify and forward approaches. Simulation results show that the system throughput is proportional to several parameters such as the maximum allowed cost at the primary network, the secondary user location, the relay user location, their transmission energies and the number of detected primary base stations. Also, it's depicted that both adaptive schemes based on relaying show a significant performance improvement in terms of throughput compared to non-cooperative adaptive scenario. Moreover, in our context, using the space-time blocks coding when cooperating outperforms the classical AF protocol.

Chapter 3

Optimal Energy Allocation in Adaptive Cooperative Cognitive Network

3.1 Introduction

In the previous chapter, energy resources are equally distributed over all nodes. We aim to improve the unlicensed system throughput under power and interference constraints. For this aim, we proposed to use a cooperative relay to assist the secondary transmission. Moreover, the adaptive modulation is used in order to compensate the throughput loss due to the relaying.

Fist of all, we propose a new energy allocation scheme for both source and relay nodes to maximize the instantaneous received SNR without disturbing the primary transmissions. We compare the performance of our proposed energy allocation method combined with adaptive modulation with the classical cooperation scheme where energy resources are equally distributed over all nodes.

Then, we propose to combine a selection scheme, where only one "best" relay is chosen, with an energy allocation scheme for source and relay nodes to maximize the instantaneous received SNR under the system

constraints. The performance of such selective AF system based on Alamouti ST code with optimized energy allocation is also studied and compared with those with uniform energy allocation.

To explain our approaches in more details, this chapter is organized as follows: we start by giving the system model of our considered adaptive cognitive cooperative network based on AF protocol. Then, we detail the formulation of our proposed energy allocation problem and provide some simulation results for the proposed system performance in terms of throughput and outage probability. After that, we propose an adaptive cooperative model based on Alamouti AF protocol and combined with a best relay selection, followed by the correspondent formulation of our proposed energy allocation problem. Finally, we provide some simulation results for this proposed system performance in terms of throughput.

3.2 Energy Allocation Optimization for Cooperative Cognitive Network: Case of Amplify and Forward Technique

3.2.1 Proposed AF System Model

Here, we consider the same cooperative system model described in subsection (2.3.1), except that we don't adopt a fixed energy allocation scheme in both relay and source nodes. Here, E_s and E_r denote the transmitted symbol energies for the SU and R, respectively. During the the first phase of the AF protocol, and for a given symbol a, the signals received at the relay and at the BS-S are respectively

$$y_{sr} = \frac{\sqrt{E_s}h_{sr}}{\sqrt{L_{sr}S_{sr}}}a + b_{sr} \tag{3.1}$$

and

$$y_{sd} = \frac{\sqrt{E_s}h_{sd}}{\sqrt{L_{sd}S_{sd}}}a + b_{sd}. \tag{3.2}$$

We recall that h_{sr} and h_{sd} are the propagation channel attenuations between SU-R and SU-(BS-S) and b_{sd} and b_{sr} are additive white Gaussian noise (AWGN) corrupting respectively the link between SU-R and SU-(BS-S) with a variance N_0 . In the second phase of the cooperation, the relay amplifies the received signal from the source with a factor γ before forwarding it to the destination. Therefore, the received signal in the indirect branch is given by

$$y_{rd} = \gamma \frac{h_{rd}}{\sqrt{L_{rd} S_{rd}}} y_{sr} + b_{rd}, \tag{3.3}$$

where h_{rd} is the propagation channel attenuation between R-(BS-S), b_{sd} is the additive white Gaussian noise of the R-(BS-S) link and the amplification factor is $\gamma = \sqrt{\frac{E_r}{\frac{|h_{sr}|^2}{L_{sr} S_{sr}} E_s + N_0}}$.

We easily show that the total received SNR expression can be written as

$$SNR = \frac{E_s}{N_0} \left(\frac{|h_{sd}|^2}{L_{sd} S_{sd}} + \frac{E_r \frac{|h_{sr}|^2}{L_{sr} S_{sr}} \frac{|h_{rd}|^2}{L_{rd} S_{rd}}}{E_s \frac{|h_{sr}|^2}{L_{sr} S_{sr}} + E_r \frac{|h_{rd}|^2}{L_{rd} S_{rd}} + N_0} \right). \tag{3.4}$$

To provide a fair comparison platform, we will consider the same total energy consumed in both cooperative and non-cooperative schemes. Then, $E_a = E_s + E_r$ where E_a is the available symbol energy of the source in the direct transmission.

3.2.2 Generated Cost due to Secondary Network Transmission

In fact, in the presence of several primary base stations, the overall cost function C_{AF} will be the maximum of cost values at the different primary base stations. For simplicity sake, we assume here the presence of one BS-P. Since cooperation is conducted in two phases, the cost at the BS-P generated after SU and R transmissions can be written respectively as follows

$$C_s = \frac{E_s R |h_{sp}|^2}{L_{sp} S_{sp}}, \tag{3.5}$$

and

$$C_r = \frac{E_r R |h_{rp}|^2}{L_{rp} S_{rp}}. \tag{3.6}$$

where $R = 1/T_s$ denotes the symbol rate and S_{sp} and S_{rp} are the shadowing, seen on the SU-(BS-P) and R-(BS-P) links respectively. Finally, the overall cost function generated after the secondary cooperative transmission will be the maximum cost of the two phases such as

$$C_{AF} = max\left(C_s, C_r\right). \tag{3.7}$$

3.2.3 Source and Relay Energy Optimization

In this section, we derive our adopted optimization approach. In fact, the optimization aims at finding out the appropriate energy repartition of both source and relay nodes in order to enhance the cognitive system performance. However, the interference cost generated at the BS-P must be kept below a prescribed threshold. Besides, the SU and R adapt their energies while keeping a fixed total available energy E_a. Therefore, our optimization problem can be formulated as follows

$$\begin{array}{c} \text{maximize} \quad SNR \\ \text{subject to} \quad E_s + E_r = E_a \\ C_s \leq C_{max} \\ \text{and} \quad C_r \leq C_{max} \end{array}. \tag{3.8}$$

That can be written with refer to (3.5) and (3.6) as

$$\begin{array}{c} \text{maximize} \quad SNR \\ \text{subject to} \quad E_s + E_r = E_a \\ E_s \leq E_{smax} \\ \text{and} \quad E_r \leq E_{rmax} \end{array}, \tag{3.9}$$

where

$$E_{smax} = \frac{C_{max} L_{sp} S_{sp}}{R |h_{sp}|^2} \tag{3.10}$$

and

$$E_{rmax} = \frac{C_{max} L_{rp} S_{rp}}{R |h_{rp}|^2}. \tag{3.11}$$

To solve our optimization problem, we propose both geometrical and analytical approaches. For the optimization, we propose to use graphical (or geometrical) method that presents an attractive way for solving nonlinear problems involving two parameters with a minimum amount of computational effort [59]. First, we have to trace the graph in two dimensions of the problem constraints as it is shown in Figure 3.1 and Figure 3.2, where the SU and the R energies are presented on the x-axis and the y-axis respectively. Because of the non-negativity energies restrictions, the feasible region is restricted to the positive quadrant. The candidate solutions are the intersection area on the valid side of each constraint line that is drawn in Figure 3.1 and Figure 3.2 as continuous lines. In fact, the point of the segment which yields the maximum value of the objective function will be the optimal solution to our problem. This is equivalent to annul the derivative function of SNR with respect to E_s as follows

$$\frac{\partial}{\partial E_s} \left\{ \frac{E_s}{N_0} \left(\frac{|h_{sd}|^2}{L_{sd} S_{sd}} + \frac{(E_a - E_s) \frac{|h_{sr}|^2}{L_{sr} S_{sr}} \frac{|h_{rd}|^2}{L_{rd} S_{rd}}}{E_s \frac{|h_{sr}|^2}{L_{sr} S_{sr}} + (E_a - E_s) \frac{|h_{rd}|^2}{L_{rd} S_{rd}} + N_0} \right) \right\} = 0. \tag{3.12}$$

Developing this expression yields to solve the following quadratic equation

$$A E_s^2 + B E_s - C = 0, \tag{3.13}$$

where

$$A = \frac{|h_{sr}|^2}{L_{sr}S_{sr}} - \frac{|h_{rd}|^2}{L_{rd}S_{rd}}, \tag{3.14}$$

$$B = 2(\frac{|h_{rd}|^2 E_a}{L_{rd}S_{rd}} + N_0) \tag{3.15}$$

and

$$C = \frac{|h_{sd}|^2}{L_{sd}S_{sd}} \frac{L_{sr}S_{sr}}{|h_{sr}|^2} \frac{L_{rd}S_{rd}}{|h_{rd}|^2} + E_a(\frac{|h_{rd}|^2}{L_{rd}S_{rd}} E_a + N_0). \tag{3.16}$$

In the case of positive discriminant $B^2 - 4AC \geq 0$, we denote by $E_s^{'}$ the potential solution of (3.13) that yields a maximum value of SNR. Since E_{smax} and E_{rmax} values depend on a randomly varying environment, we have to study the following two cases illustrated in Figure 3.1 and Figure 3.2 respectively.

1. $E_{smax} \leq E_{rmax}$

In such condition, we can obtain four different cases depending on E_a value as presented in Figure 3.1 by 1.(a), 1.(b), 1.(c) and 1.(d).

- 1.(a): $E_a \leq E_{smax}$

If $E_s^{'}$ exists and $E_s^{'} \in [0, E_a]$, then the optimal solution is $(E_s^{'}, E_a - E_s^{'})$. Otherwise, the optimal solution will be at the segment boundary $(E_a, 0)$ which means that the SU uses the whole available energy to transmit.

- 1.(b): $E_{smax} \leq E_a \leq E_{rmax}$

If $E_s^{'}$ exists and $E_s^{'} \in [0, E_{smax}]$, then the optimal solution is $(E_s^{'}, E_a - E_s^{'})$. Otherwise, it is the point at the segment boundary $(E_{smax}, E_a - E_{smax})$.

- 1.(c): $E_{rmax} \leq E_a \leq (E_{smax} + E_{rmax})$

If $E_s^{'}$ exists and $E_s^{'} \in [E_a - E_{rmax}, E_{smax}]$, then the optimal solution is $(E_s^{'}, E_a - E_s^{'})$. Otherwise, the optimal solution will be one of the segment boundary namely $(E_{smax}, E_a - E_{smax})$ or $(E_a - E_{rmax}, E_{rmax})$ which yields the maximum SNR value.

- 1.(d): $E_a \geq (E_{smax} + E_{rmax})$

For this case, and as shown in Figure 3.1, no solution is possible. So, the secondary transmission is not allowed.

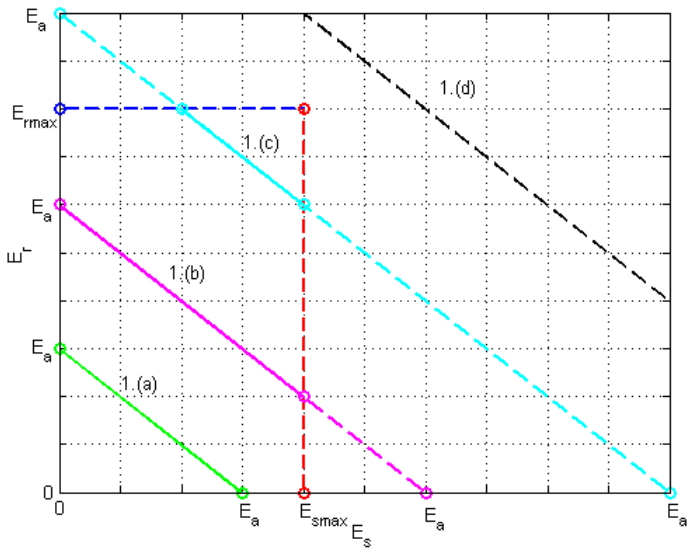

Figure 3.1: Different cases illustration where $E_{smax} \leq E_{rmax}$

2. $E_{rmax} \leq E_{smax}$

In such condition, we have also four cases presented in Figure 3.2 by 2.(a), 2.(b), 2.(c) and 2.(d).

- 2.(a): $E_a \leq E_{rmax}$

If $E_s^{'}$ exists and $E_s^{'} \in [0, E_a]$, then the optimal solution is $(E_s^{'}, E_a - E_s^{'})$. Otherwise, it is $(E_a, 0)$.

- 2.(b): $E_{rmax} \leq E_a \leq E_{smax}$

If $E_s^{'}$ exists and $E_s^{'} \in [Ea - E_{rmax}, E_a]$, then the optimal solution is $(E_s^{'}, E_a - E_s^{'})$. Otherwise, the optimal solution will be one of the segment boundary namely $(E_a, 0)$ or $(E_a - E_{rmax}, E_{rmax})$ which yields the maximum SNR value.

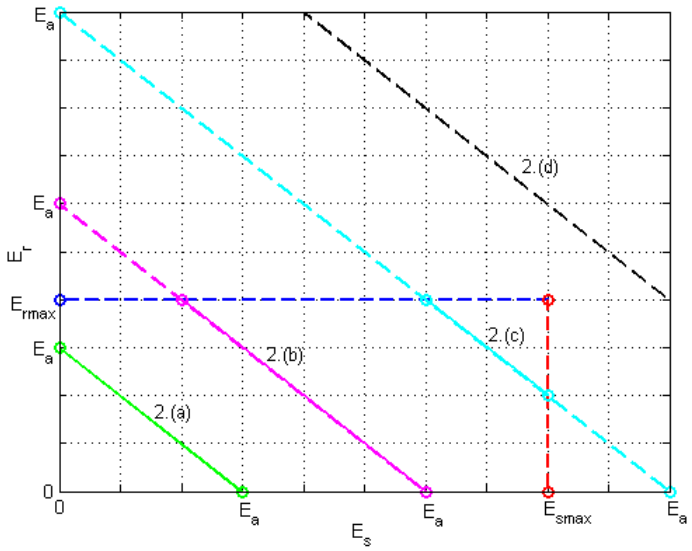

Figure 3.2: Different cases illustration where $E_{rmax} \leq E_{smax}$

- 2.(c): $E_{smax} \leq E_a \leq (E_{smax} + E_{rmax})$

If $E_s^{'}$ exists and $E_s^{'} \in [Ea - E_{rmax}, E_{smax}]$, then the optimal solution is $(E_s^{'}, E_a - E_s^{'})$. Otherwise, the optimal solution will be one of the segment boundary namely $(E_{smax}, E_a - E_{smax})$ or $(E_a - E_{rmax}, E_{rmax})$ which yields the maximum SNR value.

- 2.(d): $E_a \geq (E_{smax} + E_{rmax})$

As shown in Figure 3.2, no solution is possible for this case. So, the secondary transmission is not allowed.

3.2.4 Performances Study of the AF System

We recall that the adaptive modulation technique is used here. The outage probability is defined as the probability that the instantaneous received SNR falls below a certain threshold γ_{th}. A preliminary analysis of the system normalized throughput and outage probability evolution at the BS-S are given in Figure 3.3 and Figure 3.4 respectively, when one BS-P is considered in the network.

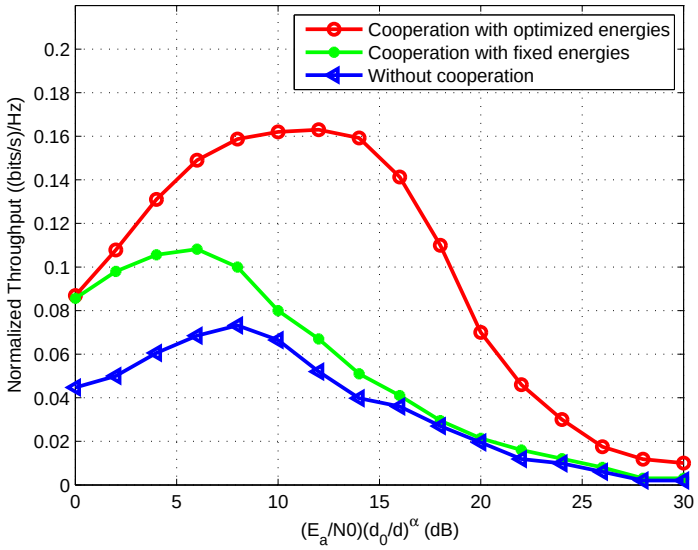

Figure 3.3: Throughput behavior as a function of $(E_a/N_0)(d_0/d)^{\alpha}$ for different schemes when $C_{max} = 0.5dB$.

We assume that $\gamma_{th} = 1$. For the fixed energy allocation scheme, we will consider the same transmitted energy in both relay and source nodes that is equal to $E_a/2$. Moreover, we assume that the SU is located at the center of the line connecting the secondary and primary base stations. We clearly depict from these curves that our proposed scheme outperforms the other schemes, and that our optimization strategy improves significantly the cognitive transmissions. Moreover, we notice that the performance gain at the BS-S decreases sharply at higher transmission energy values, since more and more the interference generated at the BS-P increases and the SU will not be authorized to transmit.

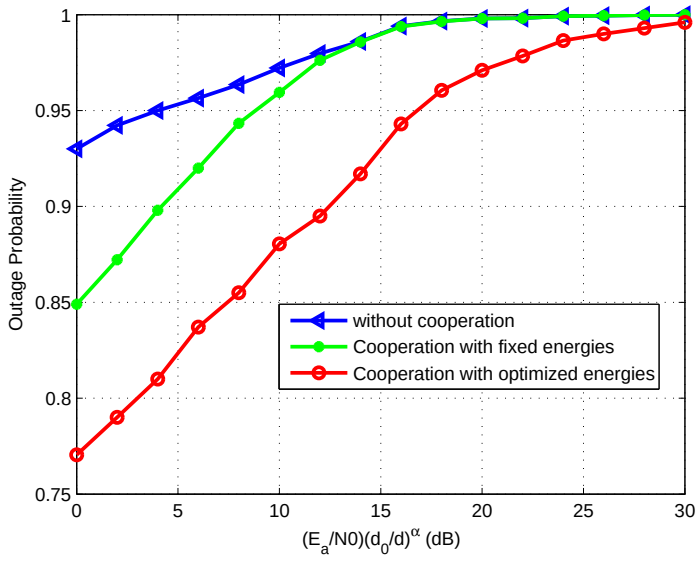

Figure 3.4: Outage probability behavior as a function of $(E_a/N_0)(d_0/d)^{\alpha}$ for different schemes when $C_{max} = 0.5dB$.

Next, we study the impact of the considered cost threshold on the throughput of our proposed optimized scheme. Figure 3.5 plots the system normalized throughput as a function of $(E_a/N_0)(d_0/d)^{\alpha}$ for different values of C_{max}. In fact, it is logical that a higher authorized C_{max} provides significant gain in terms of throughput when compared to the cases of more stringent interference constraints. For the rest of simulations, we assume that C_{max} is fixed at $0.5dB$. To study our proposed scheme with more general view, we consider a rectangular pattern where the BS-S is located at the cell center. The Relay position is varied along the cell area while keeping the BS-S, the SU and the BS-P locations unchanged. To study the impact of some parameters such as the SU position and the total available energy E_a on the system performance, we present in Figure 3.6 and Figure 3.7 the throughput and the outage probability behavior as a function of the relay location for several SU positions, respectively. In fact, Figure 3.6 and Figure 3.7 indicate for each SU position, the most prosperous relay location that maximize the acheivable system throughput and and minimize the outage probability, respectively.

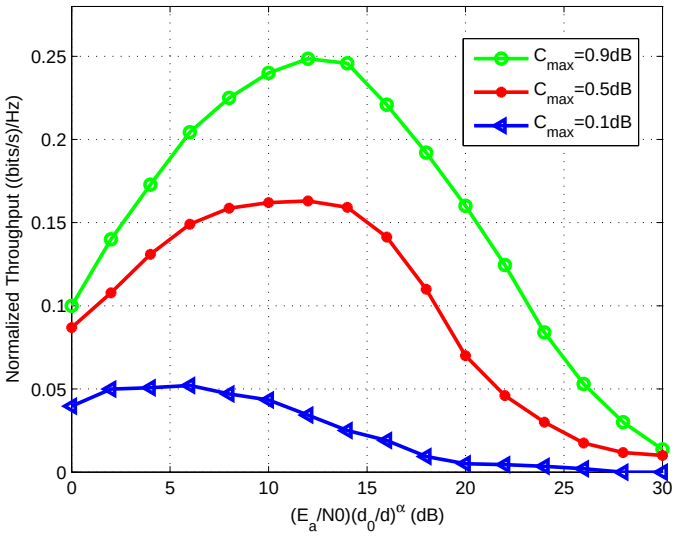

Figure 3.5: Throughput behavior of the proposed scheme as a function of $(E_a/N_0)(d_0/d)^{\alpha}$ for different C_{max} values.

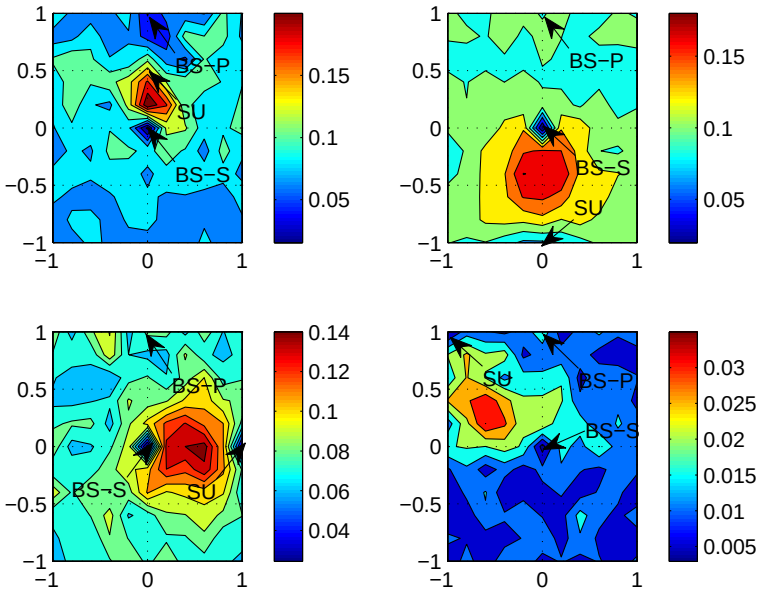

Figure 3.6: Throughput behavior as function of relay location for several SU positions when $E_a/N_0 = 1dB$.

It is expected that worst performance is seen when SU becomes near to BS-P and distant from BS-S. We also notice that the system performance becomes better at relay location between the secondary source and destination and has progressively remarkable degradations when it moves away. To illustrate the cell area repartition of the optimized relay energy for different SU positions, Figure 3.8 is plotted. As we can see, when the relay is close to BS-P, its attributed energy so that the cooperation contribution will be very low due to its generated interference. However, more SU is located in the vicinity of primary network area, more the attributed energy to the relay is important in order to help secondary transmission. Finally, we study, in Figure 3.9, the throughput behavior as a function of $(E_a/N_0)(d_0/d)^{\alpha}$ for several number of BS-Ps, N. It is observed that, with increasing N, the achievable data rate decreases significantly.

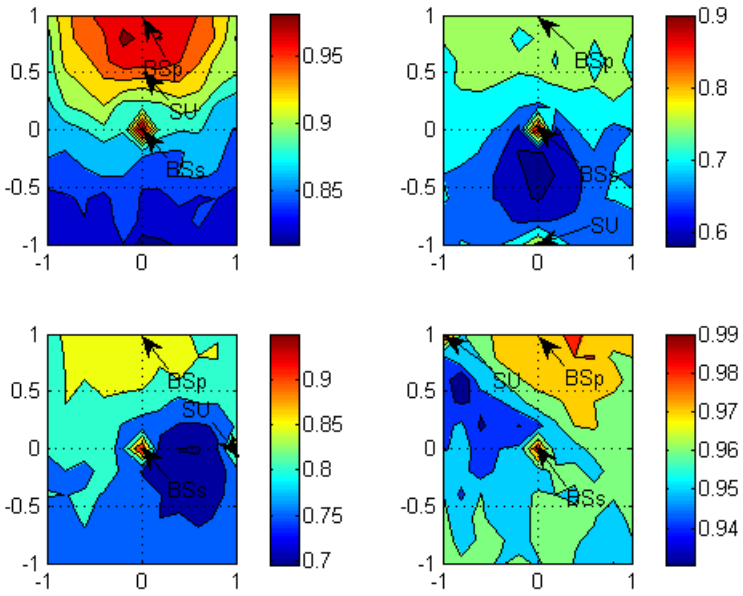

Figure 3.7: Outage probability behavior as a function of relay location for several SU positions when $E_a/N_0 = 1dB$.

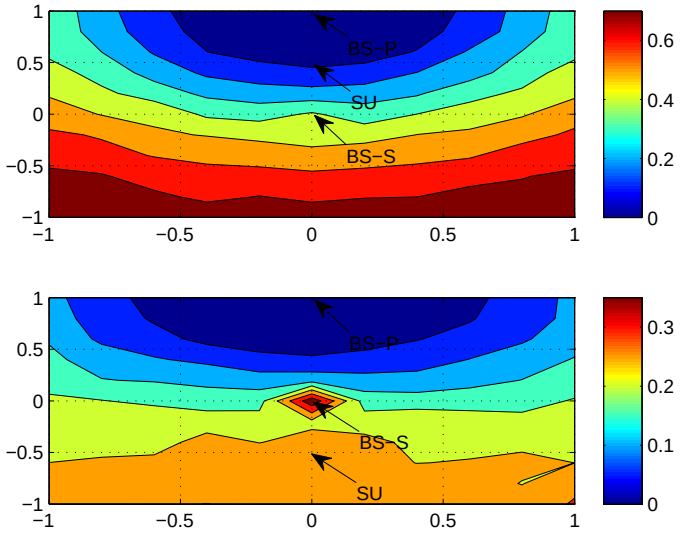

Figure 3.8: Cell area repartition of the optimized relay energy for several SU positions when $E_a/N_0 = 1dB$.

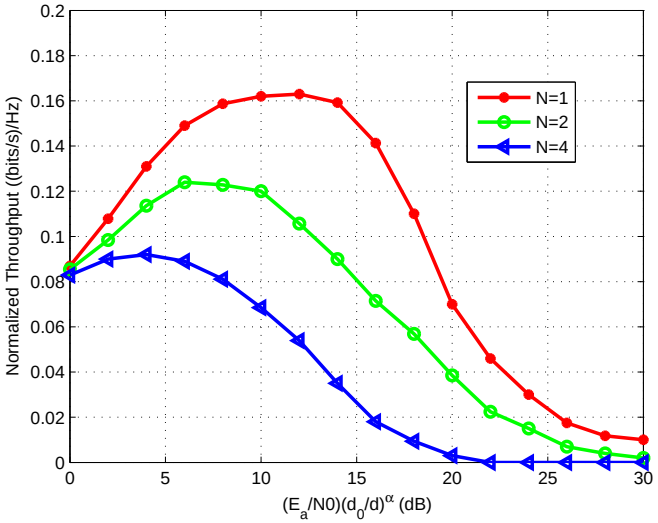

Figure 3.9: Throughput behavior as a function of $(E_a/N_0)(d_0/d)^{\alpha}$ for different numbers of BS-P.

3.3 Energy Allocation Optimization for Cooperative Cognitive Network: Case of a Selective Relay Cooperative Scheme using Alamouti ST Code

3.3.1 Proposed Selective System Model

As shown in Figure 3.10, we consider N primary base stations denoted by BS-P$_n$ where $n = 1,..N$ and a secondary radio network consisting of one terminal, one base station and M relays denoted respectively by SU, BS-S, and R$_m$ where $m = 1,..M$.

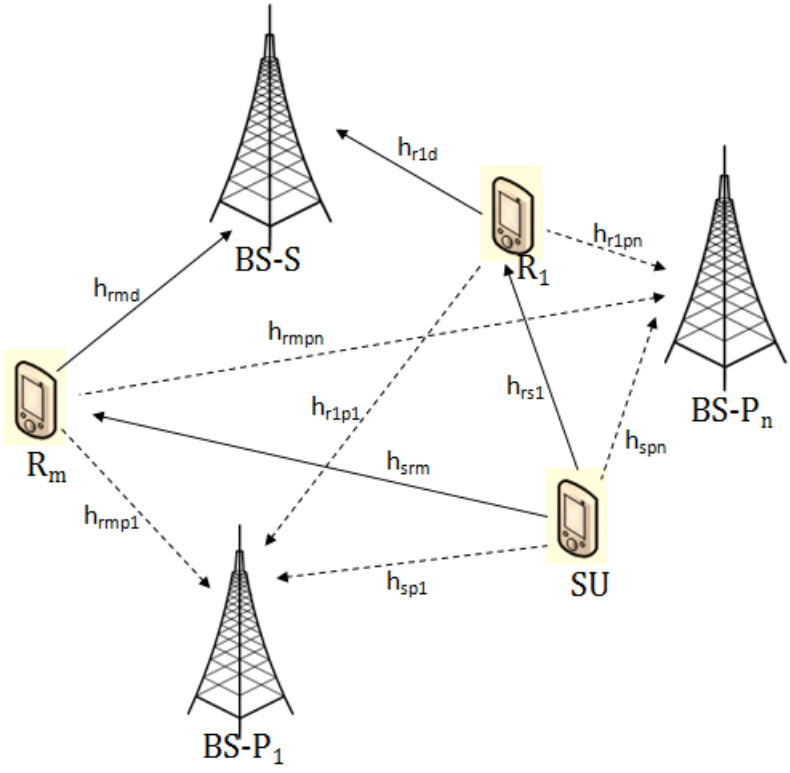

Figure 3.10: The proposed cognitive system model.

3.3.1.1 Selection Relay Criterion

Selecting a single relay for information forwarding simplifies the receiver design. Moreover, it ensures better resources allocation since the available energy will be only used by the more suitable relay. In our study, the best relay selection is based on maximization of received signal quality at the secondary base station and minimization of the received interference at the primary users. Our selection criterion is expressed as follows

$$R = \underset{m=1..M}{arg\ max} \left[\frac{\frac{|h_{r_m d}|^2}{L_{r_m d} S_{r_m d}}}{\sum_{n=1}^{N} \frac{|h_{r_m p_n}|^2}{L_{r_m p_n} S_{r_m p_n}}} \right]. \tag{3.17}$$

3.3.1.2 Cooperation Based on Alamouti ST Code

In this section, we consider an adaptive AF protocol based on the Alamouti space-time code, as schematized in Table 2.2.

At the output of the MRC combiner, the final total SNR expression for Alamouti cooperative protocol can be written as follows:

$$SNR_T = \frac{E_s}{N_0} \frac{\frac{|h_{sd}|^2}{\sqrt{L_{sd} S_{sd}}} + \gamma^2 \frac{|h_{sr}|^2}{\sqrt{L_{sr} S_{sr}}} \frac{|h_{rd}|^2}{\sqrt{L_{rd} S_{rd}}}}{1 + \gamma^2 \frac{|h_{rd}|^2}{\sqrt{L_{rd} S_{rd}}}}, \tag{3.18}$$

where $\gamma = \sqrt{\frac{E_r}{\frac{|h_{sr}|^2}{L_{sr} S_{sr}} E_s + N_0}}$ is the amplification factor of the relay.

3.3.2 Generated Cost due to the Secondary Network Transmission

For the cooperation based on Alamouti ST code, at the first and second time slots, only the secondary user is transmitting, so we have

$$C_s = \frac{E_s R |h_{sp}|^2}{L_{sp} S_{sp}}, \tag{3.19}$$

where $R = 1/T_s$ denotes the symbol rate. For the third and fourth time slots, both SU and R are transmitting to the secondary destination. Thus, the cost function at the primary destination will be the sum of these two transmissions'costs

$$C_r = \frac{E_s R |h_{sp}|^2}{L_{sp} S_{sp}} + \frac{E_r R |h_{rp}|^2}{L_{rp} S_{rp}}. \tag{3.20}$$

Finally, the overall cost function will be as follows

$$C_T = max(C_s, C_r) = \frac{E_s R |h_{sp}|^2}{L_{sp} S_{sp}} + \frac{E_r R |h_{rp}|^2}{L_{rp} S_{rp}}. \tag{3.21}$$

3.3.3 Source and Relay Energy Optimization

In this section, we derive the adopted optimization approach. In fact, the optimization aims at finding out the appropriate energy repartition of both source and relay nodes in order to enhance the cognitive system performance. Therefore, our optimization problem can be formulated as follows

$$\begin{aligned} &\text{maximize} \quad SNR_T \\ &\text{subject to} \quad E_s + E_r \leq E_a \\ &\text{and} \quad C_T \leq C_{max} \end{aligned} \quad . \tag{3.22}$$

That can be written with refer to (3.21) as

$$\begin{aligned} &\text{maximize} \quad SNR_T \\ &\text{subject to} \quad E_s + E_r \leq E_a \quad , \\ &\text{and} \quad H_s E_s + H_r E_r \leq C_{max} \end{aligned} \tag{3.23}$$

where

$$H_s = \frac{R|h_{sp}|^2}{L_{sp} S_{sp}} \tag{3.24}$$

and

$$H_r = \frac{R|h_{rp}|^2}{L_{rp} S_{rp}}. \tag{3.25}$$

For the optimization, we propose to use the geometrical method as it defined in SubSection (3.2.3). Here, we have to study the following two cases illustrated in Figure 3.11 and Figure 3.12 respectively.

1. $\frac{C_{max}}{H_s} \leq \frac{C_{max}}{H_r}$

In such condition, we can obtain three different cases depending on E_a value as presented in Figure 3.11 by 1.(a), 1.(b) and 1.(c).

- 1.(a): $E_a \leq \frac{C_{max}}{H_s}$

If $E_s^{'}$ exists and $E_s^{'} \in [0, E_a]$, then the optimal solution is $(E_s^{'}, E_a - E_s^{'})$. Otherwise, the optimal solution will be at the segment boundary $(E_a, 0)$ which means that the SU uses the whole available energy to transmit.

- 1.(b): $\frac{C_{max}}{H_s} \leq E_a \leq \frac{C_{max}}{H_r}$

If $E_s^{'}$ exists and $E_s^{'} \in \left[0, \frac{C_{max}}{H_s}\right]$, then the optimal solution is $(E_s^{'}, E_a - E_s^{'})$. Otherwise, the optimal solution will be one of the segment boundary namely $(\frac{C_{max} - H_r E_a}{H_s - H_r}, \frac{C_{max} - H_s E_a}{H_r - H_s})$ or $(\frac{C_{max}}{H_s}, 0)$ which yields the maximum SNR value.

- 1.(c): $E_a \geq \frac{C_{max}}{H_r}$

For this case, and as shown in Figure 3.11, no solution is possible. So, the secondary transmission is not allowed.

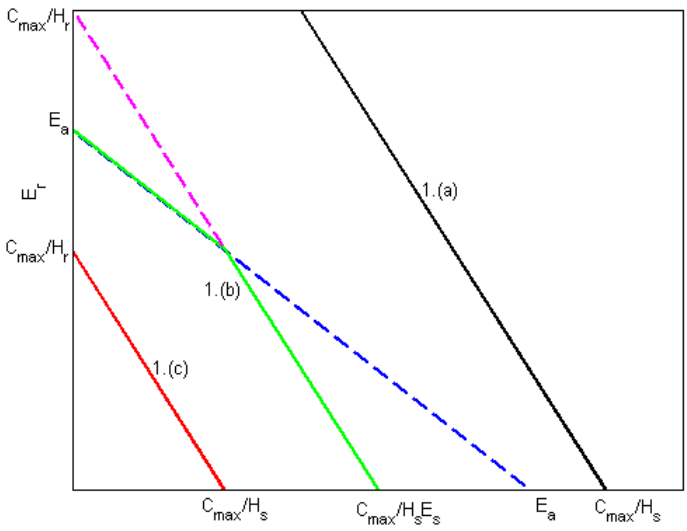

Figure 3.11: Different cases illustration where $\frac{C_{max}}{H_s} \leq \frac{C_{max}}{H_r}$

2. $\frac{C_{max}}{H_s} \geq \frac{C_{max}}{H_r}$

In such condition, we can obtain three different cases depending on E_a value as presented in Figure 3.12 by 1.(a), 1.(b) and 1.(c).

- 2.(a): $E_a \leq \frac{C_{max}}{H_r}$

If $E_s^{'}$ exists and $E_s^{'} \in [0, E_a]$, then the optimal solution is $(E_s^{'}, E_a - E_s^{'})$. Otherwise, the optimal solution will be at the segment boundary $(E_a, 0)$ which means that the SU uses the whole available energy to transmit.

- 2.(b): $\frac{C_{max}}{H_r} \leq E_a \leq \frac{C_{max}}{H_s}$

If $E_s^{'}$ exists and $E_s^{'} \in \left[0, \frac{C_{max}}{H_s}\right]$, then the optimal solution is $(E_s^{'}, E_a - E_s^{'})$. Otherwise, the optimal solution will be one of the segment boundary namely $(\frac{C_{max}-H_r E_a}{H_s-H_r}, \frac{C_{max}-H_s E_a}{H_r-H_s})$ or $(E_a, 0)$ which yields the maximum SNR value.

- 2.(c): $E_a \geq \frac{C_{max}}{H_s}$

For this case, and as shown in Figure 3.12, no solution is possible. So, the secondary transmission is not allowed.

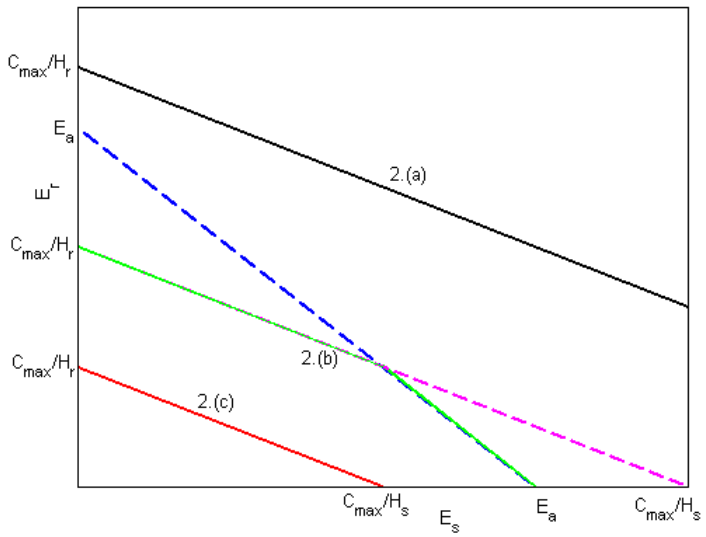

Figure 3.12: Different cases illustration where $\frac{C_{max}}{H_s} \geq \frac{C_{max}}{H_r}$

3.3.4 Throughput Study of the Selective System

To study our proposed scheme with more general view, we consider a rectangular pattern where nodes are located as it shown in Figure 3.13.

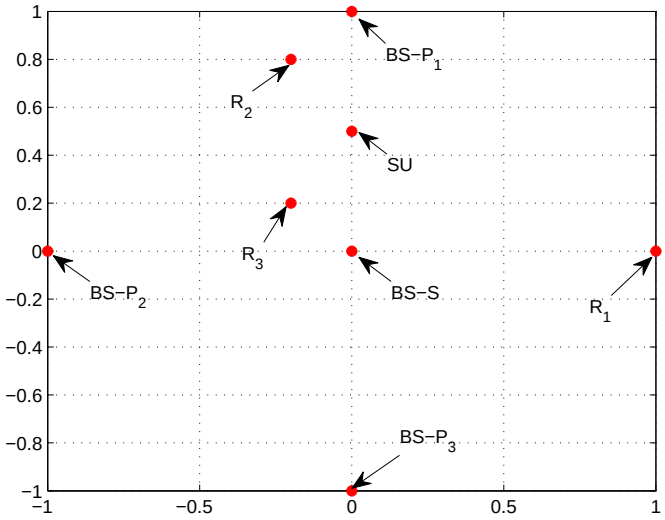

Figure 3.13: Positions of different nodes.

First of all, we consider the presence of one primary base station BS-P_1, and we present in Figure 3.14 the throughput behavior as a function of $(E_a/N_0)(d_0/d)^{\alpha}$ for each of the relay location then when applying our selective cooperative scheme, in the other words, when the best relay transmits. Figure 3.14 approves once again our selection criterion and shows that the worst throughput is seen when SU becomes near to BS-P and distant to BS-S.

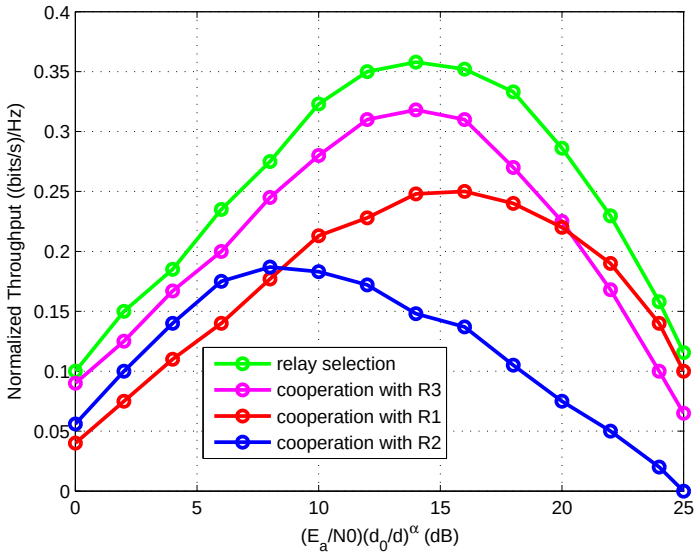

Figure 3.14: Throughput behavior of the proposed scheme as a function of $(E_a/N_0)(d_0/d)^{\alpha}$ for different relay locations.

In order to perform a preliminary comparison with other schemes, Figure 3.15 is plotted. For the fixed energy allocation scheme, we consider the same transmitted energy in both relay and source nodes that is equal to $E_a/2$. Moreover, we assume that the SU is located at the center of the line connecting the secondary and primary base stations. More precisely, Figure 3.15 illustrates the system throughput as a function of $(E_a/N_0)(d_0/d)^{\alpha}$ for different cognitive schemes. We clearly depict from these curves that our selective cooperative transmission combined with an energy allocation scheme outperforms the other schemes, and that our optimization strategy improves significantly the secondary transmissions. Moreover, we notice that the achievable throughput at the BS-S decreases sharply at higher transmission energy values, since more and more the interference generated at the BS-P increases and the SU will not be authorized to transmit. Next, we study the impact of the considered cost threshold on the throughput of our proposed optimized scheme. Figure 3.16 plots the system normalized throughput as a function of $(E_a/N_0)(d_0/d)^{\alpha}$ for different values of C_{max}.

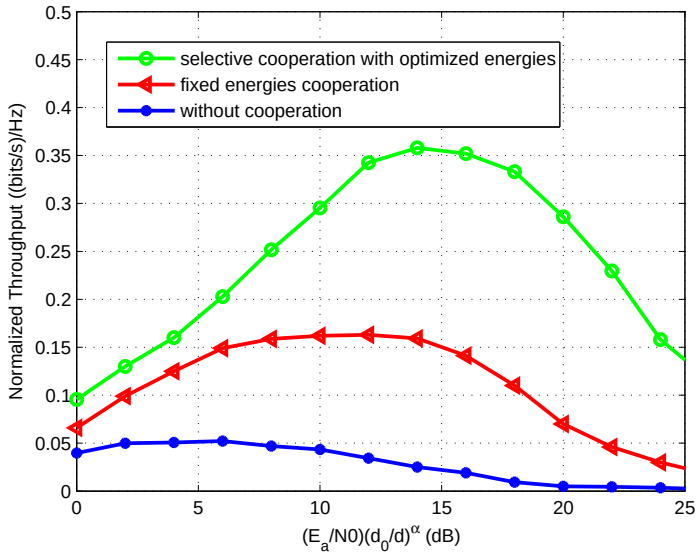

Figure 3.15: Throughput behavior of the proposed scheme as a function of $(E_a/N_0)(d_0/d)^{\alpha}$ for different schemes.

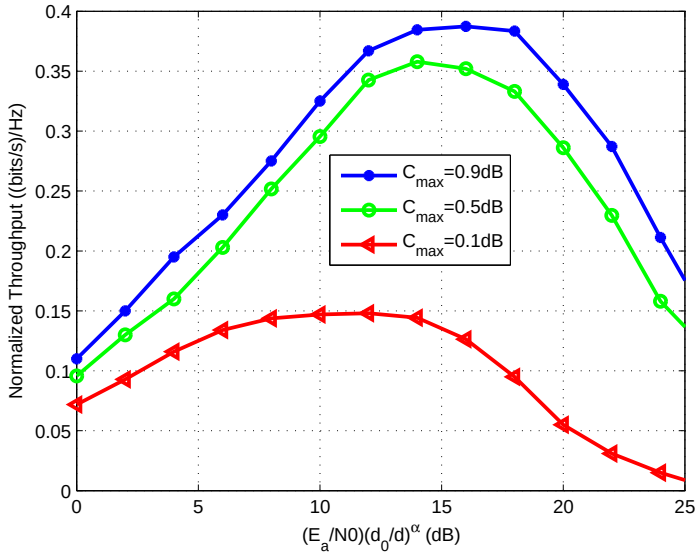

Figure 3.16: Throughput behavior as a function of $(E_a/N_0)(d_0/d)^{\alpha}$ different Cmax values.

In fact, it is logical that a higher authorized C_{max} provides significant gain in terms of throughput when compared to the cases of more stringent interference constraints.

Finally, we would like to study the effect of detecting more than one BS-P in the secondary network. In fact, Figure 3.17 shows the throughput behavior as a function of $(E_a/N_0)(d_0/d)^{\alpha}$ for several number of primary base stations, N. In particular, we consider three BS-Ps located as shown in Figure 3.13. It is observed from Figure 3.17 that, with increasing the number of BS-Ps, the achievable data rate decreases significantly.

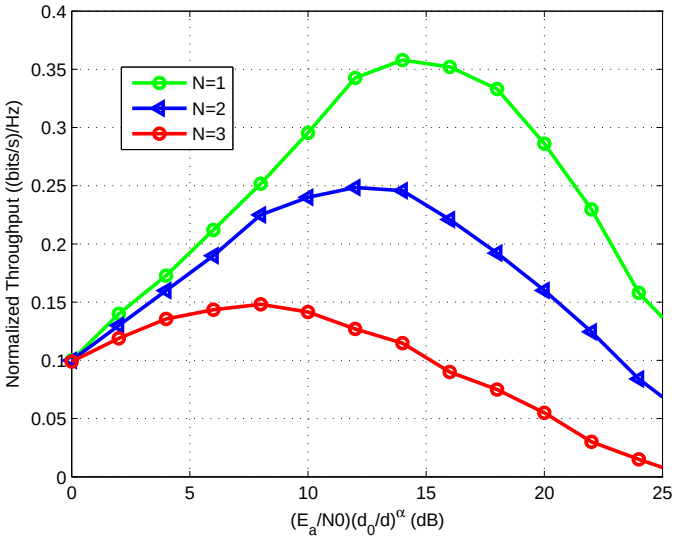

Figure 3.17: Throughput behavior as a function of $(E_a/N_0)(d_0/d)^{\alpha}$ for different numbers of BS-P.

3.4 Conclusion

In the first part of this chapter, we proposed and studied an energy allocation scheme in an adaptive cognitive network based on AF cooperation. In fact, an optimization of the SU and the relay transmitted symbol

energies is carried on to ensure the highest performance provided that the interference cost generated at the PU is below a prescribed threshold. In the second part, we proposed a selective cooperative relay combined with an energy allocation scheme in an adaptive cognitive network based on Alamouti ST cooperation.

Through numerical results, we conclude that the system performances are proportional to several parameters such as the SU location, the relay location, their transmission energies, the maximum tolerable cost at the primary network and the number of primary base stations detected in the network. In addition, we proved that our proposed strategies show superior performance gain in terms of throughput and outage probability compared to the conventional fixed allocation scheme where energy is uniformly distributed to each node.

This work will be extended in the next chapter by carrying out the optimization with multiple secondary users and carrying out an analytical optimization of the network resources.

Chapter 4

Optimal Resource Allocation Schemes for AF Multi-hop in a Cognitive Radio System

4.1 Introduction

In the previous chapter, we investigate energy optimization schemes in cognitive cooperative networks with one secondary relay. In this chapter, we consider the optimization of the energy allocation in the amplify-and-forward (AF) multi-hop cognitive system, where secondary users can access the licensed spectrum simultaneously with primary users, provided that they do not generate harmful interference at the primary network. Our optimization problem is formulated as a maximization of the instantaneous received signal to noise ratio, under interference power constraints that are imposed to protect the primary network. We propose both geometrical and analytical approaches. We start by resolving our optimization problem for two and three hops. We study our proposed energy allocation approach, combined with adaptive modulation, and compare its performances with the classical multi-hop scheme with uniform energy distribution. Then, we propose an analytical optimal solution to the problem for the 2-hop case. Note here that, up to

our knowledge, our proposed geometrical optimization approach, as well as the analytical approach in the cognitive cooperative context, have not been considered in the literature.

4.2 Cognitive Multi-hop System Model

As it shown in Figure 4.1, we consider N primary base stations denoted by BSp_n, where $n \in \{1..N\}$, and a secondary radio network consisting of a K-hop wireless transmissions in which a source terminal, SU, try to send data to a destination terminal, BS-S, via $K-1$ relay nodes. The shadowing between nodes i and j follows a log-normal distribution with parameter σ and is expressed as $S_{ij} = S_i + S_j$, where S_i is the contribution to the shadowing near the node i. For our model, we assume that the contributions to the shadowing due to the environment near nodes BS-S, BS-P_n, R_k and SU are given by

$$\text{var}(S_{BS-S}) = \text{var}(S_{BS-P_n}) = (1-\beta)\sigma^2 \tag{4.1}$$

and

$$\text{var}(S_{SU}) = \text{var}(S_{R_k}) = \beta\sigma^2, \tag{4.2}$$

where β is the correlation factor. For the relay cooperation, we consider the non-regenerative AF protocol. For a given symbol a transmitted from the secondary source, the consecutive received signals are given by

$$\begin{gathered} y_{s,1} = \sqrt{E_0}\frac{h_{s1}}{\sqrt{L_{s1}S_{s1}}}a + b_{s1} \\ \textit{and} \\ y_{k-1,k} = \gamma_{k-1}\frac{h_{k-1,k}}{\sqrt{L_{k-1,k}S_{k-1,k}}}y_{k-2,k-1} + b_{k-1,k}, \end{gathered} \tag{4.3}$$

where $k = 2,..,K$, $h_{i,j}$ is the propagation channel attenuation between nodes i and j, and b_{ij} is the additive white Gaussian noise (AWGN) corrupting respectively the link i-j with a common variance N_0. Here, E_0

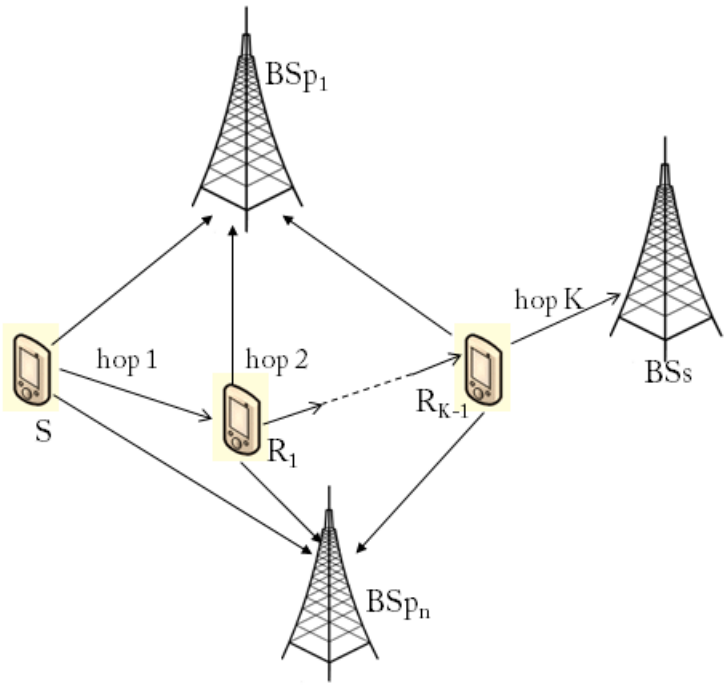

Figure 4.1: Generic system model: A multi-hop secondary network in the presence of primary base stations.

denotes the transmitted energy of the secondary source. The amplification gain at the k^{th} relay, depends on the instantaneous fading amplitude over the channel between the involved terminals, and is given by

$$\gamma_k = \sqrt{\frac{E_k}{\frac{|h_{k-1,k}|^2}{L_{k-1,k}S_{k-1,k}}E_{k-1} + N_0}}, \tag{4.4}$$

where $k = 1,..,K-1$ and E_k is the transmitted energy of the node k. We set $\gamma_0 = \sqrt{\frac{E_0}{N_0}}$.

As we consider the adaptive modulation, the source uses the calculated SNR to make decision about the constellation size of the next transmitted packet. According to (4.3), the received signal at the secondary destination is

$$y_d = \gamma_{K-1} \frac{h_{K-1,K}}{\sqrt{L_{K-1,K} S_{K-1,K}}} y_{K-2,K-1} + b_{K-1,K}. \tag{4.5}$$

Developing $y_{K-2,K-1}$, we obtain

$$y_d = \left(\prod_{k=1}^{K} \gamma_{k-1} \frac{h_{k-1,k}}{\sqrt{L_{k-1,k} S_{k-1,k}}} \right) a + \sum_{k=1}^{K} b_{k-1,k} \prod_{l=k+1}^{K} \frac{h_{l-1,l}}{\sqrt{L_{l-1,l} S_{l-1,l}}} \prod_{l=k}^{K-1} \gamma_l. \tag{4.6}$$

Let's denote $H_{i,j} = \frac{|h_{i,j}|^2}{L_{i,j} S_{i,j}}$. We can easily show that the total received SNR expression is given by

$$SNR = \frac{\prod_{k=1}^{K} \gamma_{k-1}^2 H_{k-1,k}}{\sum_{k=1}^{K} N_0 \prod_{l=k+1}^{K} H_{l-1,l} \prod_{l=k}^{K-1} \gamma_l^2}. \tag{4.7}$$

Replacing γ_k by its expression in (4.4), and using the approach given in [60], we can write the SNR as

$$SNR = \left(\prod_{k=1}^{K} (1 + \frac{1}{\theta_k}) - 1 \right)^{-1}, \tag{4.8}$$

where $\theta_k = \frac{E_{k-1}}{N_0} H_{k-1,k}$.

4.3 Imposed Interference Power Constraint on Secondary Users

4.3.1 Generated Cost due to the Secondary Network Transmission

For simplicity sake, we assume here the presence of one BS-P. The cost at the BS-P generated after the k^{th} hop transmission can be written as follows

$$C_k = \frac{E_k R |h_{kp}|^2}{L_{kp} S_{kp}}, \tag{4.9}$$

where R is the symbol rate and L_{kp} and S_{kp} are the pathloss and the shadowing coefficients, corrupting the k-(BS-P) link. Finally, the overall cost function generated after the secondary cooperative transmission will be the maximum of the K hop costs

$$C = max_{k=0..K-1}\left(C_k\right). \tag{4.10}$$

4.4 Source and Relays Energy Optimization

4.4.1 Problem Formulation

In this section, we start by formulating our optimization problem for energy allocation in the secondary network. Then, we propose two approaches for the resolution of this problem.

Our objective is to maximize the instantaneous received SNR, where the total transmit energy E_a of the cognitive network shall be constrained for practical implementation considerations. Moreover, the interference power constraint presented in Section (4.3) shall be imposed to limit the aggregated interference from the cognitive network to the primary one. With these considerations, we formulate our energy optimization problem as follows

$$\begin{aligned} &\text{maximize} \quad SNR \\ &\text{subject to} \quad \textstyle\sum_{k=0}^{K-1} E_k \leq E_a \\ &\text{and} \quad C_k \leq C_{max} \end{aligned} \quad . \tag{4.11}$$

Referring to (4.9), the last constraint of the problem (4.11) can be replaced by $E_k \leq E_{kmax}$, where $E_{kmax} = \frac{C_{max}}{R}\frac{\left|h_{kp}\right|^2}{L_{kp}S_{kp}}$.

4.4.2 Geometrical Approach

In this chapter, we propose to use a new optimization method based on geometrical approach [59] that presents an attractive way for solving nonlinear problems involving few parameters with a minimum amount of computational effort.

4.4.2.1 Energy Optimization in the Two-hop Case

An interesting special case of multi-hop transmission is the two-hop case. Developing the *SNR* expression given in (4.8), where $K = 2$, we obtain the following optimization problem

$$\begin{aligned} \text{maximize} \quad & SNR = \frac{E_0 E_1 H_{0,1} H_{1,2}}{N_0 (E_0 H_{0,1} + E_1 H_{1,2} + N_0)} \\ \text{subject to} \quad & E_0 + E_1 \leq E_a, \\ & E_0 \leq E_{0max} \\ \text{and} \quad & E_1 \leq E_{1max}. \end{aligned} \quad . \tag{4.12}$$

First, we have to trace the graph in two dimensions of the problem constraints as it shown in Figure 4.2 and Figure 4.3, where the source and the relay energies are presented on the x-axis and the y-axis, respectively. Because of the non-negativity energies restrictions, the feasible region is restricted to the positive quadrant. The candidate solutions are the intersection area of the bounded region for each constraint. In fact, the point of this area perimeter which yields the maximum value of the objective function will be the optimal solution to our problem. Since E_{0max} and E_{1max} values depend on a random varying environment, we have to study the following two cases illustrated in Figure 4.2 and Figure 4.3, respectively.

1. $E_{0max} \leq E_{1max}$

In such condition, we obtain four different cases depending on the value of E_a, as presented in Figure 4.2 by 1.(a), 1.(b), 1.(c) and 1.(d). The optimal solutions for these different cases depend on the derivative of the SNR function with respect to E_0 and E_1 and are summarized in Table 4.1.

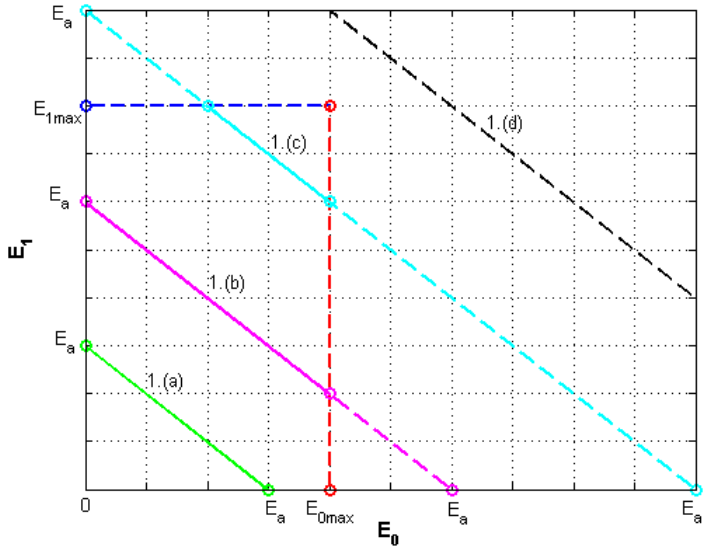

Figure 4.2: Different cases illustration for the geometrical approach, when $K = 2$ and $E_{0max} \leq E_{1max}$.

Table 4.1: Solution discussion where $E_{0max} \leq E_{1max}$.

Subcase	Optimal Solution
1.(a): $E_a \leq E_{0max}$	(E_0, E_1) if $\frac{\partial SNR}{\partial E_0} = \frac{\partial SNR}{\partial E_1}$ and $E_0 \in \left]0, E_a\right[$ and $E_1 \in \left]0, E_a\right[$
1.(b): $E_{0max} \leq E_a \leq E_{1max}$	(E_0, E_1) if $\frac{\partial SNR}{\partial E_0} = \frac{\partial SNR}{\partial E_1}$ and $E_0 \in \left]0, E_{0max}\right[$ and $E_1 \in \left]E_a - E_{0max}, E_{1max}\right[$
	(E_{0max}, E_1) if $\frac{\partial SNR}{\partial E_1} = 0$ and $E_1 \in \left]0, E_a - E_{0max}\right[$
1.(c): $E_{1max} \leq E_a \leq (E_{0max} + E_{1max})$	(E_0, E_1) if $\frac{\partial SNR}{\partial E_0} = \frac{\partial SNR}{\partial E_1}$ and $E_0 \in \left[E_a - E_{1max}, E_{0max}\right]$ and $E_1 \in \left[E_a - E_{0max}, E_{1max}\right[$
	(E_0, E_{1max}) if $\frac{\partial SNR}{\partial E_0} = 0$ and $E_0 \in \left]0, E_a - E_{1max}\right[$
	(E_{0max}, E_1) if $\frac{\partial SNR}{\partial E_1} = 0$ and $E_1 \in \left]0, E_a - E_{0max}\right[$
1.(d): $E_a \geq (E_{0max} + E_{1max})$	(E_{0max}, E_{1max})

For example, for the case 1.(a), where $E_a \leq E_{0max}$, the optimal solution is on the segment where the gradient of the SNR function $\left(\frac{\partial SNR}{\partial E_0}, \frac{\partial SNR}{\partial E_1}\right)$ is collinear with the vector $(1,1)$, and thus $\frac{\partial SNR}{\partial E_0} = \frac{\partial SNR}{\partial E_1}$. Also, the solution must satisfy the two conditions $E_0 \in \left]0, E_a\right[$ and $E_1 \in \left]0, E_a\right[$.

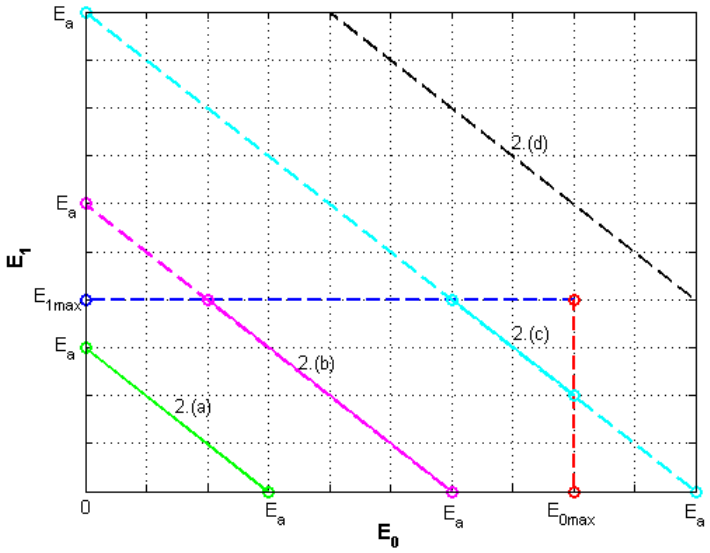

Figure 4.3: Different cases illustration for the geometrical approach, when $K = 2$ and $E_{1max} \leq E_{0max}$.

2. $E_{1max} \leq E_{0max}$

In such condition, we have also four cases presented in Figure 4.3 by 2.(a), 2.(b), 2.(c) and 2.(d). Table 4.2 summarizes the optimal solutions obtained with the geometrical method for these four cases.

Table 4.2: Solution discussion where $E_{1max} \leq E_{0max}$.

Subcase	Optimal Solution
2.(a): $E_a \leq E_{1max}$	(E_0, E_1) if $\frac{\partial SNR}{\partial E_0} = \frac{\partial SNR}{\partial E_1}$ and $E_0 \in \left]0, E_a\right[$ and $E_1 \in \left]0, E_a\right[$
2.(b): $E_{1max} \leq E_a \leq E_{0max}$	(E_0, E_1) if $\frac{\partial SNR}{\partial E_0} = \frac{\partial SNR}{\partial E_1}$ and $E_0 \in \left]E_a - E_{1max}, E_a\right[$ and $E_1 \in \left]0, E_{1max}\right[$
	(E_0, E_{1max}) if $\frac{\partial SNR}{\partial E_0} = 0$ and $E_0 \in \left]0, E_a - E_{1max}\right[$
2.(c): $E_{0max} \leq E_a \leq (E_{0max} + E_{1max})$	(E_0, E_1) if $\frac{\partial SNR}{\partial E_0} = \frac{\partial SNR}{\partial E_1}$ if $E_0 \in \left[E_a - E_{1max}, E_{0max}\right]$ and $E_1 \in \left[E_a - E_{0max}, E_{1max}\right[$
	(E_0, E_{1max}) if $\frac{\partial SNR}{\partial E_0} = 0$ and $E_0 \in \left]0, E_a - E_{1max}\right[$
	(E_{0max}, E_1) if $\frac{\partial SNR}{\partial E_1} = 0$ and $E_1 \in \left]0, E_a - E_{0max}\right[$
2.(d): $E_a \geq (E_{0max} + E_{1max})$	(E_{0max}, E_{1max})

Figure 4.4 shows the normalized throughput evolution for the optimized two-hop system as a function of $(E_a/N_0)(d_0/d)^{\alpha}$, when one BS-P is considered in the network. Moreover, we assume that the SU is located at equal distances from the BS-S and the BS-P and that the relay is located at equal distance between the SU and the secondary destination.

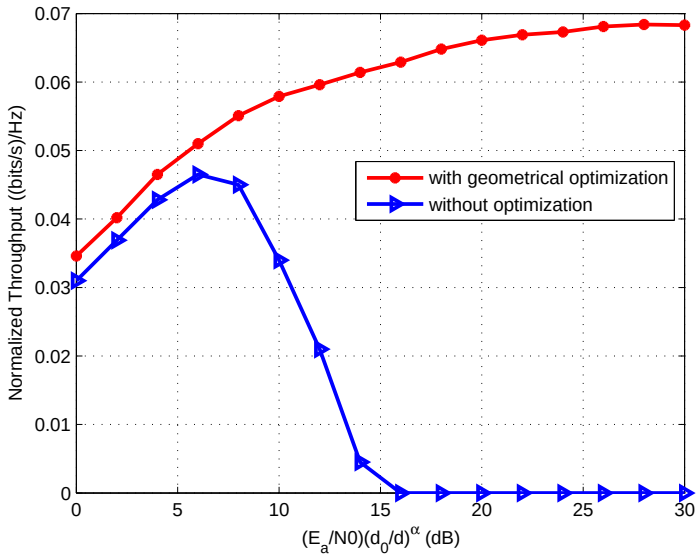

Figure 4.4: Throughput behavior as a function of $(E_a/N_0)(d_0/d)^{\alpha}$ in the dual-hop case, when $C_{max} = 0.5dB$.

The comparison is performed with the two-hop system considering a fixed energy allocation scheme, for which the same transmitted energy in both relay and source nodes is fixed to $E_a/2$. We clearly depict from these two curves that our proposed scheme outperforms the non-optimized scheme, and that our optimization strategy improves significantly the cognitive transmissions. Moreover, we notice that, with fixed energy allocation scheme, the performance gain at the BS-S decreases sharply at high transmission energy values, since more and more the interference generated at the BS-P increases and the SU will not be authorized to transmit. From Figure 4.4, we also notice that the normalized throughput of the optimized scheme keeps growing and stagnates for a certain value of $(E_a/N_0)(d_0/d)^{\alpha}$. This can be explained by the

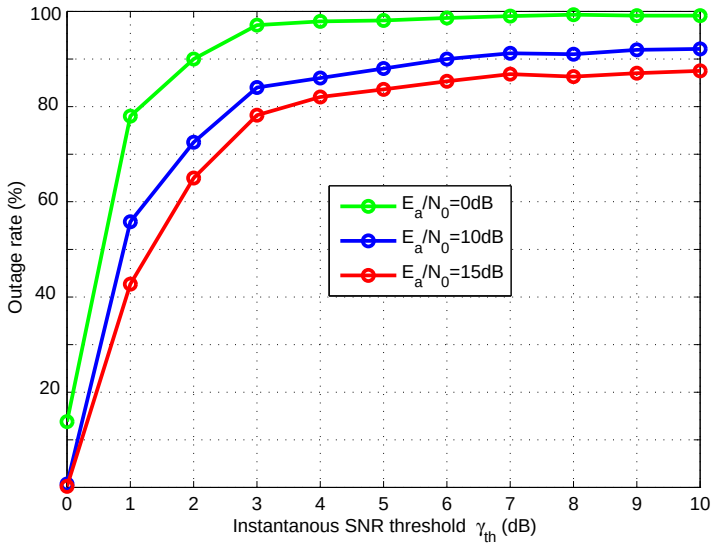

Figure 4.5: Outage rate behavior as a function of γ_{th} for several E_a/N_0 values in the dual-hop case, when $C_{max} = 0.5dB$.

inequality constraint $E_0 + E_1 \leq E_a$, that means that at higher transmission energy, the E_a value has no more impact on the system performance. In Figure 4.5, we plot the outage rate behavior as a function of γ_{th} for several E_a/N_0 values. We define the outage rate metric as the percentage that the instantaneous received SNR falls below a certain threshold γ_{th}. For example, if we fix the available energy $E_a/N_0 = 10dB$ and the threshold $\gamma_{th} = 3dB$, we can say that in 15% of measured cases, the received instantaneous received SNR at the BS-S is greater than $3dB$.

4.4.2.2 Energy Optimization in the Three-hop Case

Now, we consider a three-hop secondary radio network (K=3). Therefore, our optimization problem is formulated as follows

$$\begin{aligned} &\text{maximize} \quad SNR \\ &\text{subject to} \quad E_0 + E_1 + E_2 \leq E_a, \\ &E_0 \leq E_{0max}, \\ &E_1 \leq E_{1max} \\ &\text{and} \quad E_2 \leq E_{2max}. \end{aligned} \tag{4.13}$$

Let's trace the problem constraints graph in three dimensions as it shown in Figure 4.6.

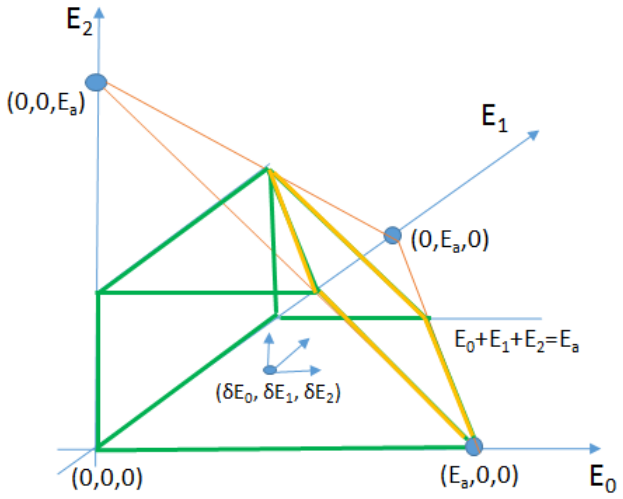

Figure 4.6: Problem constraints illustration for the three-hop case.

We note that if $E_{0max} + E_{1max} + E_{2max} > E_a$, we will have $E_0 + E_1 + E_2 = E_a$ and E_2 can be replaced by $E_2 = E_a - E_0 - E_1$. Thus, we obtain a two-variable optimization problem, as given in equation (4.14) and shown in Figure 4.7. Otherwise, the constraint $E_0 + E_1 + E_2 \leq E_a$ is always satisfied and the optimal solution will be $(E_{0max}, E_{1max}, E_{2max})$.

$$\begin{aligned} &\text{maximize} \quad SNR(E_0, E_1) \\ &\text{subject to} \quad E_0 + E_1 \leq E_a, \\ &E_0 + E_1 \geq E_a - E_{2max}, \\ &E_0 \leq E_{0max} \\ &\text{and} \quad E_1 \leq E_{1max}. \end{aligned} \tag{4.14}$$

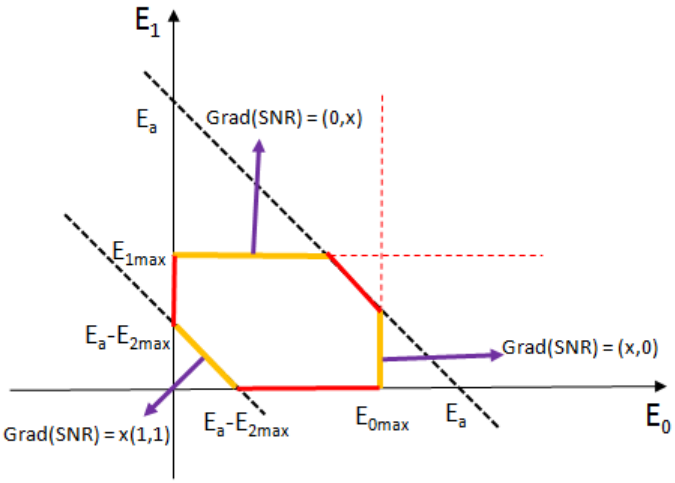

Figure 4.7: Different cases illustration for the geometrical resolution, when $K = 3$ and $E_{0max} \leq E_{1max}$.

Since the problem parameters E_{0max}, E_{1max} and E_{2max} depend on a randomly varying environment, we have to discuss the different possible cases.

When $E_{1max} \leq E_{0max}$, we obtain nine different cases depending on E_a value. The optimal solutions for these cases are given in Table 4.3. For simplicity sake we denote $E_a^{'} = E_a - E_{2max}$.

When $E_{1max} \geq E_{0max}$, we obtain also nine different cases that are omitted here for simplicity of presentation.

Table 4.3: Solution discussion where $E_{1max} \leq E_{0max}$.

Subcase	Optimal solution
1. $E_a^{'} < E_{1max}$	
1.(a): $E_a \leq E_{1max}$	(E_0, E_1) if $\frac{\partial SNR}{\partial E_0} = \frac{\partial SNR}{\partial E_1}$ and $E_0 \in \left]0, E_a^{'}\right[$ and $E_1 \in \left]0, E_a^{'}\right[$
1.(b): $E_{1max} \leq E_a \leq E_{0max}$	(E_0, E_1) if $\frac{\partial SNR}{\partial E_0} = \frac{\partial SNR}{\partial E_1}$ and $E_0 \in \left]0, E_a^{'}\right[$ and $E_1 \in \left]0, E_a^{'}\right[$
	(E_0, E_{1max}) if $\frac{\partial SNR}{\partial E_0} = 0$ and $E_0 \in \left]0, E_a - E_{1max}\right]$
1.(c): $E_{0max} \leq E_a \leq (E_{0max} + E_{1max})$	(E_0, E_1) if $\frac{\partial SNR}{\partial E_0} = \frac{\partial SNR}{\partial E_1}$ and $E_0 \in \left]0, E_a^{'}\right[$ and $E_1 \in \left]0, E_a^{'}\right[$
	(E_0, E_{1max}) if $\frac{\partial SNR}{\partial E_0} = 0$ and $E_0 \in \left]0, E_a - E_{1max}\right]$
	(E_{0max}, E_1) if $\frac{\partial SNR}{\partial E_1} = 0$ and $E_1 \in \left]0, E_a - E_{0max}\right]$
1.(d): $E_a \geq (E_{0max} + E_{1max})$	(E_0, E_1) if $\frac{\partial SNR}{\partial E_0} = \frac{\partial SNR}{\partial E_1}$ and $E_0 \in \left]0, E_a^{'}\right[$ and $E_1 \in \left]0, E_a^{'}\right[$
	(E_0, E_{1max}) if $\frac{\partial SNR}{\partial E_0} = 0$ and $E_0 \in \left]0, E_{0max}\right]$
	(E_{0max}, E_1) if $\frac{\partial SNR}{\partial E_1} = 0$ and $E_1 \in \left]0, E_{1max}\right]$
2. $E_{1max} + E_{2max} < E_a < E_{0max} + E_{2max}$	
2.(a): $E_{1max} < E_a < E_{0max}$	(E_0, E_1) if $\frac{\partial SNR}{\partial E_0} = \frac{\partial SNR}{\partial E_1}$ and $E_0 \in \left]E_a^{'} - E_{1max}, E_a^{'}\right[$ and $E_1 \in \left]0, E_{1max}\right]$
	(E_0, E_{1max}) if $\frac{\partial SNR}{\partial E_0} = 0$ and $E_0 \in \left]E_a^{'} - E_{1max}, E_a - E_{1max}\right]$
2.(b): $E_{0max} < E_a < E_{0max} + E_{1max}$	(E_0, E_1) if $\frac{\partial SNR}{\partial E_0} = \frac{\partial SNR}{\partial E_1}$ and $E_0 \in \left]E_a^{'} - E_{1max}, E_a^{'}\right[$ and $E_1 \in \left]0, E_{1max}\right]$
	(E_0, E_{1max}) if $\frac{\partial SNR}{\partial E_0} = 0$ and $E_0 \in \left]E_a^{'} - E_{1max}, E_a - E_{1max}\right]$
	(E_{0max}, E_1) if $\frac{\partial SNR}{\partial E_1} = 0$ and $E_1 \in \left]0, E_a - E_{0max}\right]$
2.(c): $E_a > E_{0max} + E_{1max}$	(E_0, E_1) if $\frac{\partial SNR}{\partial E_0} = \frac{\partial SNR}{\partial E_1}$ and $E_0 \in \left]E_a^{'} - E_{1max}, E_a^{'}\right[$ and $E_1 \in \left]0, E_{1max}\right]$
	(E_0, E_{1max}) if $\frac{\partial SNR}{\partial E_0} = 0$ and $E_0 \in \left]E_a^{'} - E_{1max}, E_{0max}\right]$
	(E_{0max}, E_1) if $\frac{\partial SNR}{\partial E_1} = 0$ and $E_1 \in \left]0, E_{1max}\right]$
3. $E_{0max} < E_a^{'} < E_{0max} + E_{1max}$	
3.(a): $E_{0max} < E_a < E_{0max} + E_{1max}$	(E_0, E_1) if $\frac{\partial SNR}{\partial E_0} = \frac{\partial SNR}{\partial E_1}$ and $E_0 \in \left]E_a^{'} - E_{1max}, E_{0max}\right]$ and $E_1 \in \left]E_a^{'} - E_{0max}, E_{1max}\right]$
	(E_0, E_{1max}) if $\frac{\partial SNR}{\partial E_0} = 0$ and $E_0 \in \left]E_a^{'} - E_{1max}, E_a - E_{1max}\right]$
	(E_{0max}, E_1) if $\frac{\partial SNR}{\partial E_1} = 0$ and $E_1 \in \left]E_a^{'} - E_{0max}, E_a - E_{0max}\right]$
3.(b): $E_a > E_{0max} + E_{1max}$	(E_0, E_1) if $\frac{\partial SNR}{\partial E_0} = \frac{\partial SNR}{\partial E_1}$ and $E_0 \in \left]E_a^{'} - E_{1max}, E_{0max}\right]$ and $E_1 \in \left]E_a^{'} - E_{0max}, E_{1max}\right]$
	(E_0, E_{1max}) if $\frac{\partial SNR}{\partial E_0} = 0$ and $E_0 \in \left]E_a^{'} - E_{1max}, E_{0max}\right]$
	(E_{0max}, E_1) if $\frac{\partial SNR}{\partial E_1} = 0$ and $E_1 \in \left]E_a^{'} - E_{0max}, E_{1max}\right]$

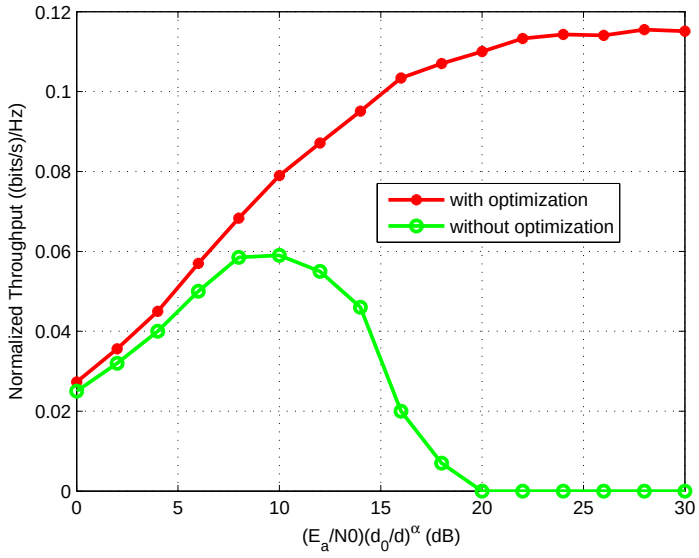

Figure 4.8: Throughput behavior as a function of $(E_a/N_0)(d_0/d)^{\alpha}$ in the three-hop case, when $C_{max} = 0.5dB$.

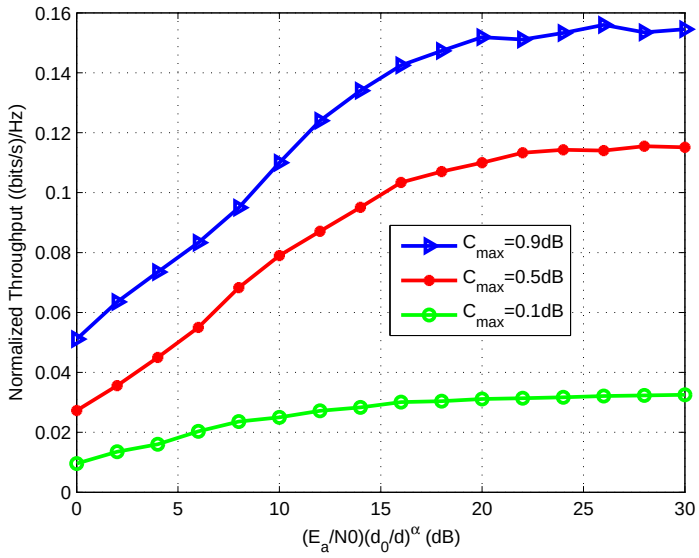

Figure 4.9: Throughput behavior of the three-hop scheme as a function of $(E_a/N_0)(d_0/d)^{\alpha}$ for different C_{max} values.

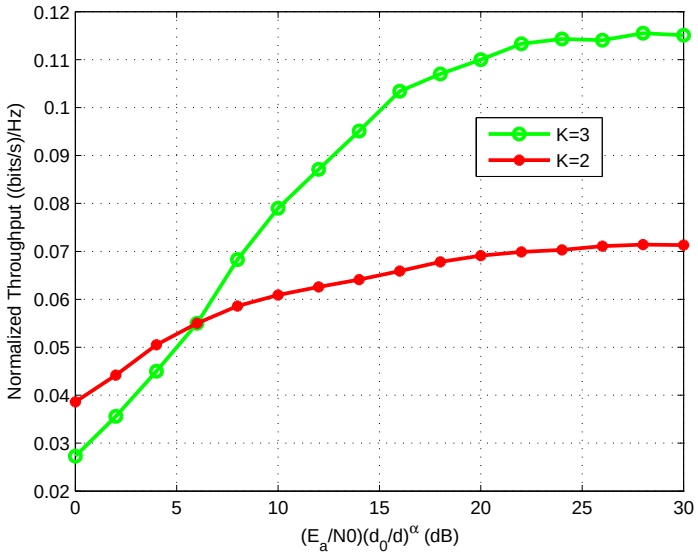

Figure 4.10: Comparison of the throughput behavior in the cases of two and three hops, when $C_{max} = 0.5dB$.

Figure 4.8 shows the throughput behavior of the optimized three-hop scheme as a function of $(E_a/N_0)(d_0/d)^{\alpha}$, when $C_{max} = 0.5dB$. We further show as benchmark, the normalized throughput of the non-optimized three-hop scheme. This Figure shows once again that our optimization scheme outperforms the fixed scheme in terms of throughput. Next, we study, in Figure 4.9, the impact of the considered cost threshold on the throughput of our proposed optimized scheme. We plot the system normalized throughput as a function of $(E_a/N_0)(d_0/d)^{\alpha}$ for different values of C_{max}. As expected, a high authorized C_{max} value provides significant gain in terms of throughput when compared to the cases of more stringent interference constraints. In Figure 4.10, we compare the normalized throughput for both two and three-hop optimized schemes as a function of $(E_a/N_0)(d_0/d)^{\alpha}$ when $C_{max} = 0.5dB$. Figure 4.10 shows that increasing the number of relaying hops (i.e. K) at low total available energy deteriorates the secondary system throughput, whereas, at high transmission energy, the three-hop scheme shows a better performance in terms of throughput. In fact, a low available energy cannot be well distributed between many nodes $(K = 3)$ especially for multi-hop scheme where each node must have some transmission energy to avoid the outage of the communication.

Thus, enough available energy is required to increase the number of hops in the secondary system.

4.4.3 Analytical Approach

In this subsection, we propose to resolve analytically the optimization problem. Note that since the objective function in (4.12) is concave and the constraints are linear, the optimization problem in (4.12) is convex and carries one optimal solution [61]. Using the Lagrange multiplier method, one has

$$L = (\prod_{k=1}^{K}(1+\frac{1}{\delta_k})-1)^{-1} - \mu(\sum_{k=0}^{K-1} E_k - E_a) - \sum_{i=0}^{K-1}\lambda_i(E_i - E_{imax}), \tag{4.15}$$

where L is the Lagrangean function. μ and λ_i, $i = 0,..K-1$ are the Lagrange multipliers. Moreover, using the Karush-Kuhn-Tucker (KKT) conditions [62], we obtain the additional following equations

$$\begin{gathered} \mu\left(\sum_{k=0}^{K-1} E_k - E_a\right) = 0 \\ \lambda_i(E_i - E_{imax}) = 0, \quad i = 0..K-1 \\ \mu \geq 0 \\ \lambda_i \geq 0, \quad i = 0..K-1 \end{gathered} . \tag{4.16}$$

Next, we resolve analytically the optimization problem for the two-hop case considering the following system of equations

$$\begin{gathered} (a): \ \frac{\partial L}{\partial E_0} = N_0 E_1 H_{0,1} H_{1,2}(E_1 H_{1,2} + N_0) - \mu - \lambda_0 = 0 \\ (b): \ \frac{\partial L}{\partial E_1} = N_0 E_0 H_{0,1} H_{1,2}(E_0 H_{0,1} + N_0) - \mu - \lambda_1 = 0 \\ (c): \ \mu(E_0 - E_1 - E_a) = 0 \\ (d): \ \lambda_0(E_0 - E_{0max}) = 0 \\ (e): \ \lambda_1(E_1 - E_{1max}) = 0 \end{gathered} . \tag{4.17}$$

According to (4.17), we have to study eight different cases depending on the Lagrange multipliers (μ,λ_0,λ_1) as described below.

1. $\mu = \lambda_0 = \lambda_1 = 0$: the equations in (4.17) lead to $E_0 = E_1 = 0$, which means that the secondary transmission is forbidden.

2. $\mu = 0, \lambda_0 > 0, \lambda_1 > 0$: we have a system of four equations system to determine four unknown parameters $(E_0, E_1, \lambda_0, \lambda_1)$, as follows

$$\begin{cases} N_0 E_1 H_{0,1} H_{1,2}(E_1 H_{1,2} + N_0) - \lambda_0 = 0 \\ N_0 E_0 H_{0,1} H_{1,2}(E_0 H_{0,1} + N_0) - \lambda_1 = 0 \\ E_0 = E_{0max} \\ E_1 = E_{1max} \end{cases} . \tag{4.18}$$

   In this case, we always have $\lambda_0 > 0$ and $\lambda_1 > 0$, which means that the optimal solution should be (E_{0max}, E_{1max}). This is an acceptable solution if and only if $E_{0max} + E_{1max} \leq E_a$.

3. $\mu = \lambda_0 = 0, \lambda_1 > 0$, we have three equations system to determine three unknown parameters (E_0, E_1, λ_1) as follows

$$\begin{cases} N_0 E_1 H_{0,1} H_{1,2}(E_1 H_{1,2} + N_0) = 0 \\ N_0 E_0 H_{0,1} H_{1,2}(E_0 H_{0,1} + N_0) - \lambda_1 = 0 \\ E_1 = E_{1max} \end{cases} \tag{4.19}$$

   In this case, we obtain at the same time $E_1 = 0$ and $E_1 = E_{1max}$, which is absurd.

4. $\mu = \lambda_1 = 0, \lambda_0 > 0$, we have three equations system to determine three unknown parameters (E_0, E_1, λ_0) as follows

$$\begin{cases} N_0 E_1 H_{0,1} H_{1,2}(E_1 H_{1,2} + N_0) - \lambda_0 = 0 \\ N_0 E_0 H_{0,1} H_{1,2}(E_0 H_{0,1} + N_0) = 0 \\ E_0 = E_{0max} \end{cases} \tag{4.20}$$

In this case, we obtain $E_0 = 0$ and $E_0 = E_{0max}$, which is absurd.

5. $\mu > 0, \lambda_0 > 0, \lambda_1 > 0$, we have five equations system to determine five unknown parameters $(E_0, E_1, \mu, \lambda_0, \lambda_1)$ as follows

$$\begin{cases} N_0 E_1 H_{0,1} H_{1,2}(E_1 H_{1,2} + N_0) - \mu - \lambda_0 = 0 \\ N_0 E_0 H_{0,1} H_{1,2}(E_0 H_{0,1} + N_0) - \mu - \lambda_1 = 0 \\ E_0 = E_{0max} \\ E_1 = E_{1max} \\ E_0 + E_1 = E_a \end{cases} . \tag{4.21}$$

If $E_{0max} + E_{1max} \leq E_a$, $\lambda_0 > 0$, $\lambda_1 > 0$ and $\mu > 0$ and the system solution is (E_{0max}, E_{1max}).

6. $\mu > 0, \lambda_0 = 0, \lambda_1 > 0$, we have four equations system to determine four unknown parameters $(E_0, E_1, \mu, \lambda_1)$ as follows

$$\begin{cases} N_0 E_1 H_{0,1} H_{1,2}(E_1 H_{1,2} + N_0) - \mu = 0 \\ N_0 E_0 H_{0,1} H_{1,2}(E_0 H_{0,1} + N_0) - \lambda_1 H_{1,2} - \mu = 0 \\ E_0 + E_1 = E_a \\ E_1 = E_{1max} \end{cases} . \tag{4.22}$$

If $E_{0max} + E_{1max} \leq E_a$, $\lambda_1 > 0$ and $\mu > 0$, the system solution is $(E_a - E_{1max}, E_{1max})$.

7. $\mu > 0, \lambda_0 > 0, \lambda_1 = 0$, we have four equations system to determine four unknown parameters $(E_0, E_1, \mu, \lambda_0)$ as follows

$$\begin{cases} N_0 E_1 H_{0,1} H_{1,2}(E_1 H_{1,2} + N_0) - \lambda_0 H_{0,1} - \mu = 0 \\ N_0 E_0 H_{0,1} H_{1,2}(E_0 H_{0,1} + N_0) - \mu = 0 \\ E_0 = E_{0max} \\ E_0 + E_1 = E_a \end{cases} . \tag{4.23}$$

If $E_{0max} + E_{1max} \leq E_a$, $\lambda_0 > 0$ and $\mu > 0$, the system solution is $(E_{0max}, E_a - E_{0max})$.

8. $\mu > 0, \lambda_0 = \lambda_1 = 0$, we have three equations system to determine three unknown parameters (E_0, E_1, μ)

as follows

$$\begin{cases} N_0 E_1 H_{0,1} H_{1,2}(E_1 H_{1,2} + N_0) - \mu = 0 \\ N_0 E_0 H_{0,1} H_{1,2}(E_0 H_{0,1} + N_0) - \mu = 0 \\ E_0 + E_1 = E_a \end{cases} . \tag{4.24}$$

In this case, we have to resolve the quadratic equations to obtain (E_0, E_1). Then, we check that $E_0 \leq E_{0max}$, $E_1 \leq E_{1max}$ and $\mu > 0$.

As we can see, the number of discussed cases depends on the number of hops, K. In fact, if we consider K-hop system, we have to study 2^{K+1}different cases.

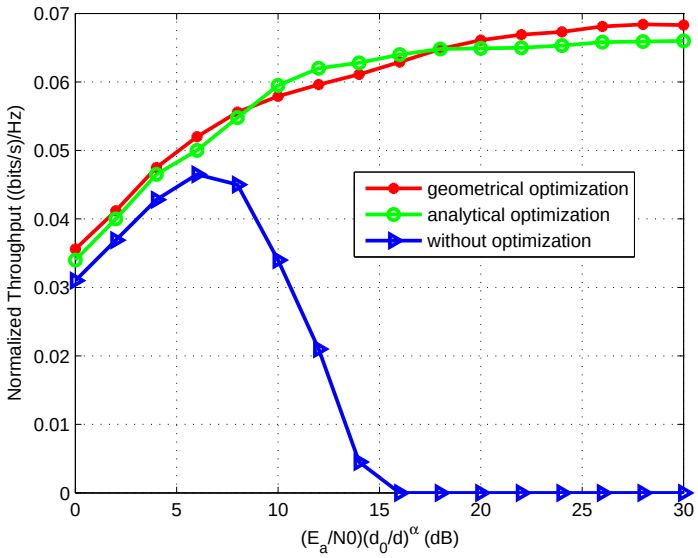

Figure 4.11: Comparison of the different optimization methods in the dual-hop transmission.

Figure 4.11 shows the normalized throughput for the two-hop system optimized with both geometrical and analytical methods, when C_{max} is fixed at $0.5dB$. As benchmark, we include in this figure the throughput of the non-optimized two-hop system and we depict from this Figure that the solution obtained by geometrical solution method and Lagrange/Kuhn-Tucker conditions algorithm lead to the same result in term of normalized throughput. However, the complexity is higher with this method compared to the geometrical

one and explodes when the number of hops increases beyond two.

4.5 Conclusion

In this chapter, we proposed two novel optimal energy allocation schemes that maximize the instantaneous received SNR in an AF multi-hop cognitive system, which guarantee that the interference cost generated at the primary network remains below a prescribed threshold. We assumed also that an adaptive modulation is considered at the secondary source. For the resolution of our optimization problems, we adopted geometrical and analytical methods. For the geometrical approach we study the two and three hops cases while for the analytical approach only the two-hop case is considered, given the resolution complexity of the problem. Through simulations, we noticed that both resolution methods lead to the same result for the two-hop system. However, the geometrical approach gives better insight to the optimization problem and makes the resolution tractable for more hops in the system. Moreover, we showed that, at sufficiently large values of transmitted SNR, the gap in throughput between energy-optimized AF multi-hop cognitive system and that with uniform energy increases with the number of hops. However, for small values of transmitted SNR, the two-hop system outperforms the three-hop system.

Chapter 5

Embedded Primary Users Identification and Channels Estimation for Underlay Cognitive Radio Network

5.1 Introduction

In this chapter, we consider an underlay cognitive radio network where secondary users can coexist with primary users in the same spectrum and region. To avoid harmful interference to the primary network, the secondary base station (BS-S) needs to identify the active primary users (PUs) and to have a perfect or partial knowledge of the primary channels. Contrary to the previous chapter, we consider, here, that the secondary base station is equipped with multiple antennas and has no prior knowledge about the interference channel state.

In the first part of this chapter, we propose a practical embedded identification scheme based on the use of random or pseudo-random sequences by the PUs to avoid extra signaling between primary and secondary

networks. Depending on the generated random sequence, the PU rotates or keeps unchanged its constellation for each transmitted symbol. Based on the signals received at the BS-S antennas, we propose a simple and efficient processing to blindly identify all active primary users, without any energy or radio resource losses. To validate our approach, we consider for our simulations random sequences and m-sequences use by the PUs. We notice also that both BPSK and QPSK modulations are studied.

In the second part of this chapter, our focus is on another identification method based on Compressive sensing technique. In fact, we propose, a novel approach for primary users identification and their channels estimation followed by the appropriate secondary transmission design. Therefore, we propose, first of all, an efficient primary users identification using compressive sensing (CS). In fact, we investigate the angular sparsity of the received signal given an unknown number of primary user source signals impinging upon the antenna array from different directions of arrival (DOA). Given multiple snapshots, multiple measurement vectors (MMV) are available at the secondary base station and considered for primary channel detection over the angular domain using the regularized MMV-FOCal Underdetermined System Solver (M-FOCUSS) algorithm. Then, we develop novel methods for paths separation and primary channels estimation based on their autocorrelation matrix properties. Finally, we focus on the downlink transmissions and propose to design a beamforming vector at the BS-S, based on the estimated channels, that maximizes the desired signal power to its corresponding secondary receiver while minimizing the total interference towards all primary receivers. For this purpose, we adopt a Gram-Schmidt orthogonalization process [26] in order to create orthogonal beams to the PUs channels. Through simulations, we analyze the recovery performance of the proposed PUs identification approach, in terms of false alarm and average minimum square error (MES) between the true and the estimated primary channel. We compare its performances with the conventional maximum to minimum eigenvalue (MME) detector. Also, we evaluate the average sum-rate at the secondary network, as well as, the average interference level at the primary network, as a function of several system parameters.

5.2 Embedded Primary Users Identification based on Pseudo-random Sequences

5.2.1 Proposed System Model

As shown in Figure 5.1, we assume that the secondary base station (BS-S), is equipped with M transmitting antennas. The secondary network coexists with a primary network consisting of one primary base station (BS-P) serving N single-antenna primary users (PUs). For the primary network, the Multi-user Multiple-Input Multiple-Output (MU-MIMO) technique is adopted. In this chapter, the secondary base station has no information about the interference link, i.e. the channels between the BS-S and the PUs. The goal of the CR system is to provide communications among SUs without causing interference to the primary system. Therefore, being able to identify the active primary users and estimate their channels are two important performance objectives.

For the uplink, the secondary base station, BS-S, listens to the primary users transmissions over K symbol periods. We consider that each primary user, with index n, has a random generator which generates a pseudo-random sequence denoted $\mathbf{q}_n = (q_{n0},..,q_{nK-1})^T \in \mathbb{C}^{K\times 1}$. This sequence will serve as a signature code for each PU. When $q_{nk} = 1$, the constellation of the k-th transmitted symbol keeps unchanged, i.e. the transmitted symbol is multiplied by $p_{nk} = 1$. When $q_{nk} = 0$, the constellation of the k-th transmitted symbol is rotated by an angle φ , i.e. the transmitted symbol is multiplied by $p_{nk} = e^{j\varphi}$, where φ depends on the constellation size.

The components of the received signal, at time kT , with T being the symbol period, to the antenna m^{th} of the BS-S, $m = 1,..,M$, from the N active primary users, can be expressed as

$$y_{mk} = \sum_{n=1}^{N} \sqrt{E_p} h_{nm} x_{nk} p_{nk} + b_{mk}, \tag{5.1}$$

where $k = 1,..,K$, x_{nk} is the transmitted information from the n^{th} active primary user at time kT with

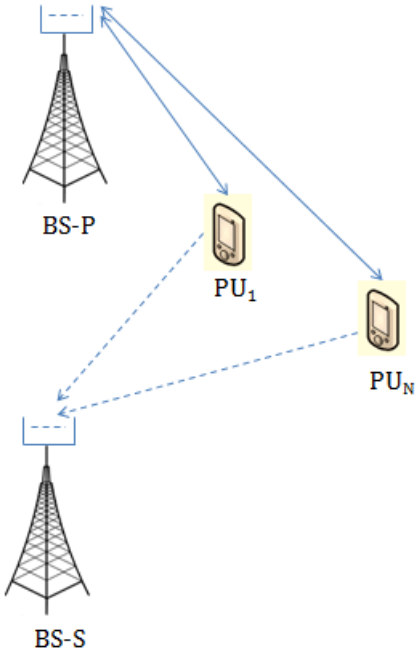

Figure 5.1: Generic system model.

transmitted energy E_p, b_{mk} represents a complex additive white Gaussian noise sample with zero mean and variance N_0. Moreover, h_{nm} denotes the interference channel sample from the n^{th} active primary user to the m^{th} antenna of the BS-S and consists of a Rayleigh slow fading channel, so that we can consider its coefficients as constant during the transmission of at least one frame. In this work, a fixed power allocation for all primary users is adopted.

To simplify our derivations, equation (5.1) can be rewritten as

$$y_{mk} = \sum_{n=0}^{N-1} h'_{nm} x'_{nk} + b_{mk}, \tag{5.2}$$

where $h'_{nm} = \sqrt{E_p} h_{nm}$ and $x'_{nk} = x_{nk} p_{nk}$.

5.2.2 Proposed Blind Channel Identification

In this subsection, we present our proposed blind identification of the active primary users. This identification is based on the pseudo-random rotation sequences use by the PUs. Next, both Binary Phase-Shift Keying (BPSK) and Quadrature Phase-Shift Keying (QPSK) modulations will be considered. We note that our approach can be easily extended to the case of other constellations (such as 16-QAM, 64-QAM and 256-QAM), for which the rotation angle φ should be different.

5.2.2.1 BPSK Modulation Case

Here, we choose $\varphi = \frac{\pi}{2}$, i.e. $p_{nk} \in \{1, e^{j\pi/2}\}$. Since the BPSK modulation uses two phases, the received signal at the BS-S in equation (5.2) is squared as follows

$$y_{mk}^2 = \sum_{n=0}^{N-1} h'^2_{nm} q_{nk} + i_{mk}, \tag{5.3}$$

where i_{mk} is an interference plus noise term given by

$$i_{mk} = \sum_{n=0}^{N-1} h'_{nm} x'_{nk} \left(\sum_{\substack{n'=0 \\ n' \neq n}}^{N-1} h'_{n'm} x'_{n'k} + 2b_{mk} \right) + b_{mk}^2. \tag{5.4}$$

We show easily that i_{mk} is an additive white Gaussian noise with variance expressed as follows

$$\sigma_i^2 = \sum_{n=0}^{N-1} E_p \left(\sum_{\substack{n'=0 \\ n' \neq n}}^{N-1} E_p + 4N_0 \right) + N_0^2. \tag{5.5}$$

As we mentionned before, each user signature consists in multiplying the original sequence by a pseudo-random sequence. We assume a prior knowledge of primary users symbol sequences bunch at the BS-S.

To identify the active users, we propose that the BS-S correlates the received sequence at each antenna m, $\mathbf{z}_m = (y_{m0}^2, .., y_{mK-1}^2) \in \mathbb{C}^{1\times K}$ with all sequences $\mathbf{q}_n = (q_{n0}, .., q_{nK-1}) \in \mathbb{C}^{1\times K}$ as follows

$$\Lambda_{nm} = \mathbf{z}_m \mathbf{q}_n^T = K h'^2_{nm} + \mathbf{i}_m \mathbf{q}_n^T. \tag{5.6}$$

Therefore, we obtain an estimation of the square of the channel realisation h'_{nm} as follows

$$\tilde{h}'^2_{nm} = \frac{\Lambda_{nm}}{K}. \tag{5.7}$$

For each identifying symbol sequence $\mathbf{q}_n$, the estimated $\tilde{h}'^2_{nm}$ in (5.7) over all receive antennas are summed and compared to a threshold denoted ξ. If the summation is above the threshold, the user PU_n is deemed to be active, otherwise, it's considered as absent.

5.2.2.2 QPSK Modulation Case

For this case, we take $\varphi = \frac{\pi}{4}$, i.e. $p_{nk} \in \{1, e^{j\pi/4}\}$. Since the QPSK modulation uses four phases, the received signal at the BS-S in equation (5.2) is raised to the power 4 as follows

$$y^4_{mk} = \sum_{n=0}^{N-1} h'^4_{nm} q_{nk} + j_{mk}, \tag{5.8}$$

where j_{mk} can be also considered as an additive white Gaussian noise, given by

$$j_{mk} = 2i_{mk} \left(\sum_{n=0}^{N-1} h'^2_{nm} q_{nk} \right) + i^2_{mk}. \tag{5.9}$$

Similarly to the modulation case, it is easy to obtain the variance of the interference plus noise term j_{mk}. This variance is omitted here for simplicity of presentation.

Then, the BS-S correlates the received sequence at each antenna m, $\mathbf{r}_m = (y^4_{m0}, .., y^4_{mK-1}) \in \mathbb{C}^{1\times K}$ with all sequences $\mathbf{q}_n = (q_{n0}, .., q_{nK-1}) \in \mathbb{C}^{1\times K}$ as follows

$$\Delta_{nm} = \mathbf{r}_m \mathbf{q}^T_n = K h'^4_{nm} + \mathbf{j}_m \mathbf{q}^T_n. \tag{5.10}$$

An estimation of the channel realization is given by

$$\tilde{h}'^4_{nm} = \frac{\Delta_{nm}}{K}. \tag{5.11}$$

For each identifying symbol sequence $\mathbf{q}_n$, the estimated $\tilde{h}'^4_{nm}$ in (5.11) over all receive antennas are summed and compared to a threshold denoted ψ. If the summation is above the threshold, the user PU_n is deemed to be active, otherwise, it's considered as absent.

5.2.3 Identification Performance Study

To evaluate the performance of our identification approach, we consider in this subsection the recovery performance for the adopted blind identification algorithm based on m-sequences technique through which

the need to send a side information from the primary network is omitted. For simulations, we consider the use of random sequences and m-sequences for simulations. We note that the m-sequences have several important randomness properties. In fact, because of their good autocorrelation [54][55] two similar PN sequences can easily be phase synchronised, even when one of them is corrupted by noise. The m-sequences are the ones of maximal possible period of $L = 2^l - 1$ where $l \in \mathbb{N}$ is the number of memory cells in the generating register. They are periodic binary sequences, obtained from primitive polynomial [63] and can be generated through shifting an original m-sequence version [55]. The most interesting property of m-sequences is their two-valued/two-level autocorrelation function $(1, -1/L)$. They are characterized by the cycle-and-add property, whereby the term-by-term sum of two cyclic shifts is a third cyclic shift of the same m-sequence. In this respect, for sufficiently long sequences, m-sequences are adequate for synchronization thanks to the absence of side-peaks and low out-of-phase autocorrelation value. We notice that the Hamming distance between two m-sequences is equal to $\frac{L+1}{2}$, so that more longer are the sequences, more different they are and less are the detection errors (more we have detection accuracy).

For measuring the performance of the approach, we simulate the identification probabiliy P_d defined as the percentage of detecting the primary user correctly at the secondary receiver (BS-S). The experiment is repeated 10^3 times with randomly drawn channel coefficients. For the m-sequence generation, we consider in Figure 5.2, the primitive polynomial $P_1 = 1 + x + x^5 + x^6 + x^8$, leading to the sequences length of $L = 255$ ($l = 8$). Here we note that N among these sequences are randomly picked out to be used in the simulation. The number of receiving antenna at the BS-S is set to $M = 4$. Figure 5.2 shows that recovery performance increases with the increase of E_p/N_0. Meanwhile, it can be seen that with the increase of the number of total primary users N in the network, the detection level decreases slightly. But we can still obtain acceptable recovery performance and accuracy. Also, from Figure 5.2, it is observed that the BPSK case offers better recovery performance in terms of identification success probability.

Next, we compare, in Figure 5.3, the performance of the proposed method for both cases of random and m-sequences. The length of both sequences is $L = 255$ and the number of active primary users is $N = 3$.

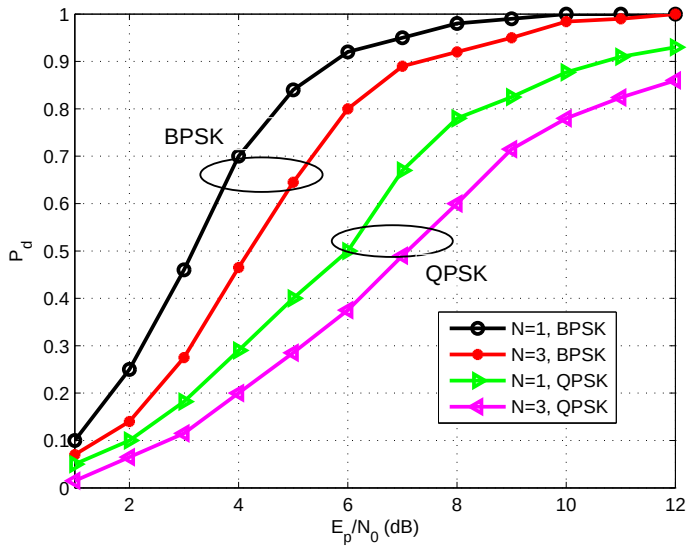

Figure 5.2: Performance of blind primary channels identification algorithm: Probability of identification success as a function of E_p/N_0 for $N = 1, 3$.

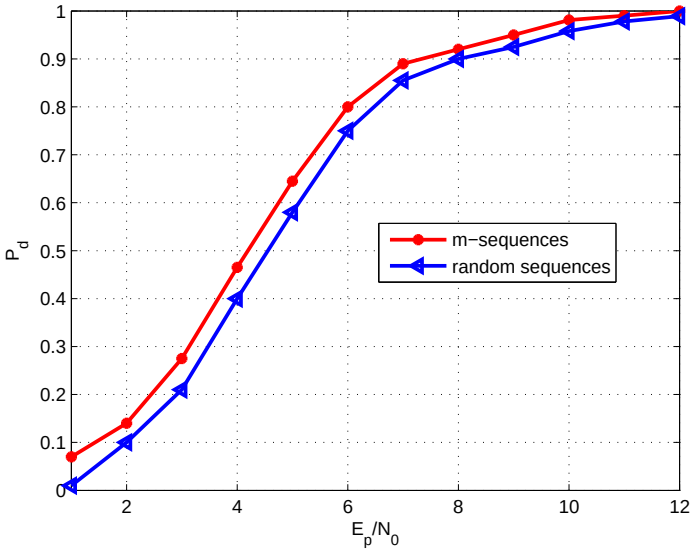

Figure 5.3: Probability of identification success as a function of E_p/N_0 for random and m-sequences techniques in BPSK case, $N = 3$.

.

Figure 5.3 shows the effectiveness of the m-sequence use in the system, compared to random sequences case especially for low average SNR (E_p/N_0) from the primary network.

5.3 Embedded Primary Users Identification and Channels Estimation based on Compressive Sensing

5.3.1 Uplink System Model

In this section, we adopt a cognitive radio system as shown in Figure 5.4, where a secondary network shares the same spectrum with a primary network. We assume that we have one secondary base station (BS-S), equipped with a uniformly-spaced linear array (ULA) of M omnidirectional antenna elements. The secondary network coexists with a primary network consisting of N primary users (PUs) with a single receiving antenna. In this work, the BS-S has no information about the interference links (channels between the BS-S and the PU).

For the primary uplink transmission, we consider a Time-Division-Duplex (TDD) mode, assuming the reciprocity of the channel. During this uplink transmission, the BS-S listens to the primary users transmissions over L symbol periods (or snapshots). In practice, the Line-of-Sight (LOS) communication links do not always exist because of the intrinsic complexity of mobile channels. Therefore, a NLOS propagation is considered here, whereby, from each PU, the BS-S can receive one or several paths. Let G_n be the number of signal paths originating from the n^{th} PU. The primary transmitted signals are impinging on the BS-S antenna array from different angles of arrival $\{\theta_g\}_{g=1}^{G}$, where $\theta_g \in \left[-\frac{\pi}{2}, \frac{\pi}{2}\right]$. The total number of signal paths arriving at the BS-S from the different active primary users is $G = \sum_{n=1}^{N} G_n$. We denote by I_n the set of path indices, of cardinality G_n, corresponding to PU_n.

The components of the received signal at the BS-S during the l^{th} observation, $l = 1, .., L$, can be expressed, in vector form, as

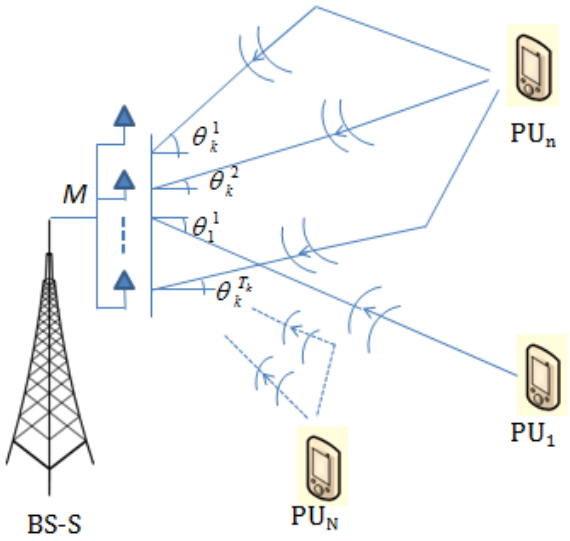

Figure 5.4: Generic uplink system model.

$$\mathbf{y}(l) = \mathbf{A}(\theta)\mathbf{s}(l) + \mathbf{b}(l), \tag{5.12}$$

where $\mathbf{y}(l) \in \mathbb{C}^{M\times 1}$, $\theta = [\theta_1, .., \theta_G]^T$ is a parameter vector corresponding to the unknown angles of arrival, $\mathbf{A}(\theta) = [\mathbf{a}(\theta_1), .., \mathbf{a}(\theta_G)] \in \mathbb{C}^{M\times G}$ is the array manifold matrix, whose columns are the steering vectors corresponding to the impinging angles of arrival. The steering vector corresponding to angle θ_g is given by $\mathbf{a}(\theta_g) = [1, \vartheta_n, \vartheta_n^2, .., \vartheta_n^{M-1}]^T$, where ϑ_n is the incremental phase between two consecutive antennas, d is the inter-antenna spacing and λ is the PU signal wavelength.

Let's s_n and ρ_n, $n = 1, .., N$, denote respectively the transmitted data and energy for n^{th} PU. The received signal from the PUs, $\mathbf{s}(l) = [\sqrt{\rho_n} s_n h_{I_n(j)}]_{n=1,..N; j=1,..G_n} \in \mathbb{C}^{G\times 1}$ is assumed to be complex Gaussian so that it looks the same in all directions. Here, $h_{I_n(j)}$ represents the fading from the n^{th} active PU through the $I_n(j)^{\text{th}}$ path. We assume that each path consists of a Rayleigh, slow fading channel, so that we can consider its

coefficients as constant during the transmission of a snapshot of L symbol periods and vary independently from one symbol period to another. Finally, $\mathbf{b}(l) \in \mathbb{C}^{M\times 1}$ is a complex Gaussian uncorrelated noise with zero mean and variance σ_b^2.

In the next subsection, we give a background of the CS theory that will be used to solve the detection problem of angles of arrivals at the BS-S, which can be seen as sparse with regards to the total possible number of angles of arrivals.

5.3.2 CS Theory Background

The topic of compressive sensing has received tremendous interest in recent years. The theory contends that we can efficiently reconstruct a sparse vector from a noisy measurement vector, given some conditions. In fact, starting with $\mathbf{y} = \mathbf{A}\mathbf{s} + \mathbf{b}$, where $\mathbf{s} \in \mathbb{C}^{G\times 1}$ is sparse vector, $\mathbf{A} \in \mathbb{C}^{M\times G}$ is the measurement matrix and $\mathbf{b} \in \mathbb{C}^{M\times 1}$ is a zero-mean random noise vector with variance σ_b^2, a near-optimal estimate of $\mathbf{s}$ can be obtained even when $M \ll G$ from the following convex optimization program

$$\min_{\widetilde{\mathbf{s}}\in\mathbb{C}^N} \left\|\widetilde{\mathbf{s}}\right\|_1 \text{ subject to } \left\|\mathbf{y} - \mathbf{A}\,\widetilde{\mathbf{s}}\right\|_2^2 \leq \varepsilon, \tag{5.13}$$

where ε is a constant that can be chosen as a function of the noise variance.

We note that CS can be used for single measurement vector (SMV) as well as for multiple measurement vectors (MMV).

In this paper, we will focus on the MMV CS that can be considered as how to recover multiple SMV with the same support simultaneously.

Given a multiple-measurement vector $\mathbf{Y} \in \mathbb{C}^{M\times L}$ and a redundant dictionary $\mathbf{A} \in \mathbb{C}^{M\times V}$, with $V \gg G$, an MMV problem, in a noisy scenario, solves the following system of equations

$$\mathbf{Y} = \mathbf{A}\mathbf{S} + \mathbf{B}, \tag{5.14}$$

where $\mathbf{S} \in \mathbb{C}^{V \times L}$ is a row sparse matrix, with a small number of rows that contain nonzero entries, and $\mathbf{B} \in \mathbb{C}^{M \times L}$ is a noise matrix. Usually, we have $L < M$. When $L = 1$, we are in the case of an SMV.

Many CS algorithms are proposed in the literature to deal with the reconstruction of $\mathbf{S}$ using a joint sparse recovery procedure that exploits the common sparse support, such as the Multi-Branch Matching Pursuit (M-BMP), the MMV-Orthogonal Matching Pursuit (M-OMP) and the MMV-FOCal Underdetermined System Solver (M-FOCUSS). In this paper, the M-FOCUSS algorithm is proposed to resolve the above problem.

5.3.3 Proposed Primary Channel Identification

5.3.3.1 Sparsity Problem Formulation

Given L snapshots, the signal model in (5.12) can be casted to a noisy MMV sparse signal representation, over an overcomplete dictionary, as follows

$$\mathbf{Y} = \mathbf{AS} + \mathbf{B}, \tag{5.15}$$

where $\mathbf{Y}$, $\mathbf{B} \in \mathbb{C}^{M \times L}$ are the observation and the noise matrices respectively, $\mathbf{A} = [\mathbf{a}(\tilde{\theta}_1), .., \mathbf{a}(\tilde{\theta}_V)]^T \in \mathbb{C}^{M \times V}$ is a known grid angle scanning matrix composed of the $V \gg G$ steering vectors corresponding to all potential angle of arrivals $\tilde{\theta}$ and $\mathbf{S} \in \mathbb{C}^{V \times L}$ is a G-row-sparse matrix such as

$$s_{vl} = \begin{cases} \sqrt{\rho_n} s_n(l) h_g \text{ if } \exists g \mid \tilde{\theta}_v = \theta_g \\ 0 \text{ otherwise} \end{cases}. \tag{5.16}$$

For sparsity problem resolution, we employ the regularized M-FOCUSS method (Reg M-FOCUSS) method [64] which is the noisy multiple snapshot extension of the iterative weighted minimum norm algorithm and considered as one of the most efficient methods for DOA estimation.

5.3.3.2 Paths/Users Separation

As we consider NLOS propagation, the sparse matrix, $\hat{\mathbf{S}} \in \mathbb{C}^{V \times L}$, recovered after the CS process, can contain within its rows several paths originating from each PU, corresponding to different angles of signal arrival. The challenge, here, is how to separate the different paths and assign each arriving signal to the appropriate PU. One idea is to investigate the autocorrelation matrix elements of $\hat{\mathbf{S}}'$, where $\hat{\mathbf{S}}' \in \mathbb{C}^{G' \times L}$ consists on the G' recovered non-null rows of $\hat{\mathbf{S}}$. In doing so, we use the fact that two signals stemming from the same primary source should have a high normalized correlation level, while those stemming from different primary sources have a very low normalized correlation level. The adopted procedure is summarized in Algorithm 5.1.

Algorithme 5.1 Primary users paths separation.

Let ξ be a certain threshold.
1. Extract the G' recovered non-null rows of $\hat{\mathbf{S}}$ in a matrix $\hat{\mathbf{S}}'$.
2. Calculate the auto-correlation matrix of $\hat{\mathbf{S}}'$:

$$\mathbf{R} = \hat{\mathbf{S}}' \hat{\mathbf{S}}'^{H}. \tag{5.17}$$

3. The following steps are repeated for each diagonal element of the auto-correlation matrix $\mathbf{R}(i,i)$, where $i = 1,..,G'$:
  for $j = i,..,G'$
    if $\frac{\mathbf{R}(i,j)\mathbf{R}(j,i)}{\mathbf{R}(i,i)\mathbf{R}(j,j)} > \xi$ then
      the row signal i and j in the matrix $\hat{\mathbf{S}}'$ stem from the same primary user, where $\mathbf{R}(i,j)$ is the $(i,j)^{\text{th}}$ entry of $\mathbf{R}$.
    end if
  end for
4. The BS-S then identifies and gathers the paths of each PU.

5.3.3.3 Primary Channels Estimation

In this section, our objective is to estimate the channel between the BS-S and each PU in order to avoid any disturbance to the primary network during the downlink secondary transmissions by transmitting orthogonal vectors to all the primary estimated channels. Nonetheless, the recovered original signal after

applying the path-separation algorithm, consists, as seen in (5.16), of the product of one path channel and the corresponding transmit information. For each primary user PU_n, we choose an index j_n from the set of its corresponding path indices I_n, and we introduce the following vector

$$\mathbf{h}_n = \sum_{i \in I_n} \mathbf{a}(\tilde{\theta}_i) \frac{\mathbf{R}(i, j_n)}{\mathbf{R}(j_n, j_n)}, \tag{5.18}$$

that can be approximated by

$$\mathbf{h}_n = \sum_{i \in I_n} \mathbf{a}(\tilde{\theta}_i) \frac{\rho_n \|\mathbf{s}_n\|^2 h_i h_{j_n}^*}{\rho_n \|\mathbf{s}_n\|^2 \left\|h_{j_n}\right\|^2}. \tag{5.19}$$

Equation (5.19) can be written as follows

$$\mathbf{h}_n = \frac{1}{h_{j_n}} \sum_{i \in I_n} \mathbf{a}(\tilde{\theta}_i) h_i = \frac{1}{h_{j_n}} \mathbf{h}'_n. \tag{5.20}$$

where $\mathbf{h}'_n$ corresponds to the desired channel estimate of the primary user PU_n, up to the multiplicative factor $1/h_{j_n}$. Therefore, the BS-S can efficiently transmit orthogonally to all $\mathbf{h}_n$ to avoid any interference to the primary network.

5.3.4 Recovery Performance Study

In our simulations, we take $V = 200$ and set the number of snapshots to $L = 50$. Also, for simplicity sake, a fixed energy ρ for all primary users is adopted. We analyze, in Figure 5.5 and Figure 5.6, the recovery performance for the adopted CS algorithm and compare its performance to the Maximum to Minimum Eigenvalue (MME) approach. We adopt two rules to compare the performances of the two algorithms: the false alarm rate R_{fa}, estimated through several simulations, and the relative mean squared error (MSE) between the true and the estimated solution, given by

$$MSE = E\left(\frac{\left\|\hat{\mathbf{S}}-\mathbf{S}\right\|^2}{\left\|\mathbf{S}\right\|^2}\right). \tag{5.21}$$

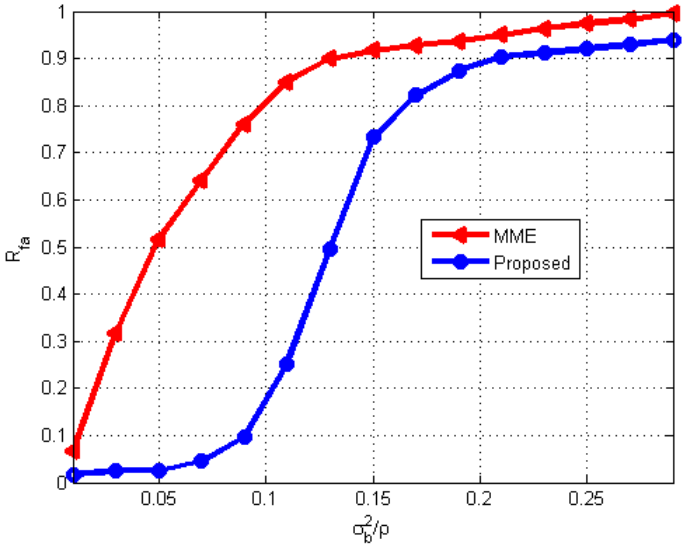

Figure 5.5: R_{fa} as a function of $\frac{\sigma_b^2}{\rho}$ for $M = 50$, $L = 50$, $V = 200$ and $N = 2$.

The plotted figures show that the recovery performance of both approaches decreases dramatically with any increase in the noise variance σ_b^2 at the secondary receiver (BS-S). Meanwhile, it can be seen that CS is better than MME in terms of robustness to noise impact.

Figure 5.7 presents the R_{fa} for different values of the number of antennas, M, at the BS-S. The simulations are carried for $N = 2$ primary users. It is shown that with the increase of M, the R_{fa} for CS and MME reduces quickly. However, with CS, we can still obtain acceptable recovery performance and accuracy, even with a small number of receive antenna, M.

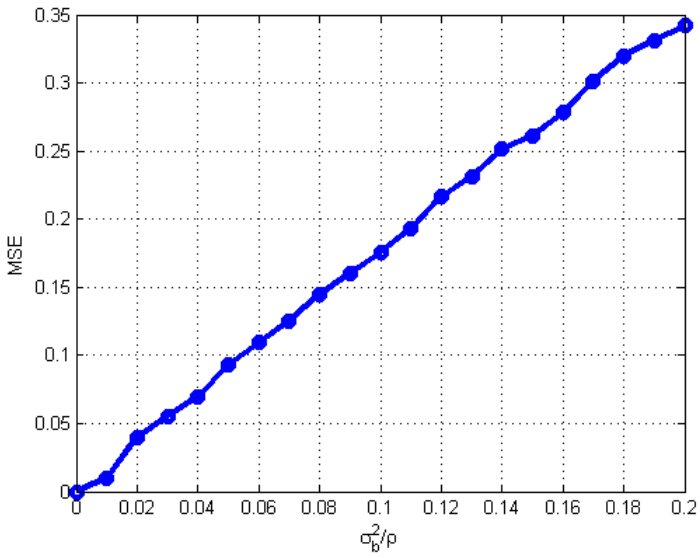

Figure 5.6: Robustness to noise for the CS based recovery algorithm, for $M = 50$, $L = 50$, $V = 200$ and $N = 2$.

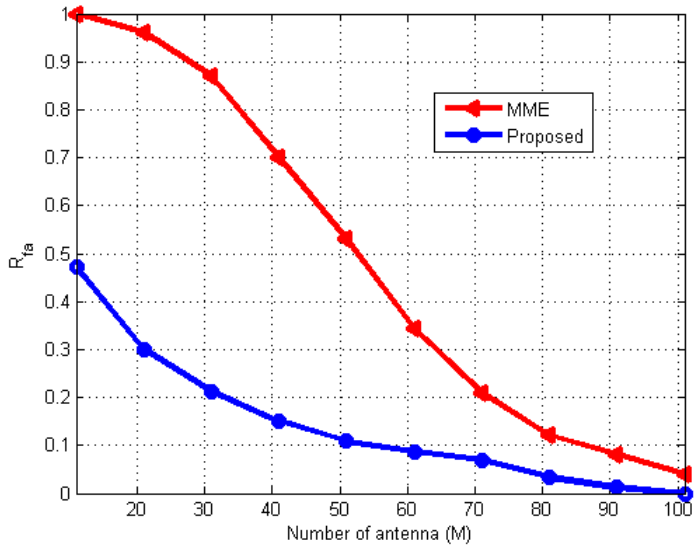

Figure 5.7: R_{fa} as a function of M for $L = 50$, $V = 200$ and $N = 2$.

In Figure 5.8, we plot the R_{fa} for different values of the number of PUs, N, and show, once again, the superior performance of CS compared to MME. Moreover, we show in the same Figure that the recovery accuracy decreases as well as N increase.

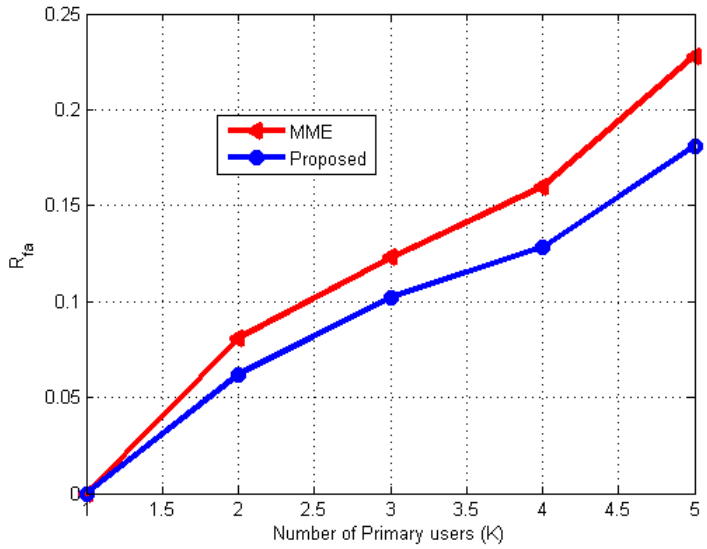

Figure 5.8: R_{fa} as a function of N for $M = 50$, $L = 50$, $V = 200$.

5.4 Orthogonal Multiple Beamforming Generation during the Downlink Transmission

5.4.1 Downlink System Model

In this subsection, we focus on the downlink transmission in the cognitive network, as shown in Figure 5.9. We assume that the secondary base station (BS-S) communicates with Q secondary users (SU) with a single receiving antenna each. The goal, here, is to schedule transmission to the secondary users, without causing interference to the primary network and minimize self interferences among SUs.

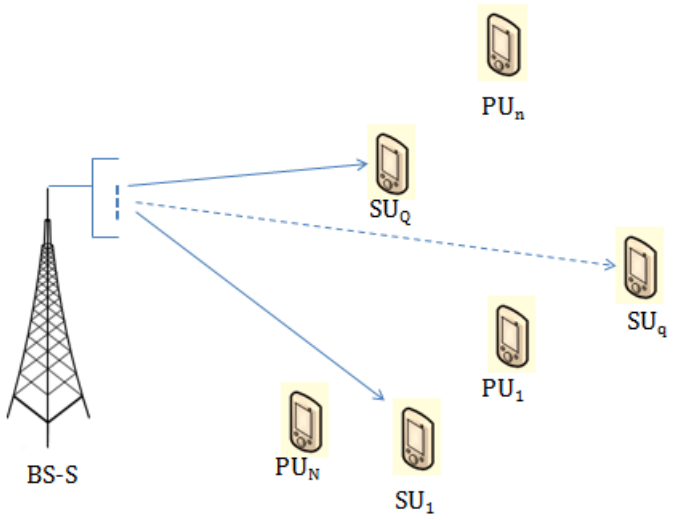

Figure 5.9: Generic downlink system model.

The signal vector $\mathbf{x} \in \mathbb{C}^{M\times 1}$ to be transmitted from the BS-S to the Q secondary users can be written as follows

$$\mathbf{x} = \sum_{q\in Q} \mathbf{w_q} s_q, \tag{5.22}$$

where s_q and $\mathbf{w_q} \in C^{M\times 1}$ denote the transmitted symbol sample and the transmit beamforming weight vector intended for the secondary user q respectively. We assume that all the secondary users have equal allocated energies ξ.

The received signal at user q is given by

$$y_q = \sqrt{\xi}\mathbf{h}_q^T \mathbf{w_q} s_q + \sum_{p\in Q, p\neq q,} \sqrt{\xi}\mathbf{h}_q^T \mathbf{w_p} s_q + z_q, \tag{5.23}$$

where $\mathbf{h}_q \in \mathbb{C}^{M\times 1}$ denotes the channel vector between the BS-S and the q^{th} SU and z_q is the additive white Gaussian noise with zero mean and variance σ_z^2. The second term is the co-channel interference (CCI)

caused by the multi-user nature of the system.

5.4.2 Orthogonal Multiple Beamforming Generation

In the proposed approach, the BS-S first senses and estimates the interference channels from the primary network and then nulls the secondary transmission to the primary network by using a beamforming technique. In other words, the BS-S generates orthogonal transmit beams to all estimated primary channels in order to eliminate the interference caused to the PU. The generated beams should also minimize the interference between the SUs. For this purpose, we adopt the Gram-Schmidt orthogonalization process [53] summarized in Algorithm 5.2.

Algorithme 5.2 Adopted orthogonalization based on Gram-Schmidt process

1. Generate independent $M-V$ arbitrary vectors set $\{\mathbf{g}_i, i = 1,..,M-V\}$.
2. Generate V orthogonal vectors sequentially by

$$\begin{cases} \mathbf{v}_1 = \mathbf{h}_1^T \\ \mathbf{v}_n = \mathbf{h}_n'^T - \sum_{j=1}^{n-1} \frac{<\mathbf{h}_n', \mathbf{v}_j>}{<\mathbf{v}_j, \mathbf{v}_j>} \mathbf{v}_j \end{cases} \text{ where } n = 2,..,V.$$

3. Generate $M-V$ orthogonal vectors $\mathbf{u}_i$ that are also orthogonal to each generated vector $\mathbf{v}_n$ in 2)

$\mathbf{u}_i = \mathbf{g}_i - \sum_{j=1}^{i-1} \frac{<\mathbf{g}_i, \mathbf{v}_j>}{<\mathbf{v}_j, \mathbf{v}_j>} \mathbf{v}_j$, where $i = 1,..,M-V$.

4. The transmit beamforming weight is the normalization of

$\mathbf{w}_i = \frac{\mathbf{u}_i}{\|\mathbf{u}_i\|}$, for $i = 1,..,M-V$

The generated transmit beams $\mathbf{w}_q$ achieve our goals in keeping the primary user interference free and minimizing the interference between the secondary users. In other words, they satisfy the following properties

$$\begin{cases} \left\|\mathbf{w}_q\right\| = 1 \\ \left|\mathbf{h}_n'^T \mathbf{w}_q\right| = 0 \quad q, p = 1,..,Q; n = 1,..,N. \\ \left|\mathbf{w}_q^H \mathbf{w}_p\right| = 0 \end{cases} \tag{5.24}$$

We recall that $\mathbf{h}'_n$ corresponds to the estimated channel vector between the BS-S and the n-th PU.

5.4.2.1 sum-rate at the Secondary Network

The signal to interference plus noise ratio, SINR, of user q is

$$SINR_q = \frac{\xi \left|\mathbf{h}_q^T \mathbf{w}_q\right|^2}{\xi \sum\limits_{p \neq q} \left|\mathbf{h}_q^T \mathbf{w}_\mathbf{p}\right|^2 + \sigma_z^2}. \tag{5.25}$$

Thus, we can consider the average sum-rate of all SU as a performance metric defined as follows

$$SR_{avg} = \frac{1}{Q} \sum_{q=1}^{Q} \log_2(1 + SINR_q). \tag{5.26}$$

5.4.2.2 Interference Level at the Primary Network

We define the interference level at the primary user as $C_v = \mathbf{w}^H \mathbf{h}_v^T E_s R$, where R denotes the symbol rate and $\mathbf{h}_v \in \mathbb{C}^{M \times 1}$ denotes the channel vector between the BS-S and the v^{th} PU.

5.4.3 Secondary Network Performance Simulation

For the downlink transmission, we set the number of primary users to $N = 2$. We evaluate, in Figure 5.10 and Figure 5.11, the secondary network performance in terms of average sum-rate as defined in (5.26) for different values of the SNR and different numbers of the secondary users Q, respectively. Figure 5.10, shows that, with the increase of M and for a fixed SUs number, the average sum-rate at the secondary network is improved.

In Figure 5.12, it's shown that with the increase of the uplink noise level σ_b, the average interference level at the primary network increases dramatically. Also, we depict from Figure 5.12, that the increase of the secondary users number in the network, can disturb more and more the primary communications.

We denote that, in Figure 5.11 and Figure 5.12, the number of antennas at the secondary base station is set to $M = 50$.

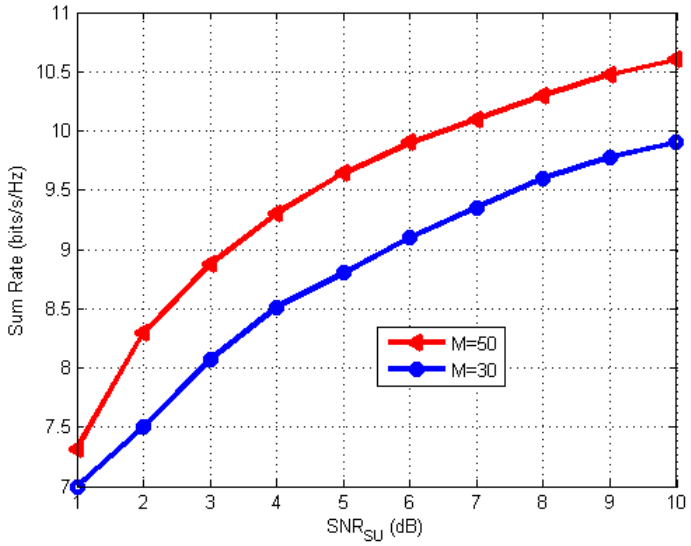

Figure 5.10: sum-rate as a function of SNR_{SU}.

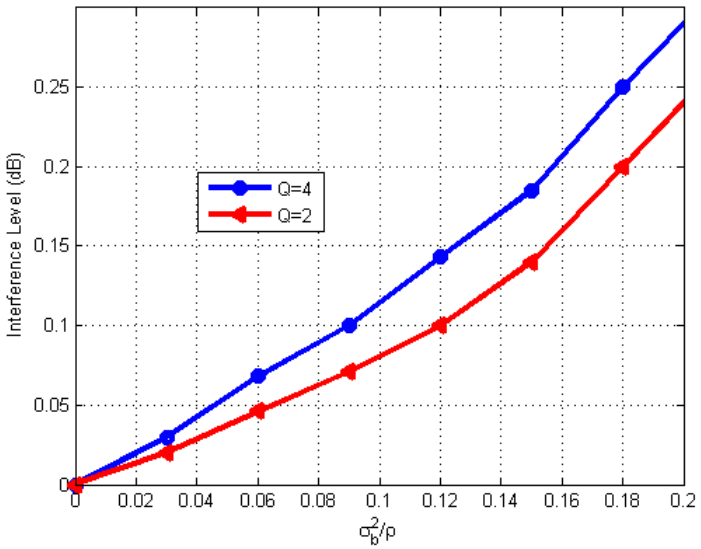

Figure 5.12: Interference level at the primary users as a function of of $\frac{\sigma_b^2}{\rho}$.

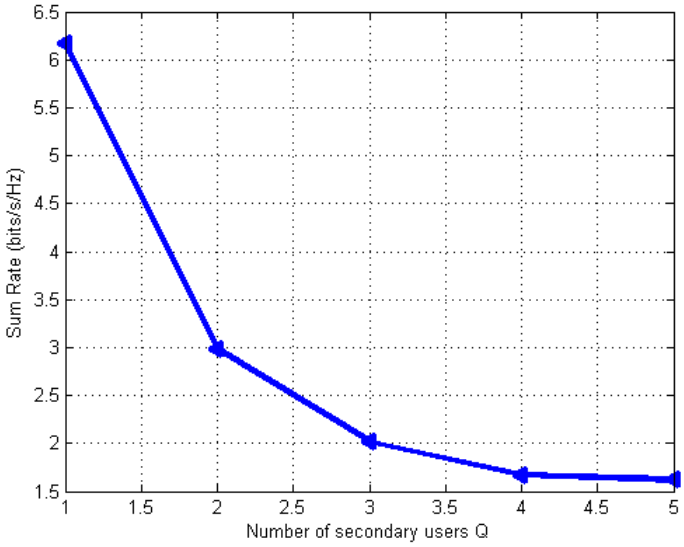

Figure 5.11: sum-rate as a function of the number of secondary users Q.

5.5 Conclusion

In this chapter, we proposed a blind identification approach based on the use of pseudo-random sequences by the primary users in a cognitive radio system, when the primary and secondary users share the spectrum concurrently. We assumed that the secondary base station does not have any information from the primary channels. Through simulation we showed that we can obtain acceptable recovery performance especially with the increase of E_p/N_0. Then, we proposed a blind identification approach of primary users based on compressive sensing in a cognitive radio context. Through simulations, we studied the effect of several parameters on the reconstruction effectiveness of the the adopted CS algorithm and showed that it outperforms the conventional Maximum to Minimum Eigenvalue (MME) approach. In addition, we proposed to design a beamforming vector at the cognitive radio base station (BS-S), based on the estimated channels, that maximizes the desired signal energy to its corresponding secondary receiver while minimizing the total interference towards all primary receivers.

Chapter 6

Conclusion and Future Work

6.1 Conclusion

In this thesis, our main objective was to improve the performance of the secondary transmissions in the cognitive radio networks. We considered the underlay case where the secondary users can share the spectrum concurrently with the primary users on condition that their generated cost remains below a certain threshold.

First, we proposed a cognitive approach based on an adaptive modulation in order to maximize the data rate at the secondary destination. We showed through simulations that the system throughput is proportional to several parameters such as the maximum allowed cost at the primary network, the secondary user location, its transmission energy and the number of detected primary base stations.

Furthermore, an adaptive cognitive strategy based on cooperation technique was proposed, when the secondary user cannot share the spectrum with the primary through a direct link to secondary destination. Two cooperative techniques were considered that are conventional and Alamouti AF approaches. Numerical results showed that adaptive modulation coupled with cooperation can be an effective way to improve

the performance of cognitive transmissions. In fact, both adaptive schemes based on relaying highlight a significant throughput improvement compared to the non-cooperative adaptive scenario. In particular, the Alamouti ST coded approach, that properly exploits the whole energy transmitted by source in the two cooperation phases, was more advantageous in terms of throughput gain compared to the classical AF protocol.

Next, we proposed and studied energy allocation schemes in an adaptive cognitive network. In fact, an optimization of the SU and the relay transmitted symbol energies was carried on to ensure the better performance provided that the interference cost generated at the PU is below a prescribed threshold. After that, our study was generalized to the cognitive multi-hop case. To solve our optimization problem, two novel optimal energy allocation schemes that maximize the instantaneous received SNR in an AF multi-hop cognitive system were adopted. More precisely, for the two and three hop cases, we proposed, to use geometrical method that presents an attractive way for solving nonlinear problems involving two parameters with a minimum amount of computational effort. We, then, proposed an analytical optimal solution to the problem for the two hop case. A variety of simulation results revealed that our energy allocation approaches, combined with adaptive modulation, gave better performances compared to the classical cooperative scheme, where energy resources are equally distributed over all nodes. Moreover, we showed that the analytical resolution leads to the same results as the geometrical one. The advantage of the geometrical method is to get more insight for the 2-hop case and makes the resolution tractable for more hops in the system.

Note here that, up to our knowledge, our proposed geometrical optimization approach, as well as the analytical approach in the cognitive cooperative context, have not been considered in the literature.

Further, we assumed that the secondary base station is equipped with multiple antennas and doesn't have any prior information about the channel from the primary users. we proposed efficient and reliable approaches for a blind active primary users identification. The first approach was based on the use of pseudo-random sequences by the primary users to avoid extra signaling between primary and secondary networks.

Depending on the generated random sequence, the PU rotates or keeps unchanged its constellation for each transmitted symbol. Both Binary Phase-Shift Keying (BPSK) and Quadrature Phase-Shift Keying (QPSK) modulations were considered. Our proposed technique revealed simple and efficient processing to blindly identify all active primary users, without any energy or radio resource losses.

The second identification approach was based on compressive sensing (CS) technique where the NLOS transmission was considered. We investigated the angular sparsity of the received signal given an unknown number of primary user source signals impinging upon the antenna array from different directions of arrival. Given multiple snapshots, multiple measurement vectors (MMV) are available at the secondary base station and considered for primary channel detection over the angular domain using the regularized M-FOCUSS algorithm. Then, we developed novel methods for paths separation and primary channels estimation based on their autocorrelation matrix properties. Through simulations, we studied the effect of several parameters on the reconstruction effectiveness of our proposed CS algorithm and showed that it outperforms the conventional Maximum to Minimum Eigenvalue (MME) approach.

Finally, we focused on the downlink transmissions and proposed to design a beamforming vector at the secondary base station, based on the estimated channels, that maximizes the desired signal power to its corresponding secondary receiver while minimizing the total interference towards all primary receivers. For this purpose, Gram-Schmidt orthogonalization process was adopted in order to create orthogonal beams to the PUs channels. Simulation results showed that the secondary network performance is proportional to several parameters such as the number of antennas at the BS-S, the uplink noise level and the number of secondary users in the network.

6.2 Future work

This thesis covered several aspects in improving performances for cognitive radio systems. Yet, there are still many remaining and emerging issues that have not been addressed.

In fact, only the amplify and forward and space-time coding protocols based on Alamouti ST code are addressed in this work. So, we can investigate the study of others cooperative techniques such as

- the simple Decode and Forward (DF), where the relay detects and decodes the received signal and then regenerates and re-encodes the signal to be forwarded to the destination.
- the hybrid AF and DF, where the relay switches between AF and DF depending on the channel conditions.
- the Demodulate and Forward technique, where the relay demodulates (without detecting) the received signal before forwarding it.

Moreover, although the considered Rayleigh model for channel fading in this thesis, is the most applicable, for instances, in the multi-paths environment, others channel fading models can be addressed such as Rice and log-normal fadings.

Next, we recall that both Binary Phase-Shift Keying (BPSK) and Quadrature Phase-Shift Keying (QPSK) modulations are studied for our primary users identification method. As a third perspective, we propose to extend to the case of other constellations, such as 16, 64 and 256 QAM, for which the rotation angles φ should be different.

Finally, it is also interesting to propose a CS-based scheduling algorithm for a cognitive radio network, where only users whose interference cost generated at the primary network is below a predefined threshold, are allowed to feedback to the secondary base station. Then, the BS-S selects the better users in terms of channel quality for the downlink transmission.

Bibliography

[1] I. F. Akyildiz, W.-Y. Lee, M. C. Vuran, and S. Mohanty, "Next generation/ dynamic spectrum access/cognitive radio wireless networks: a survey," *Elsevier Computer Networks Journal*, vol. 50, no. 13, pp. 2127 – 2159, Sep. 2006.

[2] FCC, "Spectrum policy task force," *ET Docket 02-135*, Nov. 2002.

[3] J. Mitola and G. Q. Maguire, "Cognitive radio: Making software radios more personal," *IEEE Pers. Commun.*, vol. 6, no. 6, pp. 13 – 18, Aug. 1999.

[4] H. Simon, "Cognitive radio: brain-empowered wireless communications," *IEEE Journal on Selected Areas in Communications*, vol. 23, no. 2, pp. 201 – 220, Feb. 2005.

[5] I. F. Akyildiz, W. Y. Lee, M. C. Vuran, and M. Shantidev, "A survey on spectrum management in cognitive radio networks," *IEEE Communication Magazine*, pp. 40 – 48, Apr. 2008.

[6] L. Ying-Chang, C. Kwang-Cheng, Y. L. Geoffrey, and M. Petri, "Cognitive radio networking and communications: an overview," *IEEE Transactions on Vehicular Technology*, vol. 60, no. 7, pp. 3386 – 3407, Sep 2011.

[7] J. M. III, "Cognitive radio: an integrated agent architecture for software defined radio," Ph.D. dissertation, 2000.

[8] J. Mitola, "Cognitive radio for flexible multimedia communications," *IEEE Press*, 1999.

[9] T. Yucek and H. Arslan, "A survey of spectrum sensing algorithms for cognitive radio applications," *Commun. Surveys Tuts.*, vol. 11, no. 1, pp. 116 – 130, 2009.

[10] S. Haykin, "Cognitive radio: brain-enpowered wireless communications," *IEEE Journal on Selected Areas in Communications*, vol. 23, no. 9, pp. 201 – 220, 2005.

[11] A. Goldsmith, S. Jafar, I. Maric, and S. Srinivasa, "Breaking spectrum gridlock with cognitive radios: An information theoretic perspective," *Proceedings of the IEEE*, vol. 97, no. 5, pp. 894 – 914, may 2009.

[12] Z. Zhang, K. Long, and J. Wang, "Self-organization paradigms and optimization approaches for cognitive radio technologies: a survey," *IEEE Wireless Communications*, vol. 20, no. 2, pp. 36 – 42, Apr, 2013.

[13] D. Cabric, S. M. Misha, and R. W. Broderson, "Implementation issues in spectrum sensing for cognitive radios," *in Proc. Asilomar Conf. on Signals, Systems, and Computers*, vol. 1, pp. 772 – 776, Nov, 2004.

[14] A. Sahai, N. Hoven, and R. Tandra, "Some fundamental limits on cognitive radio," *in Proc. Allerton Conference on Communication, Control and Computing*, October 2004.

[15] T. K. Phan, S. A. Vorobyov, N. D. Sidiropoulos, and C. Tellambura, "Spectrum sharing in wireless networks via qos-aware secondary multicast beamforming," *IEEE Trans. Sig. Process.*, vol. 57, no. 6, pp. 2323 – 2335, June 2009.

[16] A. Ghasemi and E. S. Sousa, "Collaborative spectrum sensing for opportunistic access in fading environments," *in Proc. IEEE DySPAN*, Nov. 2005.

[17] F. N. of Inquiry and N. of Proposed Rule Making, "In the matter of establishment of an interference temperature metric to quantify and manage interference and to expand available unlicensed operation in certain fixed, mobile and satellite frequency bands," *ET Docket No. 03-237*, Nov, 2003.

[18] A. Sendonaris, E. Erkip, and B. Aazhang, "User cooperation diversity part i: Implementation aspects and performance analysis," *IEEE Trans. Commun.*, vol. 51, no. 11, pp. 1939 – 1948, Nov 2003.

[19] J. N. Laneman, D. N. C. Tse, and G. W. Wornell, "Cooperative diversity in wireless networks: Efficient protocols and outage behavior," *IEEE Trans. Inform. Theory*, vol. 50, no. 12, pp. 3062 – 3080, Dec 2004.

[20] S. Hsin-Yi, Y. Haiming, B. Sikdar, and S. Kalyanaraman, "A distributed system for cooperative mimo transmissions," *in Proc. Global Communication Conference Globecom*, no. 30, Dec 2008.

[21] G. Holland, N. Vaidya, and P. Bahl, "A rate-adaptive mac protocol multi-hop wireless networks," *Proc. of the 7th MobiCom, Rome, Italy*, pp. 236 – 251, 2001.

[22] I. Sahnoun, I. Kammoun, and M. Siala, "Performance analysis of adaptive modulation in cooperative networks," *The Second International Conference on Communications and Networking ComNet*, 2010.

[23] K. G. Seddik, A. K. Sadek, W. Su, and K. J. R. Liu, "Outage analysis and optimal power allocation for multinode relay networks," *IEEE Signal Processing Lett.*, vol. 14, no. 6, pp. 377 – 380, June 2007.

[24] M. O. Hasna and M.-S. Alouini, "Optimal power allocation for relayed transmissions over rayleigh-fading channels," *IEEE Trans. Wireless Commun.*, vol. 3, no. 6, pp. 1999 – 2004, Nov. 2004.

[25] A. P. T. Lau and S. Cui, "Joint power minimization in wireless relay channels," *IEEE Trans. Wireless Commun.*, vol. 6, no. 8, pp. 2820 – 2824, Aug. 2007.

[26] A. Zafar, R. Radaydeh, Y. Chen, and M. S. Alouini, "Energy-efficient power allocation for fixed-gain amplify-and-forward relay networks with partial channel state information," *IEEE Wireless Commun.*, vol. 1, no. 6, Dec 2012.

[27] G. Farhadi and N. C. Beaulieu, "Power-optimized amplify-and- forward multi-hop relaying systems," *IEEE Trans. Wireless Commun.*, vol. 8, no. 9, Sep. 2009.

[28] M. HajiAghayi, M. Dong, and B. Liang, "Jointly optimal channel pairing and power allocation for multi-channel multi-hop relaying," *IEEE Trans. Signal Processing*, vol. 59, no. 10, Oct 2011.

[29] Y. Zhao, R. Adve, and T. J. Lim, "Improving amplify-and-forward relay networks: Optimal power allocation versus selection," *Trans. Wireless Commun.*, vol. 6, no. 8, Aug 2007.

[30] X. Hong, Z. Chen, C. X. Wang, S. A. Vorobyov, and J. S. Thompso, "Interference cancelation and management techniques," *IEEE Vehicular Technology Magazine*, December 2009.

[31] J. G. Proakis, *Digital Communications*, 3rd ed.

[32] W. A. Gardner, "Signal interception: A unifying theoretical framework for feature detection," *IEEE Trans. on Communications*, vol. 36, no. 8, August 1988.

[33] L. Ming, S. N. Batalama, A. D. Padosy, T. Melodia, M. J. Medley, and J. D. Matyjas, "Cognitive code-division channelization with blind primary-system identification," *IEEE Wireless Commun.*, vol. 10, no. 11, pp. 3743 – 3753, Sep. 2011.

[34] A. Ghosh, W. Hamouda, and I. Dayoub, "Blind primary user identification in mimo cognitive networks," *IEEE ICC 2013 - Signal Processing for Communications Symposium*, pp. – , June 2013.

[35] E. J. Candes, J. K. Romberg, and T. Tao, "Stable signal recovery from incomplete and inaccurate measurements," *Communications on Pure and Applied Mathematics*, vol. 59, no. 8, pp. 1207 – 1223, 2006.

[36] D. L. Donoho, "Compressed sensing," *IEEE Trans. Info. Theory*, vol. 52, pp. 1289 – 1306, Sept. 2006.

[37] M. E. Eltayeb, T. Al-Naffouri, and H. R. Bahrami, "Compressive sensing for feedback reduction in mimo broadcast channels," *IEEE Transactions on communications*, vol. 62, no. 9, pp. – , Sept. 2014.

[38] S. T. Qaseem1 and T. Al-Naffouri, "Compressive sensing for reducing feedback in mimo broadcast channels," *IEEE 17th International Conference ICC*, pp. – , 2010.

[39] K. Elkhalil, M. E. Eltayeb, A. Kammoun, T. Y. Al-Naffouri, and H. R. Bahrami, "On the feedback reduction of relay multiuser networks using compressive sensing," *cs.IT*, May 2015.

[40] Z. Tian and G. B. Giannakis, "Compressed sensing for wideband cognitive radios," *IEEE International Conference on Acoustics, Speech and Signal Processing (ICASSP)*, vol. 4, pp. IV – 1357, 2007.

[41] I. Elleuch, F. Abdelkefi, A. Nafkha, and M. Siala, "Efficient limited data multi-antenna compressed spectrum sensing exploiting angular sparsity," *IEEE 24th Annual International Symposium on Personal, Indoor, and Mobile Radio Communications, PIMRC*, pp. 1136 – 1140, Sep. 2013.

[42] Z. Chen, "Interference modelling and management for cognitive radio networks," *A thesis in partial fulfilment for the degree of Doctor of Philosophy at Heriot-Watt University School of Engineering and Physical Sciences*, April 20011.

[43] L. Zhang, Y.-C. Liang, Y. Xin, and H. V. Poor, "Robust cognitive beamforming with partial channel state information," *IEEE Trans. Wireless Commun.*, vol. 8, no. 8, pp. 4143 – 4153, Aug. 2009.

[44] J. Zhou and J. S. Thompson, "Linear precoding for the downlink of multiple input single output coexisting wireless systems," *IET Commun.*, vol. 2, no. 6, pp. 742 – 752, July 2008.

[45] L. Zhang, Y. Liang, and Y. Xin, "Joint beamforming and power allocation for multiple access channels in cognitive radio networks," *IEEE JSAC*, vol. 26, pp. 38 – 51, Jan. 2008.

[46] H. I. Ma, L. Ying-Chang, and T. H. Anh, "Joint beamforming and power control in the downlink of cognitive radio networks," *IEEE Wireless Communication and Networking Conference, Kowloon*, pp. 21 – 26, Mar. 2007.

[47] R. Suleesathira and S. Puranachikeeree, "Beamformings for spectrum sharing in cognitive radio networks," *WSEAS Transactions on Signal Processing*, vol. 9, no. 2, April 2013.

[48] H. Karama, Z. Wei, and B. L. Khaled, "Joint beamforming and scheduling in cognitive radio networks," *IEEE GLOBECOM, Washington DC, USA*, pp. 2977 – 2981, Nov 2007.

[49] Z.Wenhui, S. Sen, M. Qingmin, and Z.Weiping, "Joint user scheduling and beamforming for underlay cognitive radio system," *15th IEEE Asia-Pacific Conference on Communication, Shanghai*, pp. 99 – 103, Oct. 2009.

[50] B. Luca, C. Lorenzo, O. Marina, R. Mirco, S. R. Carlo, and A. Claudio, "A transmit beamforming technique for mimo cognitive radios," *TechRepublic*, Apr. 2011.

[51] A. Massaoudi, N. Sellami, and M. Siala, "Scheduling scheme for cognitive radio networks with imperfect channel knowledge," *IEEE 24th International Symposium on PIMRC: Mobile and Wireless Networks*, 2013.

[52] R. Rodrigues, R. Dinis, and F. Cercas, "Training sequence design for channel estimation with nonlinear oqpsk-type modulations," *in Proc. IEEE VTC-Fall*, pp. 1 – 5, Sept. 2012.

[53] M. Rice, S. Tretter, and P. Mathys, "On differentially encoded m-sequences," *IEEE Trans. Commun. Letters*, vol. 49, no. 3, pp. 421 – 424, March 2001.

[54] R. N. Mutagi, "Pseudo noise sequences for engineers," *Electronic and Commun. Engineering J.*, vol. 8, no. 2, pp. 79 – 87, April 1996.

[55] S. W. Golomb, "Shift register sequences," *Holden-Day, San Francisco, CA*, pp. – , 1967.

[56] M. Gastpar, "On capacity under receive and spatial spectrum-sharing constraints," *IEEE Trans. Inform. Theory*, vol. 53, no. 2, pp. 471 – 487, Feb. 2007.

[57] S.Alamouti, "Space-time block coding: A simple transmitter diversity technique for wireless communications," *IEEE J. Select. Areas Commun.*, vol. 16, no. 8, pp. 1451 – 1458, Oct 1998.

[58] I. Sahnoun, I. Kammoun, and M. Siala, "Throughput enhancement for secondary users in cognitive network," *IEEE 24th Annual International Symposium on Personal, Indoor, and Mobile Radio Communications, PIMRC*, 2013.

[59] B. C. Das, "Effect of graphical method for solving mathematical programming problem," *Daffodil international university journal of science and technology*, vol. 5, no. 1, January 2010.

[60] M. O. Hasna and M. S. Alouini, "Outage probability of multihop transmission over nakagami fading channels," *IEEE Commu. Letters*, vol. 7, no. 5, May. 2003.

[61] S. Boyd and L. Vandenberghe, *Convex Optimization*, 1st ed. New York: Cambridge University Press, 2004.

[62] D. Luenberger, *Linear and Nonlinear Programming*, 2nd ed. Addison-Wesley, 1984.

[63] A. Mitra, "On the construction of m-sequence via primitive polynomials with a fast identification method," *International J. of Computer and Electrical Engineering*, vol. 2, pp. 663 – 668, Sep. 2008.

[64] S. Cotter, B. Rao, K. Engan, and K. Kreutz-Delgado, "Sparse solutions to linear inverse problems with multiple measurement vectors," *IEEE Transactions on Signal Processing*, vol. 53, no. 7, pp. 2477 – 2488, 2005.